Finite Element Modelling of Eccentrically Loaded Concrete Filled Double Skin Tube Columns

by

Usongo Amika Akuta

Dissertation presented for the degree of

Master of Engineering (Civil Engineering)

in the Faculty of Engineering at

Stellenbosch University

Supervisor: Prof Trevor Haas, Pr Eng

March 2021

DECLARATION

By submitting this thesis/dissertation electronically, I declare that the entirety of the work contained therein is my own, original work, that I am the sole author thereof (save to the extent explicitly otherwise stated), that reproduction and publication thereof by Stellenbosch University will not infringe any third-party rights and that I have not precisely in its entirety or in part submitted it for obtaining any qualification.

March 2021

Signature:

SUMMARY

Columns are structural elements that transmit loads from floors, beams and other columns above to the foundation. Columns should, therefore, be robust to resist failure.

There are two (2) types of columns, i.e., short columns and long columns. Short columns generally fail as a result of crushing due to its short length. The ratio of the effective length to least lateral dimension is less than 12, with a slenderness ratio of less than 45. Short columns are generally only subjected to compressive stresses. Long columns on the other hand generally fail by buckling and the ratio of effective length to least lateral dimension is greater than 12, while the slenderness ratio of long columns is greater than 45. Due to the bending effect, these columns are subjected to both compressive and tensile stresses.

Various materials are used in column construction with reinforced concrete (RC) and structural steel being the most commonly used material. In this study, a relatively new method of column construction that was introduced into the construction sector, namely Concrete Filled Double Skin Tubular (CFDST) columns is discussed. CFDST columns have several advantages over other columns, which when carefully analysed portrays them as better structural elements compared to structural steel and RC columns.

The main objective of this study is to develop a functional general Finite Element (FE) model that predicts the behaviour and axial load capacity of eccentrically loaded circular CFDST columns. In this study four different column configurations is used to calibrate and verify the accuracy of the FE model, whereas this aspect is lacking in virtually all other research work.

While developing the general FE model, it is observed that some generally accepted parameters of the Confined Concrete Damaged Plasticity (CCDP) model contradict that found in this research. This led to proposed modifications to the magnitude of some of the CCDP parameters. Furthermore, at the end of the study, some general observations were concluded, which led to proposing new standard default values for some parameters in the CCDP model.

OPSOMMING

Kolomme is struktuurelemente wat kragte van die vloer, balke en ander kolomme na die fondament oordra. Kolomme moet dus sterk wees om faling te weerstaan.

Daar is twee (2) soorte kolomme, dws; kort kolomme en lang kolomme. Kort kolomme faal oor die algemeen as gevolg van vergruising as gevolg van die kort lengte. Hul verhouding van effektiewe lengte tot die minste laterale dimensie is minder as 12 en het 'n slankheidsverhouding van minder as 45. Hierdie type kolomme word algemeen net onderwerp aan drukspannings. Inteendeel lang kolomme faal meestal deur te knik en hul verhouding van effektiewe lengte tot die laterale dimensie is groter as 12. Die slankheidsverhouding van lang kolomme is groter as 45 en hierdie kolomme word onderhewig aan druk- en trek spannings.

Verskeie materiale word in die konstruksie van kolomme gebruik, waarvan gewapende beton en struktuurstaal die mees algemeene materiaale is. In hierdie studie word ‘n relatiewe nuwe metode vir die konstruksie van kolomme wat in die konstruksiesektor bekendgestel is bespreek, naamlik; Beton Gevulde Dubbele Vel Buise (CFDST). CFDST-kolomme het verskeie voordele, wat dit ‘n beter konstruksie-elemente maak in vergelyking met struktuurstaal en gewapende beton-kolomme.

Die hoofdoel van hierdie studie is om 'n funksionele algemene Eindige Element (FE) model te ontwikkel wat die gedrag en aksiale lasvermoë van eksentriekse gelaaide sirkel CFDST-kolomme voorspel. Hierdie studie gebruik vier verskillende kolomkonfigurasies om die FE-model te kalibreer en te verifeer om die akkuraatheid van die CFDST te bepaal. Hierdie aspek ontbreek feitlik in alle ander navorsingswerke wat die akkuraatheid van vorige studies bevraagteken.

Tydens die ontwikkeling van die algemene FE-model, is dit waargeneem dat sommige algemeene aanvaarde waardes van die parameters van die “Confined Concrete Damaged Plasticity” (CCDP) model in konflik is met die grootte van die parameters wat uit hierdie navorsing bepaal is. Dit het daartoe gelei vir die voorstel dat die grootte van sommige van die CCDP-parameters verander moet word. Verder is aan die einde van die studie 'n paar algemene waarnemings gemaak, wat gelei het tot die voorstel van nuwe standaardwaardes vir sommige parameters in die CCDP-model.

ACKNOWLEDGEMENTS

Without the following people, I will never ever have been able to make it through to the completion of this research work.

- First of all, I will like to thank the Almighty God for all He has done in my life. Without Him, I will never be anywhere close to whom I am now.

- I will like to thank my parents, brothers and sister who are such a great blessing to me, and who have been able to support me throughout this academic journey.

- My great appreciation to my supervisor Prof Haas, who not only was a mentor and guide, but also a father during difficult moments. I remain grateful for time spent with him and for all his wisdom and guidance.

TABLE OF CONTENTS

LIST OF FIGURES

LIST OF TABLES

CHAPTER 1

INTRODUCTION

Columns are structural elements, which transmit vertical loads from slabs, beams and other columns to the foundation. Conventionally, the main materials used in column construction are reinforced concrete (RC) and structural steel. In this research investigation, a new type of column known as Concrete Filled Double Skin Tubular Column (CFDST) was investigated. CFDST columns are constructed using two hollow steel tubes with the annulus filled with concrete. Various shapes of CFDST columns can be constructed using different hollow steel sections shapes. The focus of this investigation is to determine the behaviour of slender circular CFDST columns subjected to eccentric loading.

From literature, it was observed that an insignificant amount of work was conducted on slender CFDST columns and even less on slender CFDST columns subjected to eccentric loading. CDFST columns are observed to have many advantages compared with the traditional materials used in column construction. The advantages of CFDST columns are;

- Employing modular construction thus significantly increasing the speed of construction,
- The confinement of the concrete results in columns with greater ultimate load carrying capacity,
- The prevention of concrete spalling, is beneficial in seismic prone areas, resulting in greater ultimate loads in columns,
- Enhances damping characteristics and
- Reduces the overall mass of the structure resulting in smaller foundations.

The purpose of this research investigation was to develop a generalised Finite Element (FE) model that accurately predicts the ultimate axial load of CFDST columns subjected to eccentric loading. The generalised FE model was developed using the work of other researchers with specific reference to obtaining accurate concrete confinement models, materials models and interaction

properties. This was necessary as previous researchers who conducted research on CFDST columns either made assumptions that are not validated or used a single experimental column response to calibrate their work without further validation during their investigations. The generalised FE model was validated against various experimental work conducted by Koen (2015). Koen's (2015) experimental work consisted of two column lengths with two cross-sectional properties, resulting in four (4) different column specimens. The generalised FE model was calibrated to one (1) of Koen's (2015) experimental responses, where after the generalised FE model was used to predict the ultimate axial capacity of the other three (3) experimental responses for validation. Thereafter the generalised FE model was there after used to conduct a sensitivity analysis on the inner tube thickness, outer tube thickness, concrete strength, steel strength, column curvature, load eccentricity, support fixity and the concrete damage plasticity (CDP) parameter values (dilation angle, viscosity parameter, flow potential eccentricity, compressive meridian, ratio of compressive strength under biaxial loading to uniaxial compressive strength) to investigate its response on the ultimate load capacity of the CFDST columns when subjected to eccentric loading.

The content layout for this thesis is outlined as:

Chapter 2: A literature review on column and its parameters that significantly affect the axial load capacity of slender CFDST columns.

Chapter 3: Describes the process of developing a generalised FE model to predict the axial load carrying capacity of eccentrically loaded CFDST columns and validating this against Koen's experimental results.

Chapter 4: A sensitivity analysis was conducted on the parameters that may have a significant influence on the axial load capacity of slender CFDST circular columns subjected to eccentric loading.

Chapter 5: A concluding summary and proposals for future research work, which should be conducted that would lead to codified recommendations / implementation are presented.

CHAPTER 2

LITERATURE REVIEW

2.1. INTRODUCTION

Columns are structural elements, which transmit vertical loads from other elements of the structure; i.e. beams, other columns and slabs, through the foundation to the soil. The vertical loads acting on the column are compressive in nature, which can be applied either eccentrically or concentrically.

Concentric loads pass through the centroid of the cross section and do not result in bending moments developing at the ends of the column, whereas, eccentric loads do not pass through the centroid of the cross section and induces bending moments at the ends of the columns. The vast majority of research conducted on slender Concrete Filled Double Skin Tubular (CFDST) columns have only considered concentric loading, Pagoulatou *et al* (2014), Huang *et al* (2010), Hassanein and Kharoub (2014). However, the design codes of practice require a minimum load eccentricity to be applied on the cross-section of the columns. The South African concrete code (clause 4.7.2.3 in SANS 10100-1) requires that the ultimate axial load should act at a minimum eccentricity of 5% times the overall dimension of the column plane of bending under consideration and this eccentricity is required to be less than 20mm. The European code (clause 6.1(4) in EN 1992-1-1) requires that for a cross-section to be loaded by a compression force a minimum eccentricity of $h/30$ but not less than 20mm be used, where h represents the depth (width) of the section.

The American code on the other hand makes use of the ratio of end moments M_1/M_2 for determining the minimum load eccentricity (clause 6.6.4.3 to clause 6.6.4.6.4 in ACI 318-14).

Table 1.1 compares minimum eccentricity results obtained for a 2.5m and 3.5m long column using the SANS (10100-1) code, EN 1992-1-1 and ACI 318-14 codes.

Table 1.1: Difference in minimum eccentricity calculation obtained from different codes

Code	Required	Minimum eccentricity for a 2.5m long column	Minimum eccentricity for a 3.5m long column
SANS (10100-1)	5% of h and < 20mm	8.9mm (∴ use 20mm)	8.9mm (∴ use 20mm)
EN 1992-1-1	h/30 and > 20mm	5.93mm (∴ use 20 mm)	5.93mm (∴ use 20mm)
ACI 318-14	Minimum moment	The minimum load eccentricity is determined based on the ratio of end moments, M1 / M2. The end moments are determined using a lengthy process and therefore will not be elaborated upon.	

From Table 1.1 it is observed that the SANS code predicts a lower calculated minimum load eccentricity than EN 1992-1-1. Yet, the final minimum eccentricity result obtained for the SANS code is 8.9mm while the Eurocode requires a minimum eccentricity to be greater than 20mm. The American code uses the ratio of end moments for obtaining the minimum load electricity, a system different from that adopted by the SANS and Eurocode.

The above code clause comments (clause 4.7.2.3 in SANS 10100-1, clause 6.1(4) in EN 1992-1-1 and clause 6.6.4.3 to clause 6.6.4.6.4 in ACI 318-14) reinforce the point that loads must be applied eccentrically on the column's cross section. This is to account for the imperfection of the load not passing through the centroid of the cross section and also for the initial curvature of the column. Thus, as important as their work (Pagoulatou *et al* (2014); Huang *et al* (2010); Hassanein and Kharoub (2014)) are, it does not conform to codified requirements limiting their research work's implementation in the codes of practice.

Columns can be classified as either short or slender columns. Columns, which fail due to crushing, are regarded as short columns and their strength is governed by the properties of the material and the geometry of the cross-section (Bansal (2010)). Slender columns however, fail due to buckling. Slender columns have a much larger length compared to short columns for the same cross section area (Bansal (2010)). Generally, the degree of slenderness is expressed in terms of the effective slenderness ratio (L / r), where "L" is the effective length of the column, and "r" is the radius of gyration about the weaker axis. The radius of gyration is defined as the square root of the moment of inertia of the cross section divided by the cross-sectional area of the column.

Based on the slenderness ratio, structural steel columns can be classified into 3 categories namely; short steel columns which have a slenderness ratio less than 50, intermediate steel columns with a slenderness ratio between 50 and 200, while slender steel columns have a slenderness ratio greater than 200 (Alys and Ben (1999)).

However, for reinforced concrete (RC) columns, a column is considered short if the ratio of the column's effective length to its least lateral dimension is less than 12, while it is considered slender if its effective length to its least lateral dimension exceeds 12 (Krunal (2020)). These RC columns are classified based on different criteria such as the shape of the cross-section, material of construction, type of loading, slenderness ratio and type of lateral reinforcement. For RC columns, many factors must be considered to determine whether the column is short or slender (Krunal (2020)).

2.2. OTHER TYPES OF COLUMNS

RC and structural steel columns have been extensively used in the construction industry. A significant amount of attention was and still is being devoted to the analysis and design of RC and structural steel columns, to the detriment of other types of columns.

Other types of columns, which could be superior to RC and steel columns, are; steel encased columns, concrete filled steel tubular (CFST) columns and fibre laminate columns. The advantages and disadvantages of some of these columns are discussed in this chapter.

2.2.1. STEEL ENCASED COLUMNS

Steel encased columns have become widely used in the construction of tall buildings during the last two decades (Soliman *et al* (2013)). These columns are increasingly being used in the construction of high-rise buildings and bridge piers (Han *et al* (2014)), and for infrastructure in earthquake prone areas (Karim and Ipe (2016)). These columns have many advantages, as opposed to the conventional columns. According to Ellobody and Young (2006), the advantages of steel encased columns are:

- Higher ultimate load strength

- Full usage of the materials
- Higher stiffness and ductility
- Robustness against seismic loads
- Significant savings in construction time
- Particularly higher fire resistance compared to conventional steel and concrete-filled steel tube columns that require additional protection against fire.

Although steel encased columns have many advantages, they also have disadvantages, such as (Hanswille (2008)):

- High costs for formwork
- Connecting these columns to beams is very difficult and requires challenging solutions
- It is difficult to strengthen the columns
- In special cases, edge protection is necessary

Based on the disadvantages of this type of column, it seems reasonable to assume that this type of columns is not the most suited to be used for the construction of high-rise buildings (buildings higher than 75 feet or 22m).

2.2.2 CONCRETE FILLED STEEL TUBE (CFST) COLUMNS

CFST columns are constructed by filling the void of hollow structural steel sections with concrete as shown in Figure 2.1. CFST column sizes are restricted by the dimensions and shape of the hollow structural steel sections. The properties of the hollow steel sections and concrete; i.e. high strength, ductility, fire resistance and stiffness, economic and rapid construction are utilised to their optimum in the design of CFST columns (Shanmugam and Lakshmi (2001)). The steel tube provides formwork for the concrete and prohibits concrete spalling, while the concrete helps in prolonging local buckling of the steel tube (Schneider *et al* (2004)). CFST columns are commonly utilised in various structures such as bridges, high-rise buildings, subway platforms, etc., as a result of its high strength and outstanding static and dynamic characteristics (Chen and Chen (1973); Tsuda *et al* (1995); Lu and Zhao (2010); Gardner and Jacobson (1967); Lin (1988); Zeghiche and Chaoui (2005)).

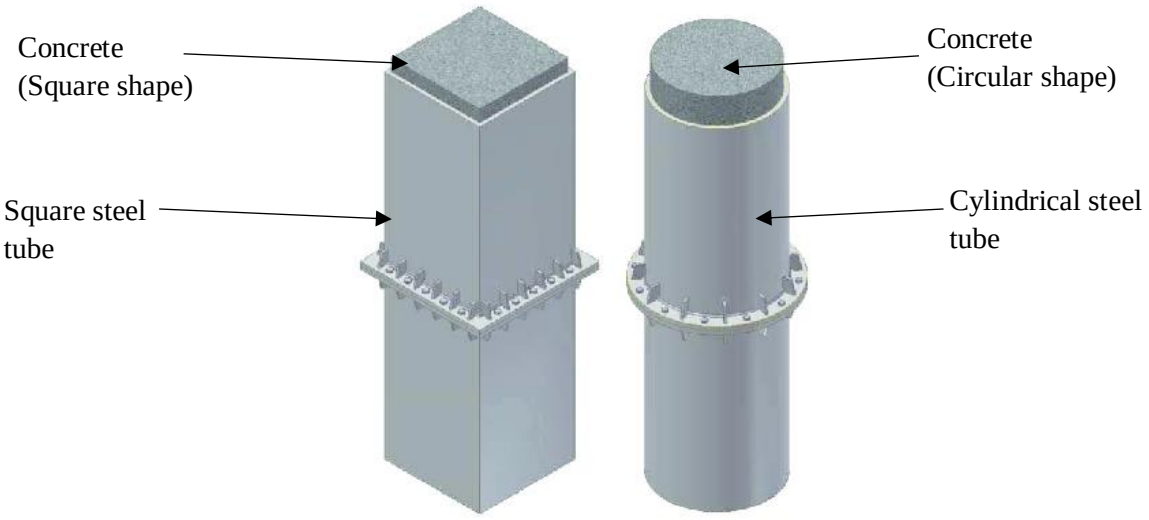

Figure 2.1: Square and circular concrete filled steel tubular columns (Liew (2015))

The advantages of CFST columns are

- CFST columns have high fire resistance. The concrete situated within the steel tube increases the steels thermal resistance thereby increasing the column's fire resistance (Kumari (2018)),
- CFST columns speed up the construction process, since the tube act as formwork thus negating the use of constructing formwork and thereby reducing construction time (Kumari (2018)),
- These columns can also be constructed without internal steel reinforcement, thereby eliminating the need for a steel reinforcing cage (Hanswille (2008)),
- CFST columns can resist significant construction loads prior to the steel tube being filled with concrete (Kumari (2018)),
- CFST columns are significantly stronger and more ductile than normal RC columns for the same cross-sectional area of steel and concrete. This is due to the concrete being confined within the steel tube, resulting in it being more ductile and able to carry more load (Han *et al* (2014)),
- These columns have excellent static and earthquake resistant properties (Kumari (2018)),
- The CFST columns can be modular constructed, placed on-site and be ready to receive its design load.

Though CFST columns have many advantages, they have some disadvantages that limit their use in construction. These disadvantages are due to the lack of construction experience by workers and companies in the use of these types of columns, a lack of understanding of the design provisions and the complex nature of the connections for CFST columns (Schneider *et al* (2004)). Also, connecting these columns to beams is very challenging, especially for circular type cross sections. These disadvantages still influence the use of these columns in the construction industry.

Dundu (2012) observed that the main parameters that influence the axial bearing capacity of CFST columns are the compressive strength of the concrete, the yield strength of the steel tube, the diameter ratio and the length of the column.

It was also discovered that increasing the compressive strength of concrete results in an increase in the load carrying capacity of CFST columns (Han *et al* (2014)). Also due to the presence of the concrete core, the buckling issue related to thin-walled steel tubes is either prevented or delayed. The concrete's infill performance is also improved due to the confinement effect exerted by the steel tube (Kurian *et al* (2016)).

The use of concrete and steel in CFST columns is very efficient with the placement of the steel on the outer perimeter of the column where its tension and bending properties are most effective, since the material lies furthest from the centroid (Kurian *et al* (2016)).

CFST columns unlike RC columns can be classified into 2 groups, namely; short or slender columns. Columns with a slenderness ratio (λ) ≤ 22 are generally considered as short and those with $\lambda > 22$ are referred to as slender (Blake (1986)). Slender columns can further be subdivided into 2 categories; intermediate and very long columns (Hassanein and Kharoob (2014)). Intermediate columns are slender columns, which fail by inelastic buckling (yielding and buckling), while very long columns fail by elastic buckling (Duggal (2014)). For circular CFST columns, the slenderness limit which distinguishes the intermediate length columns from the very long columns can be calculated according to DBJ/T13-51-2010 (2010) as$115/\sqrt{f_y/235}$, where f_y is the yield stress of steel tube in MPa.

It is observed that extensive research on the behaviour of circular and square CFST columns has been conducted (Han *et al* (2014), Farahi *et al* (2016), Johansson (2002), Shanmugam and Lakshimi (2001), etc.). From literature studies, other cross-sectional shapes like polygonal,

elliptical and round-ended rectangular CFST columns have not attracted the same research attention compared to circular and square CFST columns (Shen *et al* (2018), Hassanein and Patel (2018), Yu *et al* (2013), Ren *et al* (2014)).

Some researchers investigated CFST columns using different types of steel and concrete (Xiong *et al* (2017), Tao *et al* (2011), Liang and Fragomeni (2009), etc.). Gopal and Manoharan (2006) conducted an experimental investigation on the behaviour of eccentrically loaded intermediate slender CFST columns using fibre reinforced concrete (FRC) with circular hollow sections (CHS). They showed that using FRC instead of normal strength concrete significantly improves the column's structural behaviour (Gopal and Manoharan (2006)).

It was observed that the slenderness ratio has a significant effect on the strength and behaviour of CFST columns under eccentric loading and that fibre reinforced concrete steel tubular columns have a higher stiffness when compared to normal CFST columns (Karim and Ipe (2016)). High strength concrete and steel were observed by Xiong *et al* (2017) to have advantages for composite members subjected to compression loading in high rise buildings. Therefore, it can be concluded that a significant amount of research needs to be conducted on CFST columns using different materials; i.e. stainless-steel tubes, carbon fibre tubes, high strength concrete, ultra-high strength concrete, foam concrete, etc.

Research work conducted by Elchalakani *et al* (2002) suggests that the solid concrete core in CFST columns does not significantly contribute to the load-carrying capacity of the column. This suggestion gave rise to the concept of replacing part of this confined concrete core with a hollow steel tube. This resulted in a new type of composite columns called Concrete-Filled Double Skin Tubular (CFDST) columns (Elchalakani *et al* (2016)). This type of column was first introduced as a new form of construction for circular cylindrical shells used to resist external pressure in 1978 (Montague (1978)).

2.2.3 CONCRETE-FILLED DOUBLE SKIN TUBULAR (CFDST) COLUMNS

CFDST columns is a relatively new type of structural column that consists of inner and outer hollow structural steel tubes with the annulus filled with concrete. The advantages of the CFDST columns are

- The cavity inside the internal tubes can be used to accommodate utilities like telecommunication lines, drainage pipes, power cables, etc. (Ho and Dong (2014)),
- Lighter weight columns, due to the internal hollow section (Ho and Dong (2014)),
- Have large energy absorption capacity against earthquake loading (Lin and Tsai (2001), Tao *et al* (2004), Wei *et al* (1995), Zhao *et al* (2002)),
- Higher bending stiffness due to the inner tube (Tao *et al* (2004), Wei *et al* (1995), Zhao *et al* (2002)),
- Reducing the self-weight of the structure (Wan and Zha (2016)),
- Large reduction in cross-sectional size compared to RC or structural steel columns (Wan and Zha (2016)),
- Good ductile performance under cyclic loading (Elchalakani *et al* (2002), Aziz *et al* (2017)),
- Reasonable fire resistance due to the concrete protecting the inner tube (Han *et al* (2003), Lu *et al* (2010)),
- Higher energy absorption due to the concrete infill and the deformation of the inner tube (Tao *et al* (2004), Wei *et al* (1995)),
- Higher local buckling stability due to the support offered to the steel by the concrete infill (İpek and Güneyisi (2019)),
- Higher global stability due to increased section modulus (Hassan and Sivakamasundari (2014)),
- High ductility and strength under axial loading (Farajpourbonab (2017)),
- Significant reduction in concrete used in construction due to the hollow section, hence providing a more environmentally sustainable construction option (Elchalakani *et al* 2016),
- Fast track construction since steel tubes act as formwork, thus eliminating the need of adding and removing formwork (Hassanein *et al (*2017)),

- The tubes act as reinforcement, thus no steel cage and steel fixers required, reducing the construction time and cost (Hassanein *et al* (2013)).

Although an insignificant amount of work was conducted on CFDST columns, these columns were observed to be more advantageous as opposed to CFST columns (Aziz *et al* (2017)). Elchalakani *et al* (2002) and Elchalakani *et al* (2016) presented some advantages of CFDST columns over CFST columns, which are

- Lighter weight,
- Greater strength-to-weight ratio,
- Higher bending stiffness,
- Higher axial, flexural and torsional strengths,
- Better cyclic performance,
- Higher fire resistance capacity because the inner tube is protected effectively by the sand-witched concrete under fire conditions,
- Improved strength to weight ratio as a result of replacing the concrete in the centre with an inner steel tube which expands outwards during compression, hence increasing the confining pressure of this lighter column (Han *et al* (2011); Li *et al* (2012)).

The demand for CFDST columns has recently increased and shows a good potential for offshore construction, highway and high bridge pillars construction (Aziz *et al* (2017)).

Unfortunately, CFDST like CFST columns have a major drawback, which is that they are highly susceptible to the influence of poor concrete compaction (Han and Yang (2001)). This deficiency results in honeycombing occurring in the concrete. The interaction between the concrete and steel is thus reduced which results in a weak spot(s) in the CFDST column. This can initiate premature buckling of CFDST columns leading to reduced ultimate loads and could result in significant damage or failure (Han and Yang (2001)).

2.2.3.1 TYPES OF CFDST COLUMNS

The inner and outer tubes can be combined to create different types of CFDST columns as presented in Figures 2.2a to 2.2d. Other combinations are also possible however, these

combinations have not been investigated to date, thus creating additional research opportunities. The shape of the inner and outer tubes has a significant effect on the column's behaviour due to the confinement of the concrete (Hassanein *et al* (2018), Zhao *et al* (2002)). Thus, when the shape of the CFDST column changes, a different formulation of the confined concrete strength is required (Zhao *et al* (2002)).

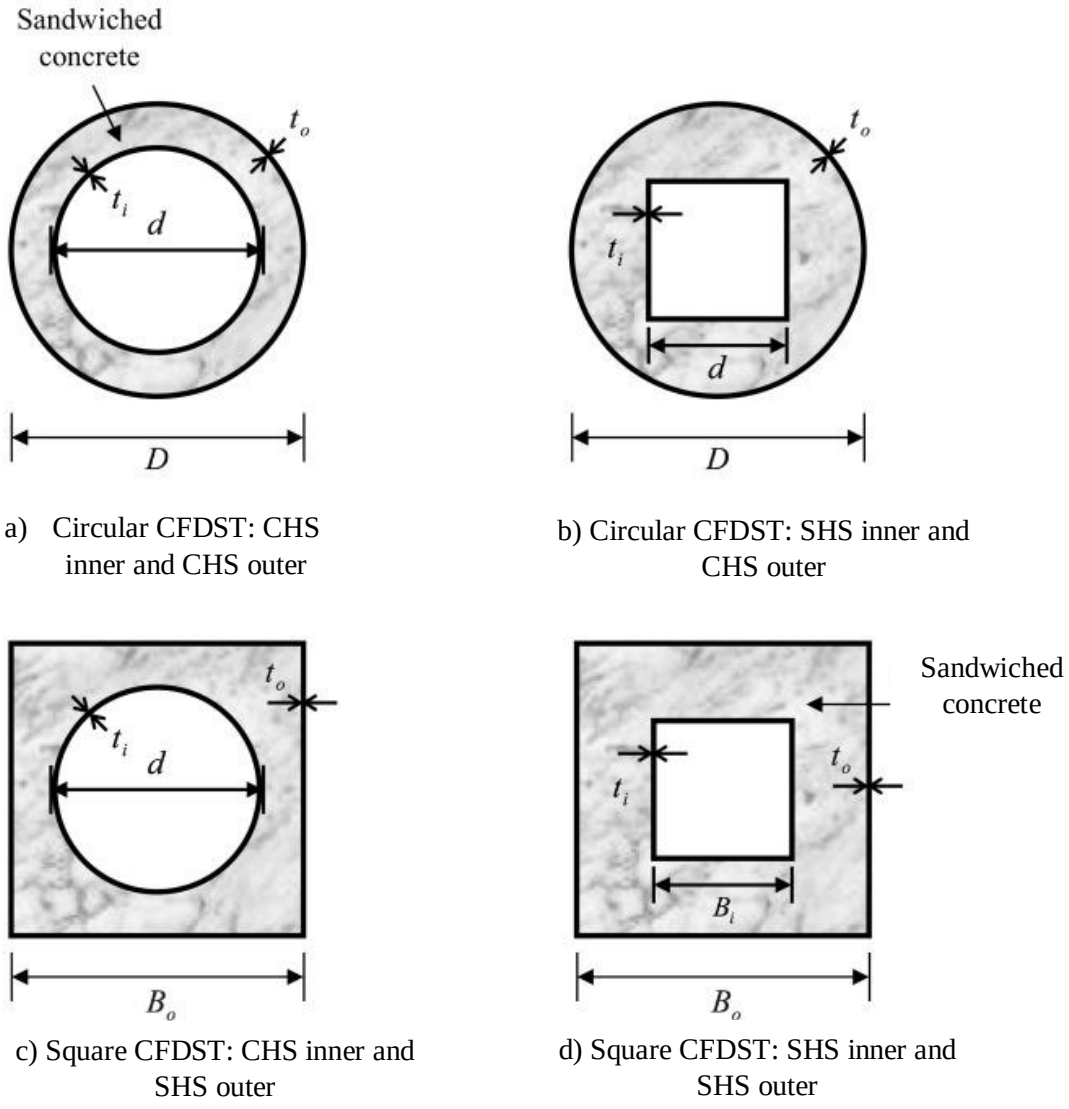

a) Circular CFDST: CHS inner and CHS outer

b) Circular CFDST: SHS inner and CHS outer

c) Square CFDST: CHS inner and SHS outer

d) Square CFDST: SHS inner and SHS outer

Figure 2.2: Different forms of CFDST columns (Hassanein et al (2018))

From the literature reviewed on CFDST columns, it was observed that circular CFDST columns received more research attention compared to other CFDST cross section shapes (Hassanein *et al* (2018), Ibañez *et al* (2017), Liang (2018); Huang *et al* (2010), Hassanein and Kharoob (2014), etc.). This is due to circular CFDST columns exhibiting better confinement effects compared to

other cross sections, resulting in circular CFDST columns being less susceptible to local buckling (Hassanein *et al* (2018)). On the other hand, beam-column joints can be easily constructed and installed for square/rectangular columns as opposed to circular columns (Huang *et al* (2010)). Due to the insignificant amount of research work conducted on square/rectangular CFDST columns, more research work is required to advance the scope and depth of knowledge for these columns.

Table 2.1 highlights the significant difference in research work between circular CFDST columns and other shaped CFDST columns.

Although research on CFDST columns were previously neglected, numerous researchers within the last decade or two conducted significant research on this new type of column. Table 2.1 presents a review of some researchers and their contribution towards developing the CFDST columns.

Table 2.1: Review of research work conducted on CFDST columns within the last 10 years

RESEARCHERS	RESEARCH ANALYSIS
H. Huang, L-H. Han, Z. Tao, X-L. Zhao (2010)	**Objective** To develop a FE model for analysing the compressive behaviour of CFDST stub columns. Two types of columns, concentrically loaded, were analysed, one with a square outer tube and a circular inner tube, and the other made of circular inner and outer tubes. **Column combination tested** Outer tube: Square Hollow section (SHS) and Circular Hollow section (CHS) Inner tube: Circular hollow section (CHS) **Positive aspects** • In general, good agreement between the results predicted by the FE model and the experimental test results obtained. **Concerns** • No variation test conducted on column length. • In practice, most columns are slender whereas this research focuses on stub columns.

	• Load eccentricity is not considered, whereas codes require the axial load to be applied eccentrically.
H-T Hu, F-C Su (2011)	**Objective** To propose and verify a proper FE material constitutive model for circular CFDST stub columns subjected to axial compressive forces using FE modelling. Also, empirical equations for predicting the lateral confining pressure of the concrete core of CFDST columns was proposed. **Column combination tested** Outer tube: CHS Inner tube: CHS **Positive aspects** • The model was verified against 5 experimental specimens by Tao *et al* (2004) and 6 experimental specimens by Zao *et al* (2002). A significant number of experimental studies were used for validating the FE model. • In general, the numerical results obtained shows good agreement with the experimental test results. **Concerns** • The columns in this study are loaded concentrically, but in practice columns are loaded eccentrically. • All experimental columns investigated were short columns, while most of columns used in practice are slender in nature.
M. Pagoulatou, T. Sheehan, X.H. Dai, D. Lam (2014)	**Objective** To conduct a FE investigation to predict the performance of (CFDST) stub columns compressed under concentric axial loads. **Column combination tested** Outer tube: CHS Inner tube: CHS **Positive aspects**

	• The average difference between the FE model results and the experimental tests results varied by 6%. **Concerns** • Stub columns are investigated; however slender columns are mainly used in construction. • Concentric loading is applied, however, in practice columns are loaded eccentrically.
S.A. Karim, B.A. Ipe (2016)	**Objective** To develop a FE model to compare the behaviour of circular, square and rectangular Fibre Reinforced Polymers (FRP) CFDST stub columns subjected to axial compression loading. **Column combination tested** Outer tube: CHS Inner tube: CHS **Positive aspects** • A new type of material, FRP is analysed in this research and used as outer steel tube. This is very novel since most research studies only focused on using carbon steel tubes. • A 5% variation between the experimental and the numerical results was achieved, which shows that there was a good correlation between the experiment conducted and FE models. • Square and rectangular CFDST columns were analysed. This is very rare since majority of research studies focuses on circular CFDST columns. **Concerns** • The FE model was validated by comparing it with just a single experimental column test result. • A graphical representation of the results showing the comparison between the experimental and FE model results is not provided. • The column investigated is a short column, while in practice columns are slender.

	• The columns in this study are loaded axially, but in practice columns are loaded eccentrically.
R.J. Aziz, L.K. Al-Hadithy, S.M. Resen (2017)	**Objective** To analyse the behaviour of circular CFDST stub columns subjected to cyclic and axial compression loads using FE analysis method. **Column combination tested** Outer tube: CHS Inner tube: CHS **Positive aspects** • Good agreement between FE model and experimental test results. • Validated FE model by comparing it with more than one set of experimental columns results as presented by different researchers. **Concerns** • Columns investigated in this study are short, but in practice, the columns used are slender. • The columns in this study are loaded concentrically but in practice, columns are loaded eccentrically.
E. Farajpourbonab (2017)	**Objective** To develop a FE model to analyse the effect of load application type, type of material and geometric parameters on the behaviour of stub CFDST columns subjected to axial loading. **Column combination tested** Outer tube: CHS Inner tube: CHS **Positive aspects** • From literature studies most researchers used ABAQUS for FE modelling. However, in this study ANSYS was used. This is quite novel and will be beneficial to people who are more acquainted with ANSYS software.

	• FE model developed showed good results when compared with that obtained from the experimental column. **Concerns** • The FE model was validated after comparing it to one (1) experimental columns configuration studied by Tao *et al* (2004). This therefore questions the accuracy and reliability of the FE model and its results. • In practice, columns are slender, but the columns tested in this paper are short columns. • Concentric loading is applied to the columns tested, but in practice, columns are loaded eccentrically.
M. Hassanein, M. Elchalakani, A. Karrech, V.I. Patel, B. Yang (2018)	**Objective** To develop a FE model for predicting the behaviour of square CFDST short columns under eccentric loading. **Column combination tested** Outer tube: SHS Inner tube: CHS **Positive aspects** • In this research the columns are eccentrically loaded. • The average difference between the experimental and the FE model results is approximately 1%, which portrays a good correlation between the FE model and experimental results. • From literature studies, it is observed that very little research work was conducted on CFDST square columns, so this research is very novel. **Concerns** • The FE model was not tested for various geometric properties. Hence, the model cannot be validated as a generalised FE model since it was not validated against experimental tests with geometric properties. • Short columns are investigated in this research, however most columns in practice are slender.

M.F. Hassanein, O.F. Kharoob (2014)	**Objective** To develop a FE model for predicting the strength and behaviour of CFDST slender columns under axial compression. It should be noted that stainless steel tubes were used instead of carbon steel tubes. **Column combination tested** Outer tube: CHS Inner tube: CHS **Positive aspects** • Stainless steel tubes were used instead of carbon steel tubes, making the research novel and interesting. **Concerns** • The FE model was compared to the experimental CFDST slender columns tested by Tao *et al* (2004). Yet these columns are made using carbon steel and not stainless steel. Thus, there remains an uncertainty in the reliability of the column FE model.
M. F. Hassanein, M. Elchalakani, V.I. Patel (2017)	**Objective** A FE model was developed for analysing the behaviour of CFDST slender columns, when subjected to axial loading. Note should be taken that stainless steel was used in the place of normal carbon steel throughout. **Column combination tested** Outer tube: CHS Inner tube: CHS **Positive aspects** • From literature, most researchers used carbon steel, thus making this research novel since the tubes tested is stainless steel. • In practice, most columns are slender, and this research focused on slender columns.

	Concerns • Columns are generally loaded eccentrically in practice, but this research focused on columns which are concentrically loaded.
M. L. Romero, C. Ibañez, A. Espinos, J.M. Partolés and A. Hospitaler (2017)	**Objective** An experimental investigation was conducted to analyse the load-bearing capacity of 14 axially loaded slender circular CFDST columns. The effect of normal strength concrete (NSC) and ultra-high strength concrete (UHSC) on these columns were assessed. **Column combination tested** Outer tube: CHS Inner tube: CHS **Positive aspects** • The effect of NSC and UHSC was investigated in this research which is quite novel. • In practice, columns are generally slender, and this research focuses on slender CFDST columns. • An eccentricity of 5mm was considered when applying the load. • A total of 37 experimental tests were conducted on the slender columns in this research, which demonstrates how intensive the study was. **Concerns** • Only one test per column type was conducted, thus rendering the reliability of the results questionable.
C. Ibañez, Manuel L. Romero, A. Espinos, J.M. Portolés, V. Albero (2017)	**Objective** Experimental study investigating the effect of ultra-high strength concrete (UHSC) on slender CFDST columns subjected to eccentric loading. **Column combination tested** Outer tube: CHS Inner tube: CHS **Positive aspects**

	• The experiment was conducted on slender columns, which are eccentrically loaded. The results obtained therefore are a good representative of the behaviour of columns used in practice. • Test conducted on ultra-high strength (UHS) concrete, which is very novel as minimal research was conducted for this configuration. **Concerns** • Only one test per column type was conducted, thus rendering the reliability of the results questionable.
Q. Q. Liang (2018)	**Objective** To obtain a mathematical model that computes the axial load-deflection behaviour of circular CFDST slender columns with high-strength concrete subjected to eccentric loading. **Column combination tested** Outer tube: CHS Inner tube: CHS **Positive aspects** • The mathematical model accurately predicts the experimental behaviour of slender CFDST columns and effectively monitors the load distributions in concrete and steel components of slender CFDST columns. • The proposed material model is an efficient computational and design technique for circular CFDST slender columns. • Most columns in practice are slender columns and this research focuses on slender columns. • The proposed model was tested against 44 experimental tests conducted by Tao *et al* (2004) and Essopjee and Dundu (2015) which shows the model was properly calibrated. **Concerns** • High strength concrete was used in this research. The concern is whether the model will produce the same level of accuracy for normal strength concrete.

	• The effect of concrete creep and shrinkage were assumed not present while developing the model, but in reality, these factors cannot be ignored. • It was assumed that the bond between the sandwiched concrete and the outer and inner steel tubes is perfect, but in reality, this is not the case. Hence this assumption makes efficiency of the model questionable.

From Table 2.1 it can be concluded that within the last 10 years significant research work was conducted on CFDST columns. Yet, the majority of the research work was focused on concentrically loaded CFDST columns. Also, from the reviewed literature, it is observed that minimal work was conducted on eccentric loading of CFDST columns. Only a handful of researchers like Portolés *et al* (2011); Espinós *et al* (2014); Haas and Koen (2014); Ibañez *et al* (2017) successfully conducted research work on eccentrically loaded slender circular CFDST columns.

Therefore, the majority of the previous research work conducted on CFDST columns presented in Table 2.1 do not comply with codified requirements (SANS 10100-1 clause 4.7.2.3 and EN 1992-1-1 clause 6.1(4)). This therefore inhibits the use of CFDST columns in industry. This will remain the case until sufficient research work addresses these concerns to develop codified requirements to ensure the robustness of requirements and confidence of structural engineers.

2.2.3.2 Finite element modelling of CFDST columns

The parameters that are used for the development of the general finite element analysis model together with the review of the work of other authors will be discussed at length in Chapter 3. The reason why this is discussed in Chapter 3 is to highlight the method that will be adopted as well as discuss those adopted by other authors, highlight what the differences are, the best suited method for this analysis and to explain how an approach will be implemented together with its parameters.

From the literature review, it was observed that the most significant parameters, which need to be considered in the development of a FE model, are

- The material models for steel and the confined concrete,

- The element type, mesh density and support boundary conditions,
- The interaction between the steel tube-concrete interface,
- Significant verification after calibration of the FE model prior to conducting sensitivity analysis.

2.2.3.3 Review of work conducted on CFDST's

Table 2.2 represents a brief summary of previous research work conducted on CFDST columns in terms of the various parameters considered by different investigators to show the gaps in the literature in a matrix format.

The investigation aims to develop a generalised FE model to determine the behaviour and ultimate load of slender CFDST columns subjected to eccentric loading. Table 2.2 therefore highlights these three parameters to determine whether any investigator had previously conducted research, which combines all these three parameters. Based on Table 2.2, no investigator had previously considered all these three parameters in their investigation, which thus reinforces the need for this research.

Table 2.2: Analysis of research work conducted on CFDST columns – Main Parameters

		Huang *et al* (2010)	Hu and Su (2010)	Uenaka *et al* (2010)	Han *et al* (2011)	Hu and Su (2011)	Dong and Ho (2012)	Fanggi and Ozbakkaloglu (2013)	Hassanein *et al* (2013)	Pagoulatou *et al* (2014)	Hassanein and Kharoob (2014)	Essopjee and Dundu (2015)	Koen (2015)	Karim and Ipe (2016)	Hassanein *et al* (2017)	Ibañez *et al* (2017)	Farajpourbonab (2017)	Aziz *et al* (2017)	Romero *et al* (2017)	Hassanein *et al* (2018)	Liang (2018)
Shape of steel inner tubes	Circular	√	√	√	√	√	√	√	√	√	√	√	√	√	√	√	√	√	√		√
	Square							√												√	
	Other																				
Shape of steel outer tubes	Circular	√	√	√	√	√	√	√	√	√	√	√	√	√	√	√	√	√	√		√
	Square	√			√															√	
	Other																				
Type of Steel	Carbon steel	√	√	√	√	√	√	√	√	√		√	√			√	√	√	√	√	√
	Stainless steel								√		√				√						
	Other													√							
Type of Concrete	NSC	√	√	√	√	√	√	√	√	√		√	√	√		√	√	√	√	√	
	UHSC							√			√				√	√			√		√
	Other																				
Type of Analysis	Experimental			√	√		√	√				√	√			√			√		
	Numerical analysis		√			√															√
	Finite element analysis	√			√				√	√	√			√	√		√	√		√	
Column Loading	Concentric	√	√	√	√	√	√	√	√	√	√	√		√	√		√	√	√		
	Eccentric												√			√				√	√
Type of column	Stub	√	√	√		√	√	√	√	√		√		√			√			√	
	Slender				√						√	√	√		√	√			√		√

Table 2.3 - Continued: Analysis of research work conducted on CFDST columns – Secondary Parameters

		Huang *et al* (2010)	Hu and Su (2010)	Uenaka *et al* (2010)	Han *et al* (2011)	Hu and Su (2011)	Dong and Ho (2012)	Fanggi and Ozbakkaloglu (2013)	Hassanein *et al* (2013)	Pagoulatou *et al* (2014)	Hassanein and Kharoob (2014)	Essopjee and Dundu (2015)	Koen (2015)	Karim and Ipe (2016)	Hassanein *et al* (2017)	Ibañez *et al* (2017)	Farajpourbonab (2017)	Aziz *et al* (2017)	Romero *et al* (2017)	Hassanein *et al* (2018)	Liang (2018)
PARAMETERS STUDIED	Inner tube diameter							√									√				
	Outer tube diameter					√						√					√				
	Diameter ratio			√					√												√
	Inner tube thickness							√									√			√	
	Outer tube thickness							√									√	√		√	
	Inner tube shape							√													
	Hollow section ratio	√			√					√	√							√		√	
	Diameter to thickness ratio			√	√	√				√											√
	Slenderness ratio										√				√						√
	Steel tube strength	√			√				√	√		√	√				√			√	√
	Concrete strength	√						√	√	√	√				√		√			√	√
	Length of columns					√						√									
	Eccentricity ratio																			√	
	Width to thickness ratio of inner steel tube	√																			

	Concrete-steel contribution ratio	Inner concrete contribution ratio	Steel tube thickness ratio	Load distribution of steel tube and concrete	Concrete confinement	Load application type	Sustained loading
Huang *et al* (2010)							
Hu and Su (2010)					✓		
Uenaka *et al* (2010)							
Han *et al* (2011)							✓
Hu and Su (2011)					✓		
Dong and Ho (2012)							
Fanggi and Ozbakkaloglu (2013)							
Hassanein *et al* (2013)			✓				
Pagoulatou *et al* (2014)							
Hassanein and Kharoob (2014)			✓		✓		
Essopjee and Dundu (2015)							
Koen (2015)							
Karim and Ipe (2016)							
Hassanein *et al* (2017)					✓		
Ibañez *et al* (2017)	✓	✓					
Farajpourbonab (2017)						✓	
Aziz *et al* (2017)							
Romero *et al* (2017)							
Hassanein *et al* (2018)							
Liang (2018)				✓	✓		

A review of Table 2.2 shows some of research work conducted on the CFDST columns in the last 10 years, while indicating the immense voids in certain aspects of research not covered.

From Table 2.2 it is observed that the majority of research work, i.e. 18/20, focused on columns with a circular cross section compared to the other cross-sectional shapes. This shows that other CFDST column cross sectional shapes like octagonal, polygonal, elliptical CFDST columns require research to determine their efficiency in terms of their behavioural response to loading (axial or bending), finite element modelling, fire testing and so much more.

Most of the research work was conducted using carbon steel for the inner and outer tubes (17/20) and (16/20) respectively, and normal strength concrete to fill the gap between the tubes. Thus, a significant amount of research can be conducted on other types of tube materials; i.e. fibre reinforced polymers tubes (FRP), carbon fibre tubes, stainless steel tubes as well as other types of concrete; i.e. foam concrete, light weight concrete, ultrahigh strength concrete, etc.

Eighty percent (16/20) of the research work in Table 2.2 focused on columns which were concentrically loaded, as opposed to 20% (4/20) of the research which focused on eccentrically loaded columns. Of the 20% of research work on eccentrically loaded columns, 75% (3/4) was focused on slender columns. Therefore, a significant amount of investigation is required on eccentrically loaded CFDST columns.

From Table 2.2 it is observed that the concrete and steel tube strength were the most studied parameters (9/20), compared to parametric studies conducted on the inner tube thickness (3/20) and outer tube thickness (4/20), inner tube diameter (2/20) and outer tube diameter (3/20).

From Table 2.2 it is observed that an insignificant amount of research work was conducted on verifying the effect the inner tube shape and the width to thickness ratio of the inner steel tube have on the columns. From the 20 research papers studied on the topic, only one investigation was found to have conducted work on these topics. This shows that these topics have been significantly ignored.

From Table 2.2, it can be concluded that until recently no research work on FE modelling of eccentrically loaded CFDST columns was conducted. Koen (2015) conducted experimental investigations on eccentrically loaded CFDST columns resulting in 4 different geometric columns. The parameters used by Koen (2015) is presented in Chapter 3.

This research work will therefore be conducted using Koen's experimental work as a basis for the calibration and validation of the eccentrically loaded FE CFDST column model that was developed. In order to develop a functional model, a careful study of previous research work on CFDST columns and especially the FE modelling of CFDST columns will be reviewed in Chapter 3.

ABAQUS was used for the development of the FE model. This research was conducted to investigate the effect of eccentric loading on circular CFDST columns through FE analysis and to conduct sensitivity analysis on certain parameters.

2.2.3.3 TESTING EULER THEORY AND SECANT FORMULA FOR DETERMINING COLUMN AXIAL LOAD ON CFDST COLUMNS

Instead of using the FE method for determining the peak axial load of the columns, another method for obtaining the axial load of a column is using the Euler Theory.

When discussing column failure load determination, the topic cannot be discussed without mentioning Euler theory and Secant formula. The Euler theory has proven to be effective in approximating the critical buckling load, P_{cr}, of slender columns subjected to concentric loading. The application of the theory is brief and hence very practical for quickly calculating the column's critical buckling load (P_{cr}).

Equation 2.1 presents the Euler theory as

$$P_{cr} = \frac{\pi^2 EI}{(L_{eff})^2} \qquad \text{(Eq 2.1)}$$

where

E is the Young's Modulus of the material

I is the second moment of inertia of the cross section

L_{eff} is the effective column length defined as the distance between the two zero moment points along the length of the column

The Euler theory cannot be used on columns where the load is eccentrically applied. The Euler theory also assumes that the material is homogeneous. The CFDST columns are not homogeneous and therefore cannot be used.

A method for determining the critical load of a column subjected to eccentric loading can be obtained using the Secant formula as presented in Equation 2.2:

$$\sigma_{max} = \frac{P}{A}\left[1 + \left(\frac{ec}{r^2}\right) sec\left(\frac{L}{2r}\sqrt{\frac{P}{AE}}\right)\right] \quad \text{(Eq 2.2)}$$

where,

σ_{max} = Maximum compressive stress

P = Axial compressive load

A = Cross section area of the member

e = Eccentricity of the load

c = Distance from the centroid to the extreme compression fibre

E = Young's Modulus

I = Second moment of inertia of the cross section

r = Radius of gyration

L = Length of the member.

It can be observed that the Secant formula cannot be used on CFDST columns, because the cross section of CFDST columns is not homogeneous. Also, in CFDST columns there is some interactions between the concrete and the steel, which the Secant formula unfortunately does not take into consideration.

The Secant formula is unable to consider the confinement of concrete, which is a very important parameter in modelling CFDST columns. Also, the Secant formula assume the columns are perfectly straight. These factors significantly influence the ultimate load carrying capacity of the column. Since the Secant formula does not consider these factors, it cannot be used to determine the ultimate load of CFDST columns.

This therefore implies that the only accurate method for determining the ultimate load of CFDST columns is by combining advanced theories developed by some researchers and the FE method that will be discussed in this thesis.

2.3. CONCLUDING SUMMARY

A significant amount of research attention was and is still being devoted to the analysis and design of RC and structural steel columns, compared to other types of composite columns. Some of the other types of columns include steel encased columns, concrete filled steel tubular (CFST) columns, fibre laminate columns and concrete filled double skin tubular (CFDST) columns. These composite columns have advantages when compared to concrete and steel columns.

Due to the numerous advantages portrayed by these composite columns, they are mostly used in the construction of high-rise buildings, construction of bridges and much more. Researchers like Xiong *et al* (2017), Tao *et al* (2011), Liang and Fragomeni (2009), Hassanein and Patel (2018), Yu *et al* (2013), Ren *et al* (2014) and a few others studied the behaviour of CFST columns and it was observed that these columns were among the most beneficial composite columns based on the numerous advantages the columns portrayed.

Yet, it was observed that one of the major disadvantages of using CFST columns is that these columns are very heavy. The process of making CFST columns lighter led to the development of CFDST columns. The hollow middle section of CFDST columns makes them lighter than CFST columns and this gives CFDST columns numerous advantages over CFST columns like, lighter weight, increased earthquake resistance, increased fire-resistant properties, higher bending resistance, etc. These columns are good for offshore construction, highway and high bridge pillar construction as observed by Han and Yang (2001).

An in-depth analysis of previous research work conducted on CFDST columns depicted in Table 2.2, shows that most research work conducted on CFDST columns focused on analysing the behaviour of stub CFDST columns which were concentrically loaded. Very little research work focused on eccentrically loaded CFDST columns, and the least research work was conducted on eccentrically loaded CFDST slender columns. A careful study of some design codes of practice like the South African concrete code (SANS 10100-1 clause 4.7.2.3), the European code (EN

1992-1-1 clause 6.1(4)), and the American code (ACI 316-14 clause 6.6.4.3 to clause 6.6.4.6.4) reveals that a minimum load eccentricity is required to be applied on the cross-section of columns. Therefore, most previous studies conducted on CFDST columns did not conform to the codified requirements which requires that a minimum load eccentricity be applied to the columns. Also, in the construction of buildings and structures, most of the columns are slender and not stub column. This adds to proving that most of the research conducted on CFDST columns did not focus on the practical analysis of these columns in the industry.

Koen (2015) conducted experimental investigations on eccentrically loaded CFDST columns, while Liang (2018) conducted numerical analysis of eccentrically loaded CFDST slender columns. No research study was focused on the development of a FE model which predicts the behaviour of eccentrically loaded CFDST slender columns.

In this research, the effect of eccentric loading on circular CFDST columns is investigated and Koen's experimental work is used as a basis for calibrating and validating the eccentrically loaded FE CFDST column model developed. A sensitivity analysis on certain parameters not observed by some previous researchers as observed in Table 2.2 is conducted at the end of the research.

CHAPTER 3

METHODOLOGY

3.1 INTRODUCTION

Koen (2015) conducted an experimental investigation on CFDST columns subjected to eccentric loading. His experimental work was conducted on four (4) different variations of circular CFDST columns. He conducted three (3) specimen tests per column configuration to ensure accuracy of the experimental test results, which resulted in 12 experimental tests. Except for one (1) specimen, which produced an outlier, the remaining test results per column configuration produced reliable results. The average of each column's configuration was used as the column's response. Koen's (2015) experimental results were used as a reference for calibrating and validating a generalised FE model, which was developed in this research. The FE model was calibrated to one (1) experimental test response, where after it was validated against the remaining three (3) experimental results. A series of adjustments were required to ensure that the FE model's predicted results fall within 5% of all the experimental results. Once the generalised FE model produced discrepancies of less than 5% compared to the experimental results, the generalised FE model was considered calibrated and fully validated to conduct sensitivity analysis on various parameters.

3.2 KOEN'S EXPERIMENTAL RESULTS

Prior to Koen's (2015) work, no known research work was conducted on slender CFDST columns subjected to eccentric loading. It is observed from the literature reviewed that within the last decade, not more than 3 research papers were published on the topic of eccentric loading of slender CFDST columns.

From Table 2.2, it is clear that previous research work on CFDST columns was predominantly focused on the analysis of stub columns and slender columns subjected to concentric loading. This, therefore, does not comply with design requirements, which states "*At no section in a column should the design moment be taken as less than that produced by regarding the design ultimate*

axial load as acting at a minimum eccentricity e_{min} equal to 0,05 times the overall dimension of the column in the plane of bending under consideration. It should not, however, be more than 20 mm." (SANS (10100-1) clause 4.7.2.3). Thus, more research is required on slender CFDST columns subjected to eccentric loading to make codified provisions for these types of columns.

Koen (2015) conducted experimental tests on 4 different CFDST column variations. The two (2) column parameters, which were varied are, the column length and the hollow section ratio (χ) of the columns.

The hollow section ratio can be defined by Equation 3.1 as

$$\chi = \frac{D_i}{(D_o - (2 \times t_o))} \quad \text{(Eq 3.1)}$$

where,

D_i = Outer diameter of the inner tube

D_o = Outer diameter of the outer tube

t_o = Wall thickness of the outer tube

The columns were labeled according to their length and sizes. The shorter columns of 2.5m length was given the prefix **"S"**, while the longer columns of 3.5m length was given the prefix **"L"**. The columns with the smaller hollow section ratio were labeled "**TK**" (thick columns) while those with a larger hollow section ratio were labeled "**TN**" (thin columns). The "TK" columns have a larger concrete cross sectional area than the "TN" columns. For example, STK column refers to the shorter length column with the thicker concrete infill while LTN column refers to the longer column with a thinner concrete cross section. Figure 3.1 shows the different cross sections of the TK and the TN column models.

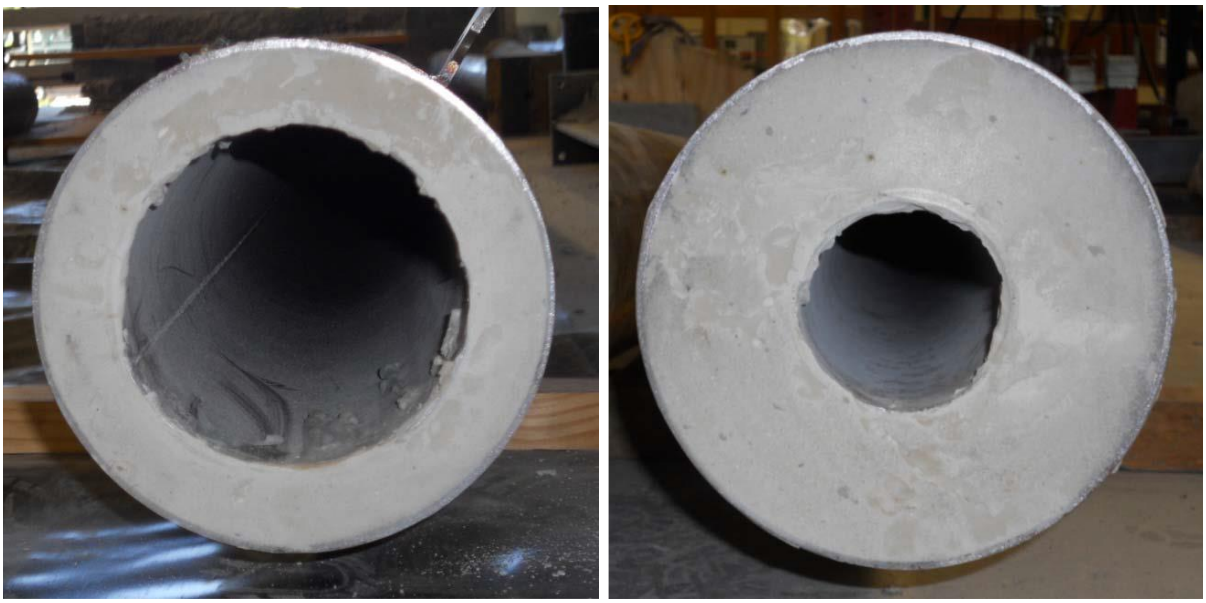

Figure 3.1: The different column models tested by Koen (2015), with the thin concrete annulus (TN) on the left and the thick concrete annulus (TK) on the right (Koen (2015))

Table 3.1 presents a summary of the four (4) different CFDST column's geometric properties including its hollow section ratio.

Table 3.1: Summary of the test specimen geometric properties (Koen (2015))

Specimen identification	Outer CHS (diam x thick) [mm]	Inner CHS (diam x thick) [mm]	Length [mm]	Thickness of Concrete fill [mm]	Hollow-section ratio
LTK	177.8 x 3.0	76.2 x 3.0	3 500	49.3	0.444
LTN	177.8 x 3.0	127.0 x 3.0	3 500	23.9	0.444
STK	177.8 x 3.0	76.2 x 3.0	2 500	49.3	0.739
STN	177.8 x 3.0	127.0 x 3.0	2 500	23.9	0.739

Figure 3.2 shows the 3.5 m column mounted in the Amsler compression-testing machine prior to experimental testing. The load was applied through bearing plates at an eccentricity of 20 mm. The three (3) wooden boxes around the column were attached to linear varying displacement transducers (LVDTs), which measured the transverse deflection of certain points along the length

of the column during the experimental test. A load cell placed at the bottom of the column measured the axial force, while a vertical LVDT measured the vertical displacement of the bottom bearing plate.

Figure 3.2: 3.5m column being tested by Koen (2015)

One of the major problems faced when constructing CFDST columns is ensuring that no honeycombing exists within the column. To resolve this problem, Koen (2015) used self-compacting concrete, as this approach eliminates the need for vibrating the concrete. The self-compacting concrete developed by Koen (2015), had a 28-day cube strength of 52.8 MPa with a standard deviation of 2.5 MPa. The concrete strength was determined from 40 cube tests, which were cured under ideal conditions; i.e. in a water bath.

The inner and outer steel tubes used throughout the experiment have a yield strength of 300 MPa and an ultimate strength of 450 MPa.

To ensure that each test specimen is consistently loaded with the same eccentricity, alignment pins were attached to bearing plates at the top and bottom supports. Pot bearings were used at both ends of the test specimen to simulate pinned end conditions. A total of 3 base plates were used in order to include a pot bearing and a load cell at the bottom configuration. One base plate was required to include the alignment pin at the top support. Figure 3.3 shows the setup of the load cell and bearing plates.

Figure 3.3: Load cell and bearing setup by Koen (2015)

A hydraulic actuator (Amsler), which can either be load or displacement controlled, with a compression capacity of 2 MN was used to conduct the experiment. In order to obtain quasi-static conditions, the tests were conducted using the displacement-controlled option with a rate of 1 mm/min.

To reduce the effect any load misalignment might have on the test results, an eccentricity of 20mm was chosen in accordance with SANS (10100-1), clause 4.7.2.3 requirements.

From observation of the data collected by Koen (2015), it was observed that the horizontal and vertical displacement readings began recording once the column was loaded with approximately 20 kN (preload). The raw experimental results were therefore normalised to account for the preload.

The ultimate loads with the corresponding vertical and lateral midspan displacements are presented in Table 3.2.

Table 3.2: Peak load and corresponding displacement data after normalisation (Koen (2015))

Test specimen	Peak Load [kN]	Vertical Deflection at peak load [mm]	Lateral midspan deflection at peak load [mm]
STK	798	5.9	16.9
STN	736	7.2	21.8
LTK	663	6.0	26.2
LTN	614	6.7	26.8

From Table 3.2, we can observe the following differences between the peak forces for the different type of columns.

- 7.0 % decrease from STK to STN
- 16.6 % decrease from STK to LTK
- 7.7 % decrease from LTK to LTN
- 17.2 % decrease from STN to LTN
- An average strength reduction of 7.35% is observed from the thick annulus (TK) columns to the thin annulus (TN) columns.
- An average strength reduction of 16.9% from the short (S) columns to the long (L) columns.

If we consider Euler critical load theory, $P_{cr} = \frac{\pi^2 EI}{{L_{eff}}^2}$, we observe a reduction of 50% in the critical load when all the parameters remain constant except for changing the length, i.e. when length changes from 2.5 m to 3.5 m. This however does not conform to the results of the experimental tests, which shows a reduction of 16.9% when the lengths are changed from 2.5 m to 3.5 m. The interaction between the tubes and the concrete has a substantial effect on the ultimate load carrying capacity of the columns. Based on the experimental results obtained, it confirms that the Euler theory cannot be used to determine the ultimate load of CFDST columns.

3.3 DEVELOPMENT OF GENERALISED FE MODEL

From the literature reviewed, it was observed that different FE techniques were used by Huang *et al* (2010); Hu and Su, (2011); Hassanein *et al* (2013); Pagoulatou *et al* (2014); and Liang (2018); in examining the strength and behaviour of circular CFDST columns. Yet, none of these studies focused on modelling eccentrically loaded slender CFDST columns. Various researchers used a variety of modelling techniques and in some cases different magnitudes of the parameters in their development of their FE model.

Most researchers, like Huang *et al* (2010), modelled the steel tubes of CFDST columns with shell elements (S4R), while the concrete core and end-plates were modelled with 8-node brick elements (C3D8R). It was observed that most researchers used shell elements (S4R) to model the steel tubes. This is to capture the outwards local modes induced from the lateral expansion of the infilled concrete. Other researchers, like Aziz *et al* (2017) used an 8-node hexahedron continuum shell element (SC8R) with reduced integration to model the steel tubes. The advantage of using reduced integration is that it reduces the analysis time and also provides good approximation to real-life behaviour (ABAQUS (2014)). These researchers used ABAQUS to conduct their numerical modelling.

Unlike previous researchers, Hassanein *et al* (2018) used solid element (C3D8) to model the steel tubes and the concrete. From research conducted by Hassanein *et al* (2018), Dai and Lam (2010) and Dai *et al* (2014), it was observed that thin-walled steel tubes in CFST columns are mostly discretized by shell elements to capture the outwards local buckling modes induced from the lateral expansion of infilled concrete. It was however observed that the size (height and length) of these shell elements are approximately 3 to 5 times larger than the tube thickness, hence affecting the discretization of the surfaces especially the interaction between the steel tube and concrete core. Solid element (C3D8R) was observed to better capture both the deflected shape of steel tubes and effective mesh at the contact surface (Dai and Lam (2010) and Dai *et al* (2014)). Hassanein *et al* (2018) further observed that replacing the tube's shell elements with solid elements resulted in an insignificant increase in computational time.

The above observations made by Hassanein *et al* (2018), Dia and Lam (2010) and Dai *et al* (2014) demonstrate the benefits of using solid elements for modelling both the steel and the concrete as opposed to using shell elements as presented by previous researchers. From the above

observations, it was decided that for this research, the steel tubes and the concrete will be modelled using the eight-node solid element (C3D8R) with reduced integration.

3.3.1 Analysis Type

There are two options, which can be used to model CFDST columns in ABAQUS, i.e. a static general analysis approach or a buckling analysis approach. In the static general procedure, the numerical analysis is simulated by applying a force or displacement boundary condition to the column. The approach will yield the necessary output as requested in ABAQUS, ranging from forces, displacements, stresses to strains. In the buckling analysis, a linear perturbation analysis is performed to determine the eigenvalues of the column (buckling shape), which is then used in the risks analysis to obtain the same data / information as requested in the static procedure. In this analysis no force or displacement boundary condition is applied to the column. Researchers are generally silent on which analysis technique was used.

Based on preliminary analysis work conducted by Prof Trevor Haas (personal communication, September 18, 2018), it was concluded that the two analysis methods using the same geometric and material properties yield results within 3% of each other. The analysis time of both methods differed insignificantly to conclude which method is better. Therefore, based on personal communique with Prof Trevor Haas (personal communication, September 18, 2018), it was decided to use the static analysis approach to conduct the numerical analysis in ABAQUS.

3.3.2 Interaction properties

Since CFDST columns consist of an outer tube, a concrete core and an inner tube, the properties in the contact formulation between these material surfaces must be correctly defined to yield accurate results. Thus, two contact formulations are required, namely, the outer surface of the concrete core and the inner surface of the outer tube as well as the inner surface of the concrete core and the outer surface of the inner tube. The contact formulation must be defined for the normal and tangential directions.

Previous researchers used a “Hard” contact pressure overclosure relationship together with the default constraint enforcement method for normal behaviour. For the tangential behaviour, researchers used a penalty formulation together with a friction coefficient of 0.25 or 0.3 (Hu and Su (2011), Hassanein and Kharoob (2014), Aziz *et al* (2017), Pagoulatou *et al* (2014)). The term

"normal behaviour" as used in ABAQUS refers to the pressure developed between the surfaces of the concrete and steel tubes while the "tangential behaviour" refers to the extent of friction and the occurrence of slippage between the concrete and steel surfaces as a result of high shear stresses (Pagoulatou *et al* (2014)).

A "hard" contact pressure-overclosure minimizes the penetration of the slave surface into the master surface at the constraint locations. This does not allow the transfer of tensile stresses across the interface. A "hard" contact pressure-overclosure model in the normal direction is used in order to simulate the bond between the external tube or the internal tube and the sandwiched concrete of the CFDST columns.

Since simulating ideal friction behaviour is very difficult, ABAQUS uses the penalty friction formulation with an allowable "elastic slip" for simulating friction. This "elastic slip" represents the small amount of relative motion between the surfaces, which occurs when the surfaces should be sticking to each other (ABAQUS (2014)).

In order to effectively implement the contact formulation, researchers also used a surface-to-surface contact formulation (ABAQUS (2014)). The surface-to-surface contact formulation is used to model contact interaction between the concrete and steel surfaces. These surfaces are defined as master or slave surfaces; with the inner steel tube's outer surface and outer steel tube's inner surface set as the master surfaces, while the concrete core's inner and outer surfaces are set as the slave surfaces. The main difference between the master and the slave surface as stated by ABAQUS standard user manual (2014) is that the master surface can penetrate the slave surface, but the slave surface cannot penetrate the master surface. Since CFDST columns are a composite made of 2 steel tubes with sandwiched concrete in-between, 2 interactions will therefore be required when modelling the columns.

3.3.3 Loading and Boundary conditions

The columns will be analysed using the General Static approach. This approach can either be conducted through a load or displacement-controlled analysis. Most researchers like Pagoulatou *et al* (2014) and Aziz *et al* (2017) used a displacement-controlled loading system to model the loading of the CFDST columns. Other researchers, like Hu and Su (2010) simulated their CFDST columns through a compressive load.

It was observed that different researchers used different approaches to establish the boundary conditions. Some researchers like Pagoulatou *et al* (2014) used the nodes of the endplates to define the boundary conditions. Others like Hassanein *et al* (2018) used fixed reference points at the top and bottom of the columns for defining the boundary conditions.

From the results obtained by these and other researchers, it is observed that any of the above approaches for defining the loading and boundary conditions can be used and will yield accurate results if implemented correctly.

In this research, the displacement-controlled loading system was implemented as the loading mechanism. Two boundary conditions were defined. The first labeled as "RP Bottom" was defined 100 mm below the column and 20 mm off centre from the positive x-axis. The 100 mm offset is to account for the base plates and pot bearings at the top and bottom of the column. All three translational degrees of freedom (DOF) at this point were initially restrained in order to simulate a pin connection. At the start of the simulation, the translational DOF in the longitudinal direction of the column was released to allow the compressive displacement control boundary condition of 20 mm to be engaged. The second boundary condition labeled "RP Top" was set 100mm above the column and 20mm off centre from the positive x-axis. All three translational DOF were restrained for this reference point. Only the rotational DOF about the "*y*" axis, i.e. along the length of the column, was activated to prevent numerical instability. Figure 3.4 shows the location of these boundary conditions on the CFDST column, with the *x*, *y* and *z* axis defined.

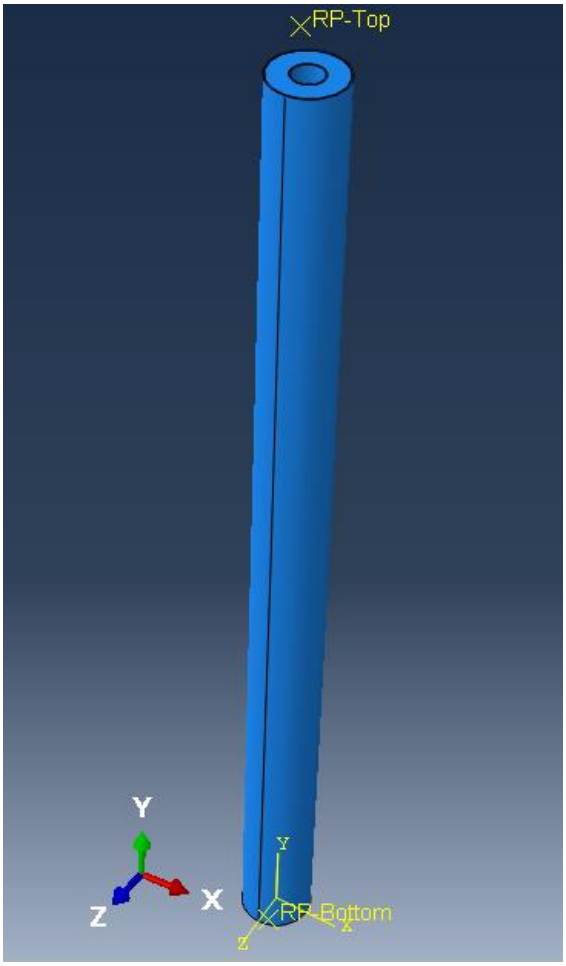

Figure 3.4: Boundary conditions defined on the CFDST LTK column model

The top and bottom surfaces of the column (tubes and concrete surfaces) were restrained to the respective RP's. Thus, the RP's acts as the master point while the surfaces act as the slave. Thus, the DOF of the column's top and bottom surfaces are dependent on the translational and rotational behaviour of the RPs.

3.3.4 Material properties

CFDST columns are a composite made of concrete sandwiched between two steel tubes. The material properties section therefore will describe the methods used in modelling the confined concrete and the steel tubes.

3.3.4.1 Confined concrete modelling

The tubes of the column confine the concrete core, resulting in increased strength of the concrete. Thus, it is important that the confinement be considered in the development of the generalised FE model. Various researchers use different methods in developing the confined concrete model.

Two approaches for modelling the confined concrete will be compared in this study. The Pagoulatou *et al* (2014) approach will be compared to the Hassanein *et al* (2013) approach for modelling the confined concrete. Some observations are made of the two approaches at the end of this section.

3.3.4.1.1 Pagoulatou Approach

The confined concrete model used by Pagoulatou *et al* (2014) is hereafter referred to as the Pagoulatou's approach in this research. This model was used in this study for modelling the confined concrete of the CFDST columns. A narrative of the steps used in this research for developing the confined concrete FE model with Pagoulatou's approach is now described.

3.3.4.1.1.1 Obtaining the Confined Concrete Compressive Strength (f_{cc})

After casting and testing 40 concrete cubes in temperature-controlled curing baths, Koen (2015) obtained an average cube strength, f_{cu}, of 52.8 MPa with a standard deviation of 2.5 MPa.

The unconfined concrete cylinder compressive strength f_c can then be obtained using Equation 3.2.

$$f_c = 0.8 \times f_{cu} \qquad \text{(Eq 3.2)}$$

The value of f_c obtained for this research work was 42.24 MPa.

Having obtained the value of f_c, the magnitude of the confined concrete compressive strength, f_{cc}, can be obtained using Equations 3.3, which was proposed by Mander *et al* (1988).

$$f_{cc} = f_c + k_1 f_l \qquad \text{(Eq 3.3)}$$

where,

- k_1 is a constant with a numerical value set to 4.1 (Richart *et al* (1928)).

- f_l is the lateral confining pressure obtained as the absolute minimum magnitude of Equations 3.7 to 3.9.

The resultant f_{cc} was obtained as 54.56 MPa for the thick (TK) columns and 46.29 MPa for the thin (TN) columns.

3.3.4.1.1.2 Confined Concrete Strain

The magnitude for the corresponding confined concrete strain, ε_c, varies from 0.002 to 0.003 depending on the effective compressive strength of the concrete. In this case, it is set as 0.003 and the confined concrete strain, ε_{cc}, is obtained using Equation 3.4 proposed by Mander *et al* (1988):

$$\varepsilon_{cc} = \varepsilon_c \left(1 + k_2 \frac{f_1}{f_c}\right) \quad \text{(Eq 3.4)}$$

where,

- k_2 is a constant with a numerical value set to 20.5 (Richart *et al* (1928)).

Figure 3.4 presents the curves for predicting the pre-yield and post-yield behaviour of unconfined and confined concrete under axial compressive load proposed by Mander *et al* (1988) and used by Pagoulatou *et al* (2014). From Figure 3.4, we notice the significant increase in the strength of the concrete when subjected to confinement. Some of the parameters shown in Figure 3.5 are defined in Equations 3.2 to 3.4, while others are defined in the next section.

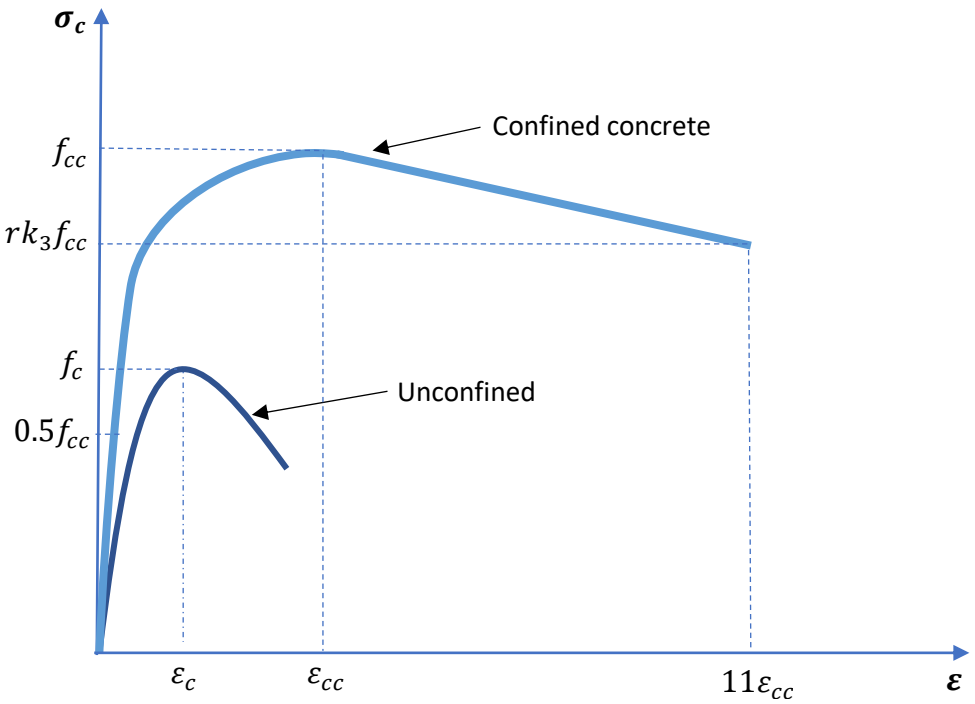

Figure 3.5: Stress strain graph of confined and unconfined concrete (Hu and Su (2011))

3.3.4.1.1.3 Modulus of Elasticity (E_{cc}) of Confined Concrete

The Modulus of Elasticity, $E_{cc,}$ is important in modelling the confined concrete. The recommendations in ACI Committee 318 was used to determine the initial modulus of elasticity, E_c, of the concrete. In order to obtain the modulus of elasticity of confined concrete, E_{cc}, the same formula is applied, but in this case the compressive strength of concrete, f_c, is replaced with the compressive strength of confined concrete, f_{cc}, as shown in Equations 3.5 and 3.6 (ACI 318-14).

$$E_c = 4700\sqrt{f_c} \quad \text{(Eq 3.5)}$$

$$E_{cc} = 4700\sqrt{f_{cc}} \quad \text{(Eq 3.6)}$$

Note, f_c should be in MPa.

The Poisson's ratio, μ_c, of concrete was also determined according to the recommendations in the ACI Committee 318 as $\mu_c = 0.2$.

The confining pressure around the concrete, f_l, is obtained from Equations 3.7 to 3.9 as proposed by Hu and Su (2011).

$$fl_1 = 8.525 - 0.166\left(\frac{D_o}{t_o}\right) - 0.00897\left(\frac{D_i}{t_i}\right) + 0.00125\left(\frac{D_o}{t_o}\right)^2 + 0.00246\left(\frac{D_o}{t_o}\right)\left(\frac{D_i}{t_i}\right) - 0.0055\left(\frac{D_i}{t_i}\right)^2 \geq 0$$

(Eq 3.7)

$$\frac{fl_2}{f_{yi}} = 0.01844 - 0.00055\left(\frac{D_o}{t_o}\right) - 0.0004\left(\frac{D_i}{t_i}\right) + 0.00001\left(\frac{D_o}{t_o}\right)^2 + 0.00001\left(\frac{D_o}{t_o}\right)\left(\frac{D_i}{t_i}\right) - 0.00002\left(\frac{D_i}{t_i}\right)^2 \geq 0$$

(Eq 3.8)

$$\frac{fl_3}{f_{yo}} = 0.01791 - 0.00036\left(\frac{D_o}{t_o}\right) - 0.00013\left(\frac{D_i}{t_i}\right) + 0.00001\left(\frac{D_o}{t_o}\right)^2 + 0.00001\left(\frac{D_o}{t_o}\right)\left(\frac{D_i}{t_i}\right) - 0.00002\left(\frac{D_i}{t_i}\right)^2 \geq 0$$

(Eq 3.9)

where

- f_{yi} is the yield stress of inner steel tube
- f_{yo} is the yield stress of the outer steel tube
- fl represents the confining pressure around the concrete core.
- The magnitude of fl_1, fl_2, and fl_3 are obtained from Equations 3.7 to 3.9.

A magnitude of fl is then obtained, with fl being the absolute minimum magnitude of the three equations, i.e. fl_1, fl_2, and fl_3.

The stress-strain relationship of concrete is obtained using Equation 3.10, which was proposed by proposed by Saenz *et al* (1964). This equation is adopted widely and helps in predicting the nonlinear behaviour of concrete.

$$\sigma_c = \frac{E_{cc}\varepsilon}{1+(R+R_E-2)\left(\frac{\varepsilon}{\varepsilon_{cc}}\right)-(2R-1)\left(\frac{\varepsilon}{\varepsilon_{cc}}\right)^2+R\left(\frac{\varepsilon}{\varepsilon_{cc}}\right)^3} \quad \text{(Eq 3.10)}$$

$$R = \frac{R_E(R_\sigma-1)}{(R_\varepsilon-1)^2} - \frac{1}{R_\varepsilon} \quad \text{(Eq 3.11)}$$

$$R_E = \frac{E_{cc}\varepsilon_{cc}}{f_{cc}} \quad \text{(Eq 3.12)}$$

From research conducted by Hu and Schnobrich (1989), they obtained R_σ and R_ε as a constant of 4.

- $R_\sigma = 4 \; and \; R_\varepsilon = 4$

rk_3f_{cc}, is the ultimate stress point of the concrete stress-strain curve, which is obtained from Equation 3.13. Its corresponding strain magnitude is obtained from $11\varepsilon_{cc}$.

The magnitude of k_3 can be obtained as

$$k_3 = 1.73916 - 0.00862\left(\frac{D_o}{t_o}\right) - 0.04731\left(\frac{D_i}{t_i}\right) + 0.00036\left(\frac{D_o}{t_o}\right)^2 + 0.00134\left(\frac{D_o}{t_o}\right)\left(\frac{D_i}{t_i}\right) - 0.00058\left(\frac{D_i}{t_i}\right)^2 \geq 0 \quad \text{(Eq 3.13)}$$

The value *r* is a reduction factor.

- r = 1.0 for concrete strength ≤ 30 MPa (Giakoumelis and Lam (2004)).
- r = 0.5 for concrete strength ≥ 100 MPa (Mursi and Uy (2003)).
- Therefore, for concrete strength in between 30 and 100 MPa, the value of r is obtained through linear interpolation.

The yield stress and cracking strain of the concrete are required as input parameters in ABAQUS.

The tensile yield stress (f_t) of the concrete is obtained from Equation 3.14

$$f_t = 0.6\sqrt{\gamma_c \times f_c} \quad \text{(Eq 3.14)}$$

where

$$\gamma_c = 1.85 D_c^{-0.135} \quad (0.85 \leq \gamma_c \leq 1.0) \qquad \text{(Eq 3.15)}$$

$$D_c = D_o - 2t_o \qquad \text{(Eq 3.16)}$$

The value γ_c incorporates the effect of the column size and was proposed by Liang (2018).

The confined concrete tensile cracking strain ε_{crack} is 10% of the confined concrete strain ε_{cc} as expressed in equation 3.17 (Liang (2018)).

$$\varepsilon_{crack} = 0.1 \times \varepsilon_{cc} \qquad \text{(Eq 3.17)}$$

3.3.4.1.1.4 Concrete Damage Plasticity (CDP) parameters

The CDP model describes the plasticity of concrete by adopting a unique yield function with the non-associated flow and a Drucker-Prager hyperbolic flow potential function. Due to the difference in strength and failure mechanisms in both tension and compression, independent uniaxial stress-strain relations for concrete in compression and tension are required (ABAQUS (2014)).

The inelastic behaviour of concrete is well represented by the CDP model since it uses the concepts of isotropic damaged elasticity in combination with isotropic tensile and compressive plasticity. Hence, the tensile cracking and compressive crushing can clearly be observed using the CDP model (ABAQUS (2014)).

Therefore, the behaviour of plain or reinforced concrete elements subjected to both static and dynamic loads are provided for by the CDP model in ABAQUS (2014).

In ABAQUS, there are various input parameters, which need to be defined in the concrete damaged plasticity section. These parameters are the dilation angle, Ψ, flow potential eccentricity, e, the compressive meridian, K_c, ratio of the compressive strength under biaxial loading to uniaxial compressive strength, f_{bo}/f_c, and the viscosity parameter, μ.

Han *et al* (2010) proposed the use of constant values for the CDP parameters. These were 30°, 0.1, 0.667 and 1.16 to represent Ψ, *e*, K_c and f_{bo}/f_c. This notion of using constant values for the CDP parameters was refuted by Tao *et al* (2013) who rather reported that constant values may not be suitable for use in some cases and the complex nature of passively confined concrete need to be considered.

3.3.4.1.1.4.1 Dilation angle (Ψ)

The dilation angle is a material parameter determined from experimental data, which is required by ABAQUS to define the plastic flow potential. Magnitudes of 20° and 30° are predominantly used by most researchers as the dilation angle (Aziz *et al* (2017), Hassanein and Kharoob (2014), Hassanein *et al* (2017)). Tao *et al* (2013) suggest that the dilation angle for circular CFDST columns can be obtained using Equation 3.18.

$$\Psi = \begin{cases} 56.3(1-\xi_c) & for\ \xi_c \leq 0.5 \\ 6.672e^{\frac{7.4}{4.68+\xi_c}} & for\ \xi_c \geq 0.5 \end{cases} \quad \text{(Eq 3.18)}$$

where ξ_c = confinement factor

$$\xi_c = \frac{A_s f_y}{A_c f_c} \quad \text{(Eq 3.19)}$$

$$A_s = \left(\frac{\pi {D_o}^2}{4} - \frac{\pi {D_{co}}^2}{4}\right) + \left(\frac{\pi {D_{ci}}^2}{4} - \frac{\pi (D_i - 2t_i)^2}{4}\right) \quad \text{(Eq 3.20)}$$

$$A_c = \left(\frac{\pi {D_{co}}^2}{4}\right) - \left(\frac{\pi {D_{ci}}^2}{4}\right) \quad \text{(Eq 3.21)}$$

where:

D_i and D_o are the outside diameters of the inner and outer tubes

D_{ci} and D_{co} are the inner and outer diameters of the confined concrete

The location of D_o, D_i, D_{co} and D_{ci} are shown in Figure 3.6.

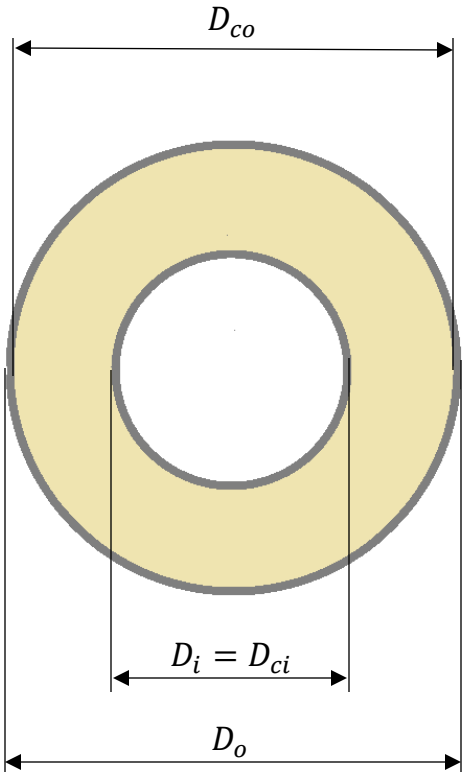

Figure 3.6: Circular CFDST column cross-section

3.3.4.1.1.4.2 Ratio of compressive strength under biaxial loading to uniaxial compressive strength (f_{bo}/f_c)

A magnitude of 1.16 has generally been used in research work to represent the value of f_{bo}/f_c. Papanikolaou and Kappos (2007) proposed Equation 3.22 to effectively determine this ratio.

$$\frac{f_{bo}}{f_c} = 1.5(f_c)^{-0.075} \quad \text{(Eq 3.22)}$$

3.3.4.1.1.4.3 Ratio of the second stress invariant on the tensile meridian to that on the compressive meridian (K_c)

This parameter is required for determining the yield surface of concrete plasticity model. K_c is defined as the ratio of the distances between the hydrostatic axis and the compressive and tensile meridians. Figure 3.7 obtained from the ABAQUS documentation (SIMULIA 2014) portrays the deviatoric cross section of this failure surface as defined in the CDP model.

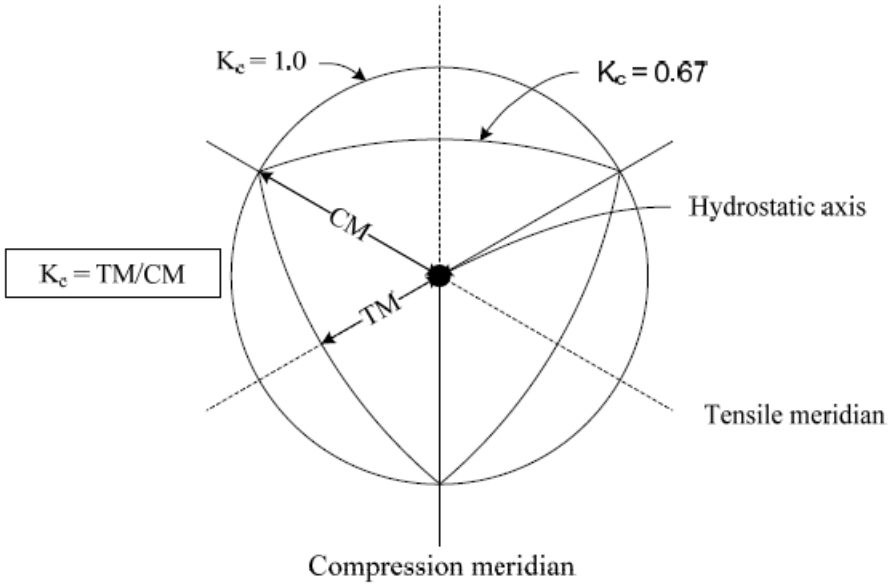

Figure 3.7: Cross-section of failure surface in CDP model as displayed in SIMULIA (2014)

The magnitude of K_c is generally assumed as 0.667 (Hassanein and Kharoob (2014), Aziz *et al* (2017)). However, Yu *et al* (2010) proposed Equation 3.23 to determine K_c as

$$K_c = \frac{5.5 f_{bo}}{3 f_c + 5 f_{bo}} \quad \text{(Eq 3.23)}$$

Substituting Equation 3.22 into Equation 3.23, yields Equation 3.24.

$$K_c = \frac{5.5}{5 + 2(f_c)^{0.075}} \quad \text{(Eq 3.24)}$$

In ABAQUS, K_c has a default value of 0.667.

3.3.4.1.1.4.4 Flow potential eccentricity (e)

This parameter changes the shape of the plastic potential meridian's surface in the stress space. The flow potential eccentricity e is defined as being a small positive value, which expresses the rate of approach of the plastic potential hyperbola to its asymptote. The form of a hyperbola is assumed by the plastic potential surface when in the meridional plane of the CDP model. From research work conducted by Tao *et al* (2013), it was observed that a default value of 0.1 could be

used as the flow potential eccentricity. The plastic potential surface in the meridional plane is presented in Figure 3.8.

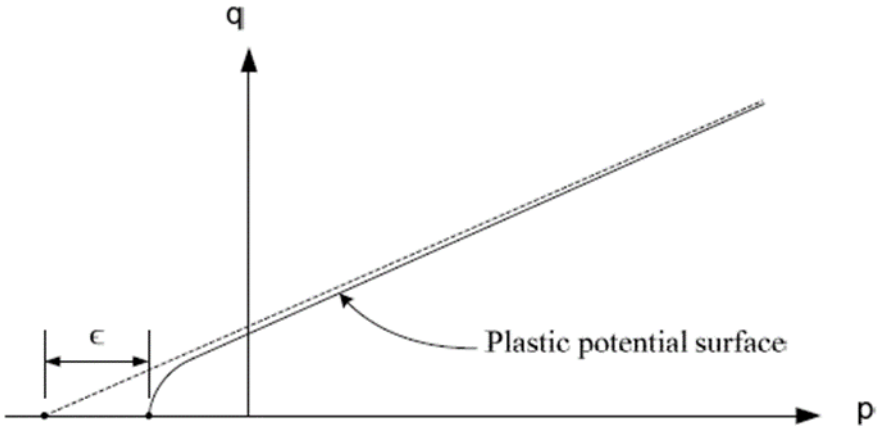

Figure 3.8: Depicts hyperbolic plastic potential surface in the meridional plane as obtained from the ABAQUS documentation (SIMULIA 2014).

3.3.4.1.1.4.5 Viscosity parameter

The viscosity parameter is used to allow the model to slightly exceed the plastic potential surface in certain insufficiently small solution steps. This means that this parameter is used for the viscoplastic regularization of the constitutive equations. Tao *et al* (2013) proposed a default value of zero (0) for the viscosity parameter.

There are other methods, which can be used for modelling confined concrete apart from the approach used by Pagoulatou *et al* (2014). In this research study, one of the other approaches for modelling the confined concrete that was examined is that used by Hassanein *et al* (2013) termed here as Hassanein approach.

3.3.4.1.2 Comparison of Hassanein and Pagoulatou's confined concrete model approaches

Besides the approach used by Pagoulatou *et al* (2014), Hassanein *et al* (2013) also modelled the confined concrete using a different approach. The confined concrete stress strain graph for the STK model using both Pagoulatou and Hassanein is presented in Figure 3.9. The linear region of

both responses is virtually identical. However, the approach used by Hassanein portrays the confined concrete as having a relatively short inelastic behaviour and strain after yielding, while Pagoulatou's approach portrays the concrete to have a very significant inelastic behaviour and a larger strain after yield.

Initial FE analysis using both approaches yielded an insignificant difference in response. It was decided to use Pagoulatou's approach in the development of the generalised FE model.

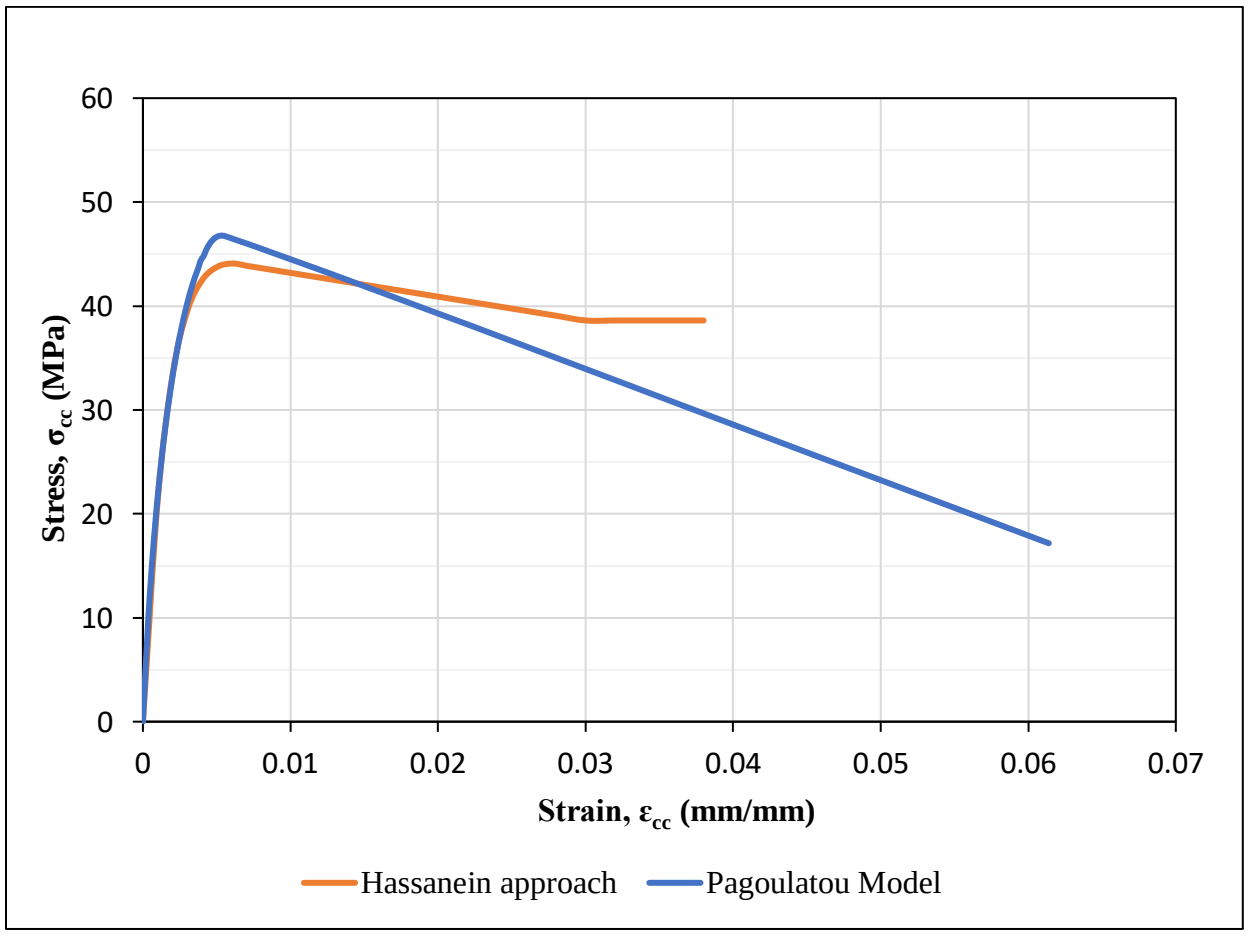

Figure 3.9: Confined concrete stress strain graph modeled using Hassanein and Pagoulatou approaches

3.3.4.2 Steel Modelling

The steel stress-strain curve was simulated using a bilinear kinematic model. From literature studies, it is observed that most research studies conducted on CFDST columns make use of this

approach for modelling the steel tubes (Pagoulatou *et al* (2014), Hassanein *et al* (2013), Hassanein *et al* (2014)).

In ABAQUS, steel is treated as an elastic material up to the point at which it yields and then as a plastic material from its yield point to its final strain which is considered as 3%. The material model requires parametric inputs such as the yield stress, f_y, the Young's Modulus, E_s, the Poison's ratio, μ, and plastic behaviour which will help define the overall steel behaviour. The steel constitutive model is used to obtain the stress-strain relationship to simulate the behaviour of the steel tubes. This constitutive model is developed with the equations proposed by Han and Huo (2003):

These equations are:

$$\sigma_s = E_s(T) \times \varepsilon \qquad for\ \varepsilon \leq \varepsilon_{sy}(T) \tag{Eq 3.25}$$

$$\sigma_s = f_{sy}(T) + E_1(T) \times \left[\varepsilon - \varepsilon_{sy}(T)\right] \qquad for\ \varepsilon > \varepsilon_{sy}(T) \tag{Eq 3.26}$$

With $E_1(T) = 0.01 \times E_s(T)$

where:

- $E_s(T)$ represents the initial modulus of elasticity
- $f_{sy}(T)$ is the yield strength of steel after fire exposure to a given temperature T
- $\varepsilon_{sy}(T)$ is the corresponding stress strain expressed by the equation:

$$\varepsilon_{sy}(T) = \frac{f_{sy}(T)}{E_{sy}(T)} \tag{Eq 3.27}$$

The temperature coefficient in Equations 3.25 to 3.27 is ignored during the calculation in this case. This is because Koen's experimental work was carried out in a laboratory at normal room temperature, so the temperature has no influence on the stress and strain of the steel tube.

Figure 3.10 presents the stress strain model used in this research study.

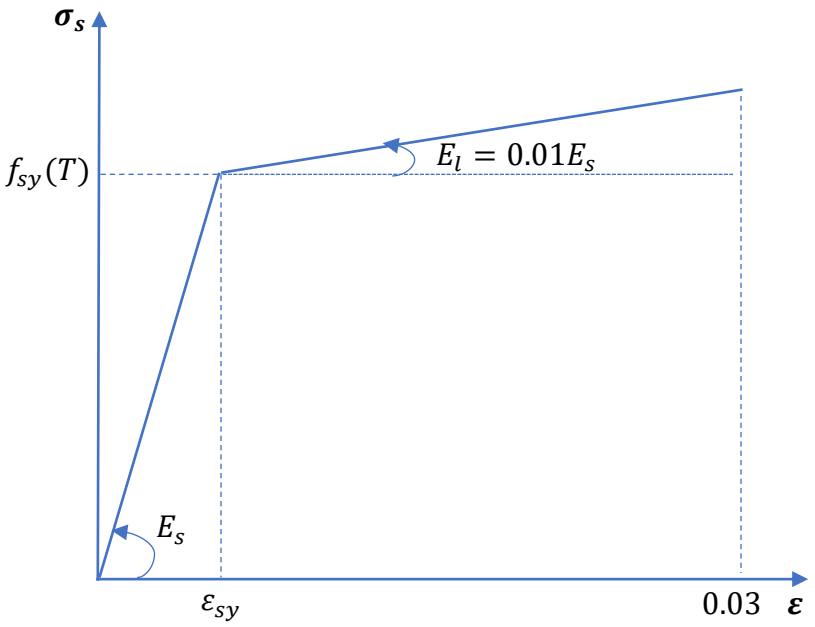

Figure 3.10: Stress strain graph for inner and outer steel tubes (Pagoulatou et al (2014))

3.3.5 Partitioning of Columns

In order to mesh the columns effectively, it was observed that the columns needed to be partitioned. This is due to circular CFDST columns not having edges compared with square or rectangular columns. Partitioning the columns creates edges, hence enabling greater flexibility to define the column mesh.

The surfaces of the columns were then partitioned as illustrated in Figures 3.11 and 3.12.

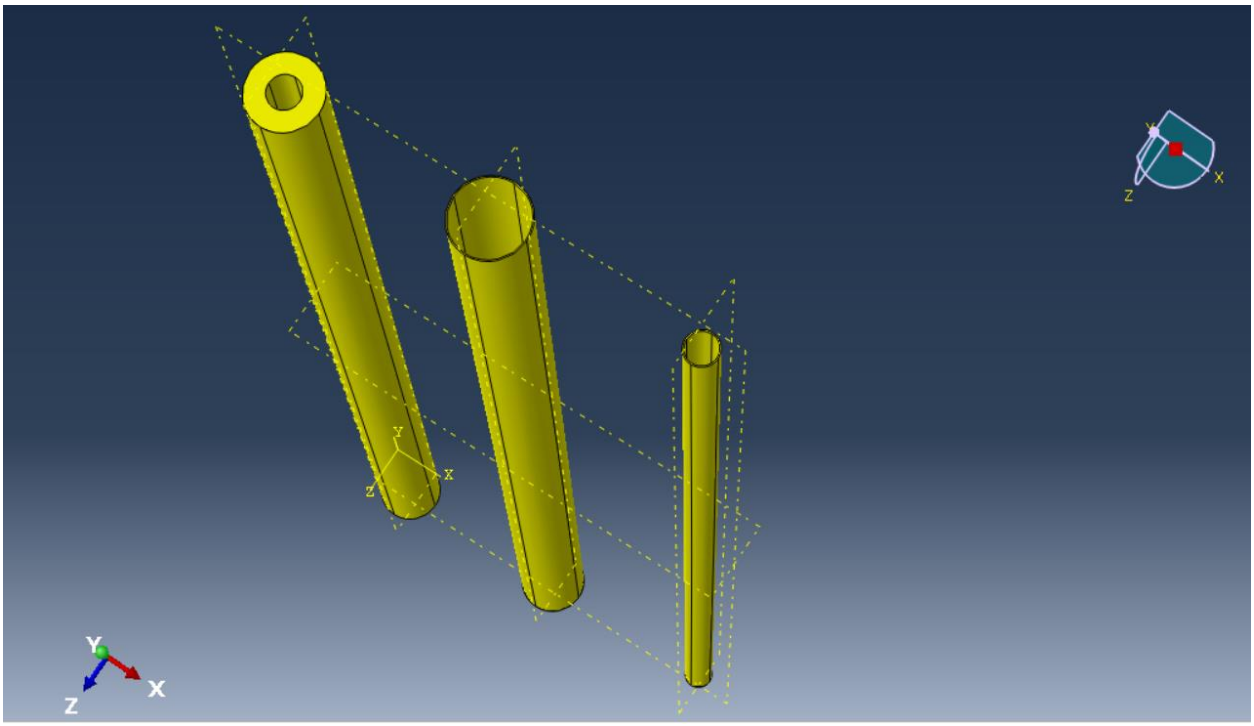

Figure 3.11: Partitioned CFDST columns (column parts partitioned separately)

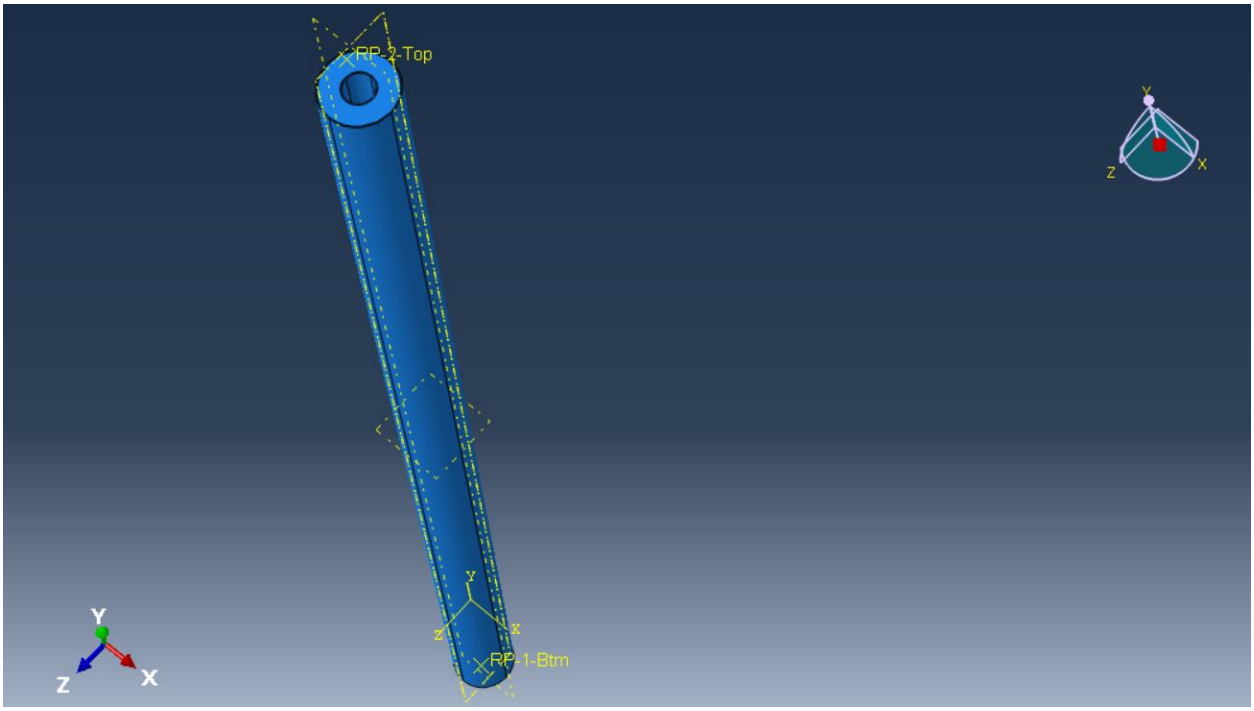

Figure 3.12: Completed partitioned CFDST columns

3.3.6 Meshing of the columns

The columns were meshed using different meshing schemes to obtain an ideal mesh size that accounted for efficiency and accuracy. Several simulations were conducted to determine the optimal mesh configuration. The final mesh arrangements for the columns were obtained as 20 segments along the height and 48 along the circumference. The number of elements through the thickness of the tubes was selected as 1, while the number of elements through the thickness of the concrete core was obtained as 7. Although the length of the element is greater than 10 times than its thickness, the model produced accurate results while being computationally efficient. Figure 3.13 shows the meshing configuration of the STK column.

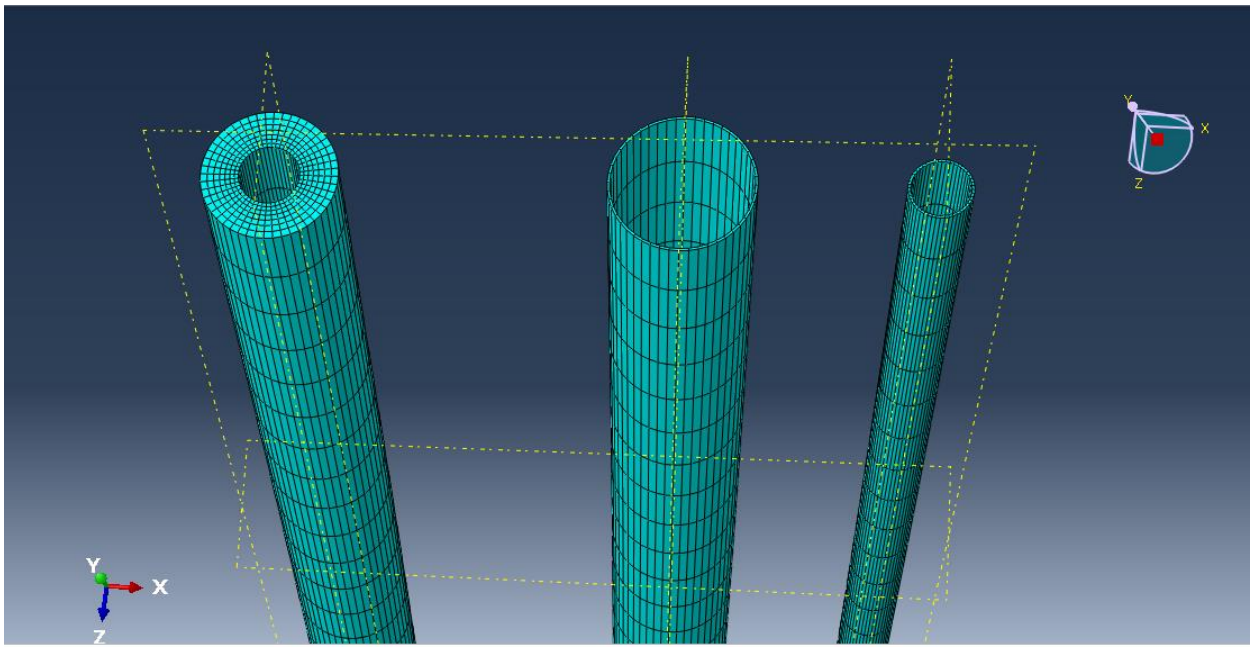

Figure 3.13: STK CFDST column meshing

3.3.7 Initial FE results compared with experimental test results

The generalised FE model was calibrated to the STK model. Once satisfactory calibrated, the modelling techniques were used to validate the FE model against the other three CFDST columns. This section, therefore, explores the calibration and validation of the general FE model. Figures 3.14 and 3.15 presents the FE model's response for the axial force vs horizontal midspan

displacement and the axial force vs axial (vertical) displacement of the STK model, respectively. The responses were obtained using the parameters as outlined in sections 2.3.1 to 2.3.6.

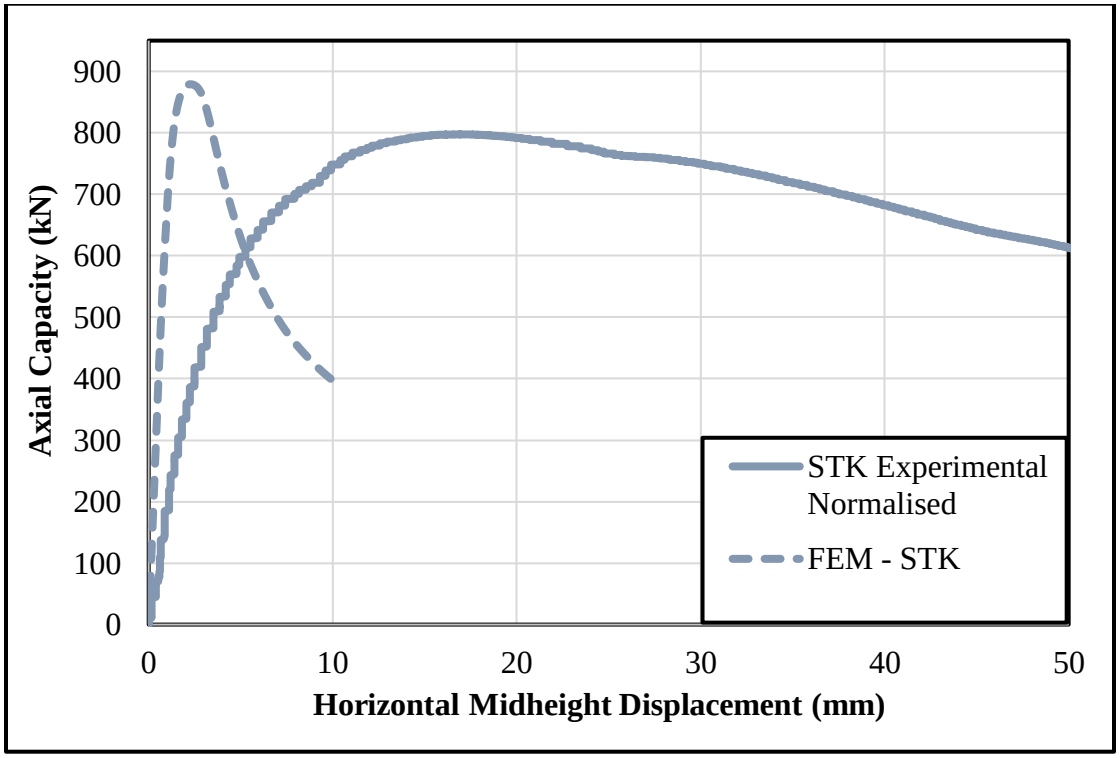

Figure 3.14: Comparison of the initial STK FE and experimental axial force vs horizontal midspan displacement responses

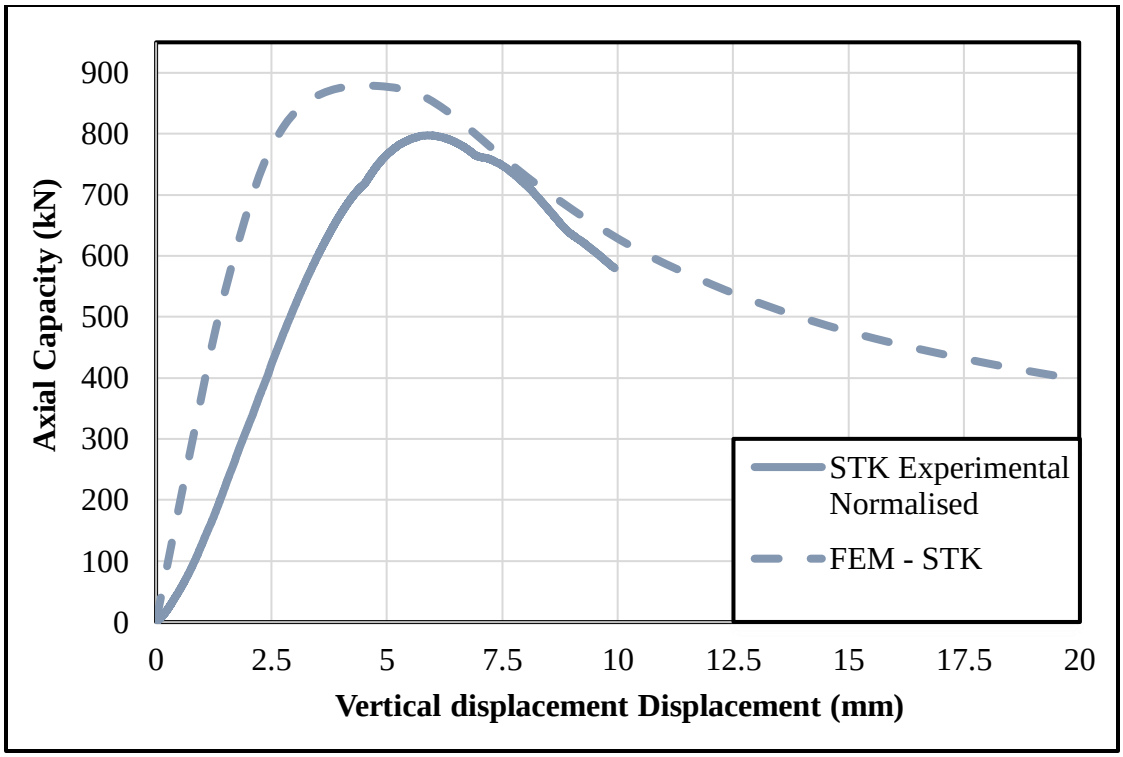

Figure 3.15: Comparison of the initial STK FE and experimental axial force vs axial displacement responses

After reviewing the responses obtained in Figures 3.14 and 3.15, it was observed that the FE STK model produced a greater axial force than the experimental STK. The FE model has a greater stiffness compared to the experimental results. Thus, the initial FE model required the adjustment of certain parameters to yield better responses. The entire modelling process together with the parameters used in the FE model was carefully reviewed. Upon review of the FE model, two major factors were identified that could explain the discrepancy of the results. The two factors are: incorrect concrete strength resulting from the curing conditions and the wrong assumption that perfectly straight columns were used.

3.3.8. Adjustment of the confined concrete compressive strength (f_{cc})

After casting and testing 40 concrete cubes in temperature-controlled curing baths (ideal conditions), Koen (2015) obtained an average cube strength (f_{cu}) of 52.8 MPa with a standard deviation of 2.5 MPa.

After studying the research work conducted by Naderi *et al* (2009), it was observed that different concrete curing conditions result in different concrete strength for different concrete mixes as shown in Figure 3.16. Since the curing conditions of concrete confined in the tubes is different from the ideal conditions, we can expect a reduction in concrete strength as observed in Figure 3.16. Based on the observations of the curing conditions, it was assumed that the concrete between the tubes cure similarly to the indoor condition as shown in Figure 3.16. This results in a concrete strength reduction to 43 MPa, which was used to determine the confined concrete strength profile. FE simulations were conducted with this reduced confined concrete strength profile.

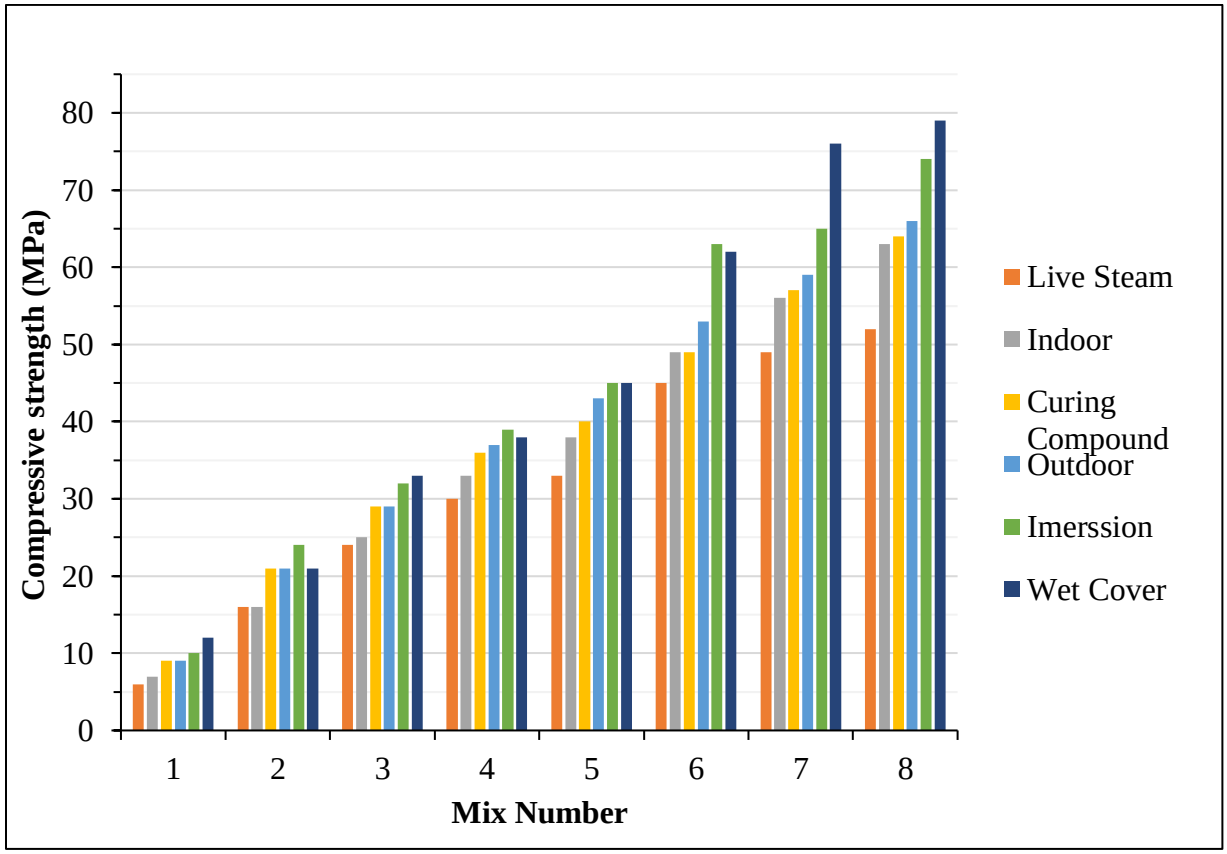

Figure 3.16: Concrete compressive strength of eight different concrete mixtures cured under different curing conditions (Naderi et al (2009))

3.3.9. Columns not being perfectly straight

After a visit to the laboratory and measuring a number of steel tubes, it was observed that these tubes are not perfectly straight and had an initial curvature of approximately 2 mm at midspan for a 2.5 m length. It was also observed that for columns with a diameter of 177.8 mm and 2.5 m long,

a curvature of 2 mm is undetectable to the human eye. Initial FE simulations on a single tube with various curvatures showed a significant reduction in the ultimate load of the column.

According to the Chinese code GB50017-2003, the initial geometric imperfection at mid-height of the CFDST slender column could conservatively be obtained using the formula L/1000. Therefore, the initial imperfection for the 2.5m and 3.5m long columns will be 2.5mm and 3.5mm respectively. These values validate the initial approximate curvature value of 2mm for the CFDST columns used in this study.

3.3.10. Updated results obtained after updated parameters

Once the parameters in sections 3.3.4.1.1 were adjusted, an updated FE response of the STK column model was obtained and compared with the experimental STK column, which is shown in Figures 3.17 and 3.18.

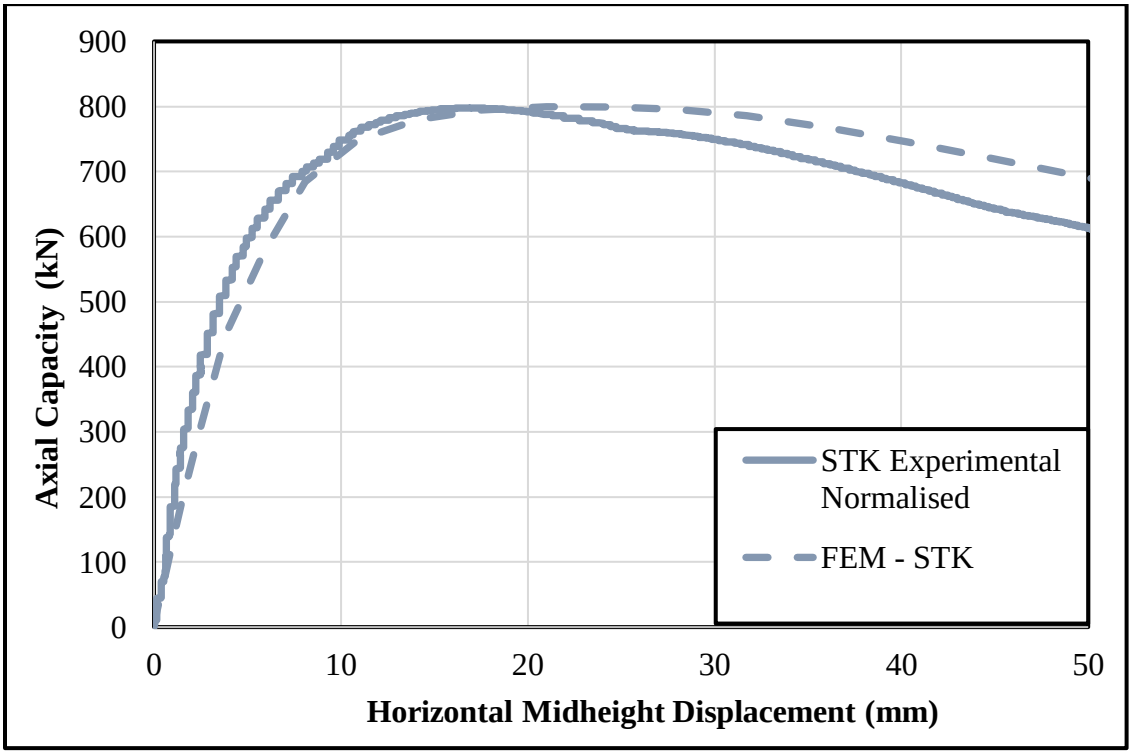

Figure 3.17: Updated comparison of the STK FE and experimental axial force vs horizontal midheight displacement responses

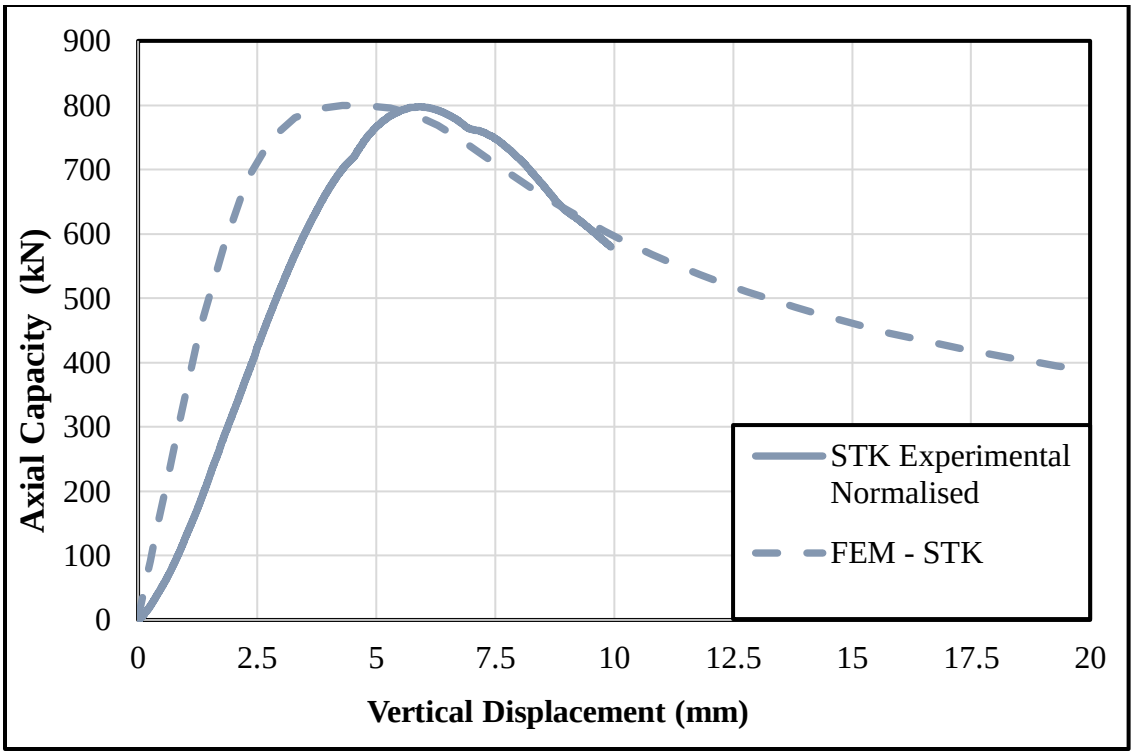

Figure 3.18: Updated comparison of the STK FE and experimental axial force vs vertical midheight displacement

The updated STK responses displayed in Figures 3.17 and 3.18 prove that the FE model is functional and accurate. From these results, a peak load percentage difference of only 0.21% was observed between the experimental and FE model. Since we were only interested in the ultimate response of the columns, the initial stiffness of the columns was ignored.

3.4 VALIDATION OF GENERALISED FE MODEL

The general FE model was calibrated to the experimental STK test results. From Figures 3.17 and 3.18, it is observed that there is a good correlation between the responses in terms of the ultimate load. It is important that the general FE model be validated against other experimental results to ensure accuracy. The generalised FE approach used for the STK model was used in modelling the STN, LTK and LTN models for verification against its equivalent experimental responses. It is important to note that some researchers calibrated their FE model to a single experimental result but did not validate their FE model against other experimental results (Farajpourbonab (2017),

Karim and Ipe (2016)). Figures 3.19 to 3.21 presents the axial load vs midspan displacement responses of the STN, LTK and LTN columns obtained from the STK modelling techniques together with the equivalent experimental responses.

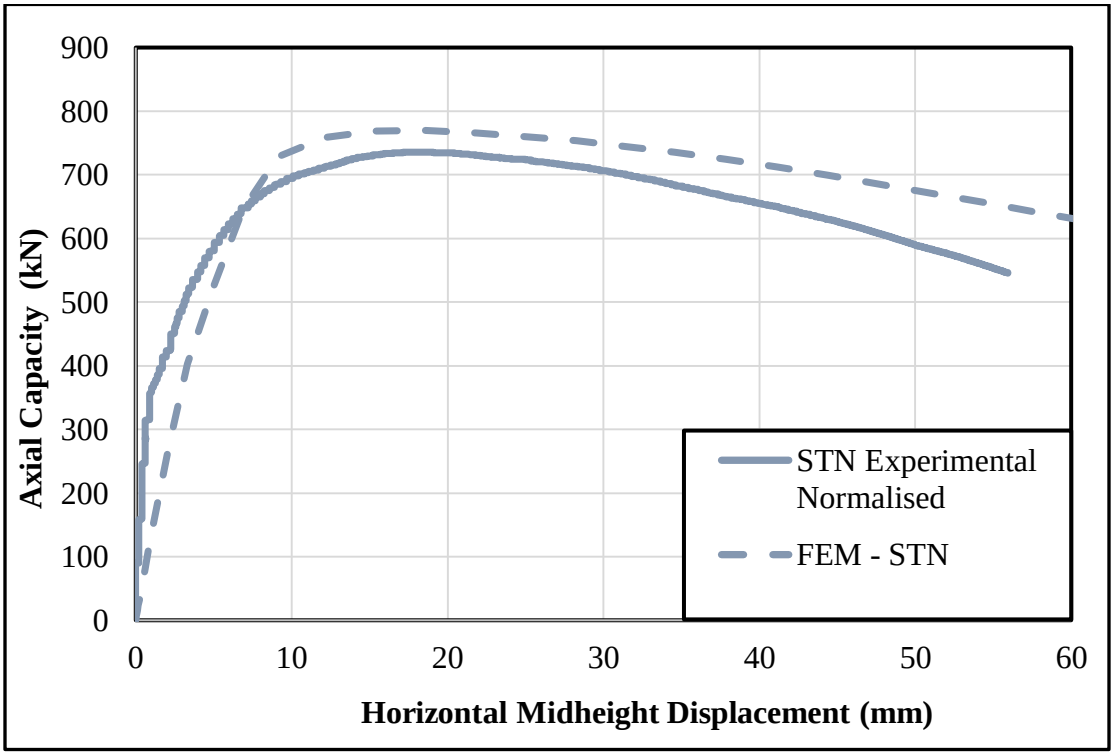

Figure 3.19: Comparison of the STN FE and experimental axial force vs horizontal midheight displacement responses obtained without validation

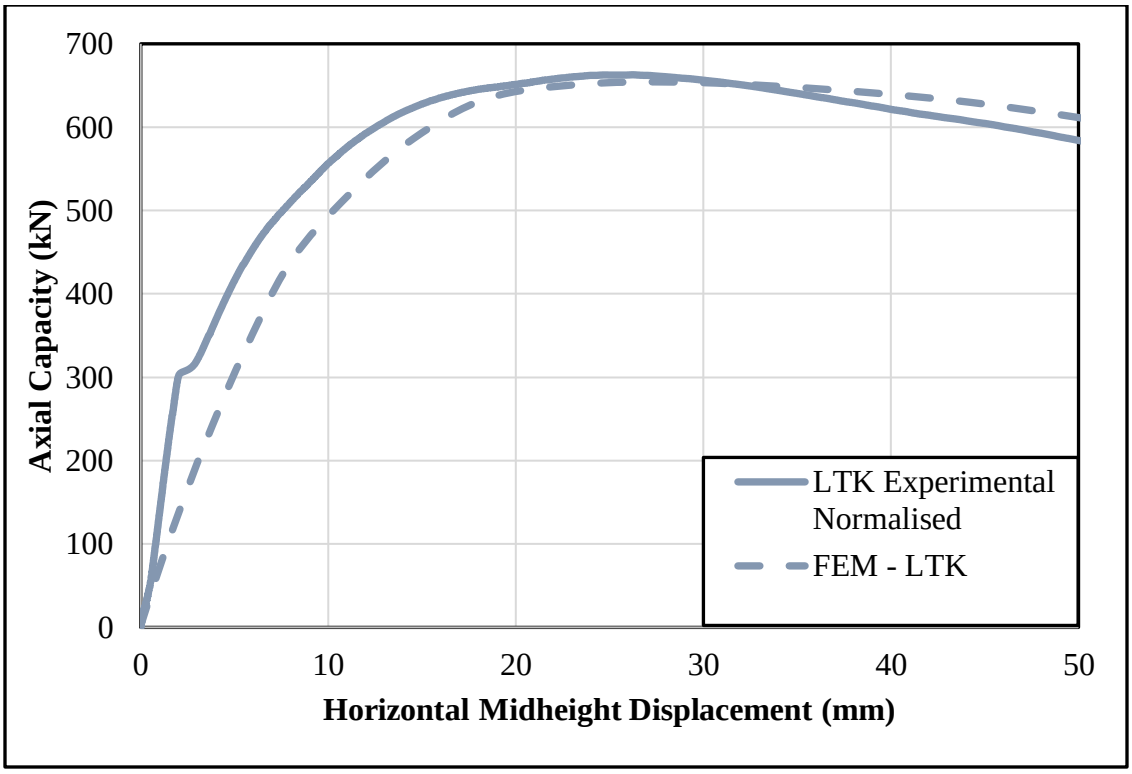

Figure 3.20: Comparison of the LTK FE and experimental axial force vs horizontal midheight displacement responses obtained without validation

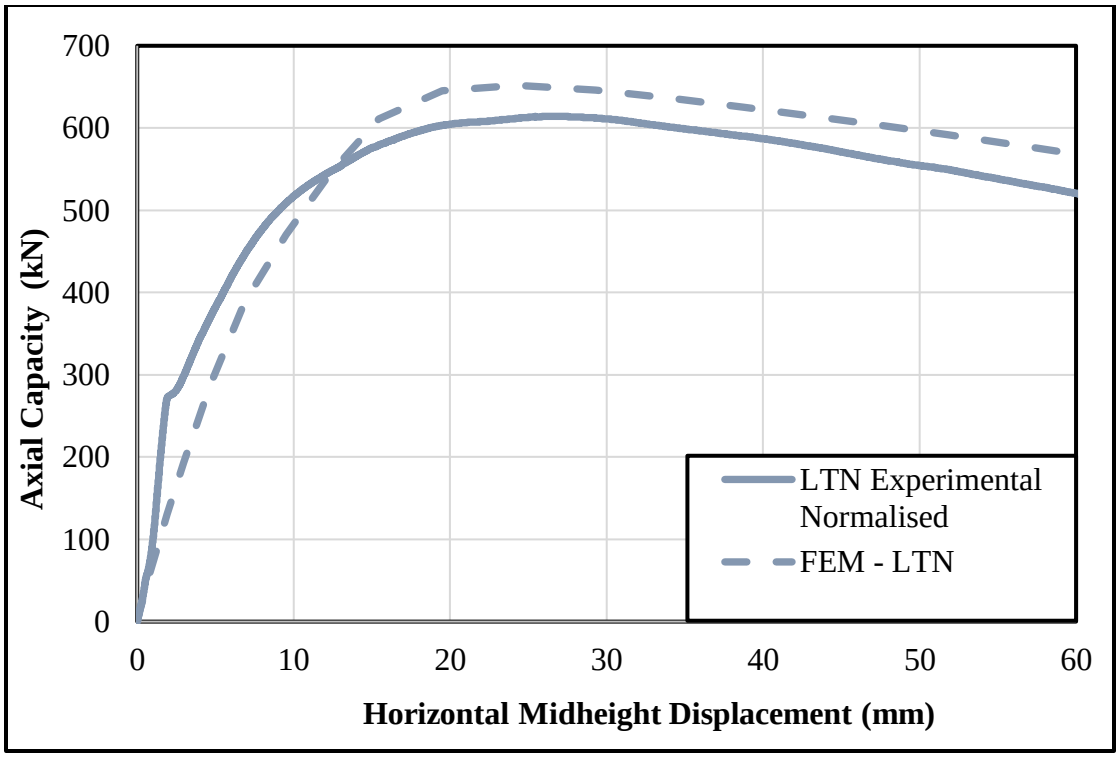

Figure 3.21: Comparison of the LTN FE and experimental axial force vs horizontal midheight displacement responses obtained without validation

From Figures 3.19 to 3.21, it can be observed that the STN, LTK and LTN FE model predictions do not provide the same accuracy as the STK column's FE model. Errors of 4.04%, -1.67% and 2.99% was observed between the FE and experimental responses of the STN, LTK and LTN, respectively. Failure to account for these errors, will only lead to amplified errors during the sensitivity analysis if the FE models are not calibrated and properly validated. The error in these particular cases are small, i.e. less than 5%, however, no guarantee exists that the error could be significant in this case or in the case of other researchers work.

Thus, this observation proves the results of many researchers who calibrated their FE model without validation and immediately proceeded with conducting sensitivity studies on various parameters, could be questionable. Thus, calibrating FE models without validation does not conform to best practice.

Certain geometric and material properties required minor adjustments to obtain better accuracy between the experimental and FE responses.

3.5. RESULTS AND DISCUSSION

The general FE model required several minor tweaks to certain parameters to obtain accurate peak forces that were within 3% of Koen's (2015) experimental test results. The major problem associated with the incorrect force vs displacement results were due to errors in the formulas obtained from various journal articles related to the confined concrete model (Pagoulatou *et al* (2014), Hassanein *et al* (2018)). The parameters which required adjustment are:

- The confined concrete properties of the TN columns were recalculated. The new obtained concrete strength for the TN columns is 17.7% less than that of the LTK columns,
- All concrete damage plasticity input parameter values remain the same, except for the dilation angle which was reduced by 20.2% for the TN columns after calculations,
- The column length of the STK column was increased by 40% to represent the long column models (LTN and LTK),
- The inner tube diameter of STK column was reduced by 40% to represent the TN column models.

After these parameters were slightly adjusted, the FE models were analysed. The comparison between the FE model and experimental test results axial force vs midspan lateral deformation for the STK, STN, LTK and LTN models are shown in Figures 3.22 to 3.25.

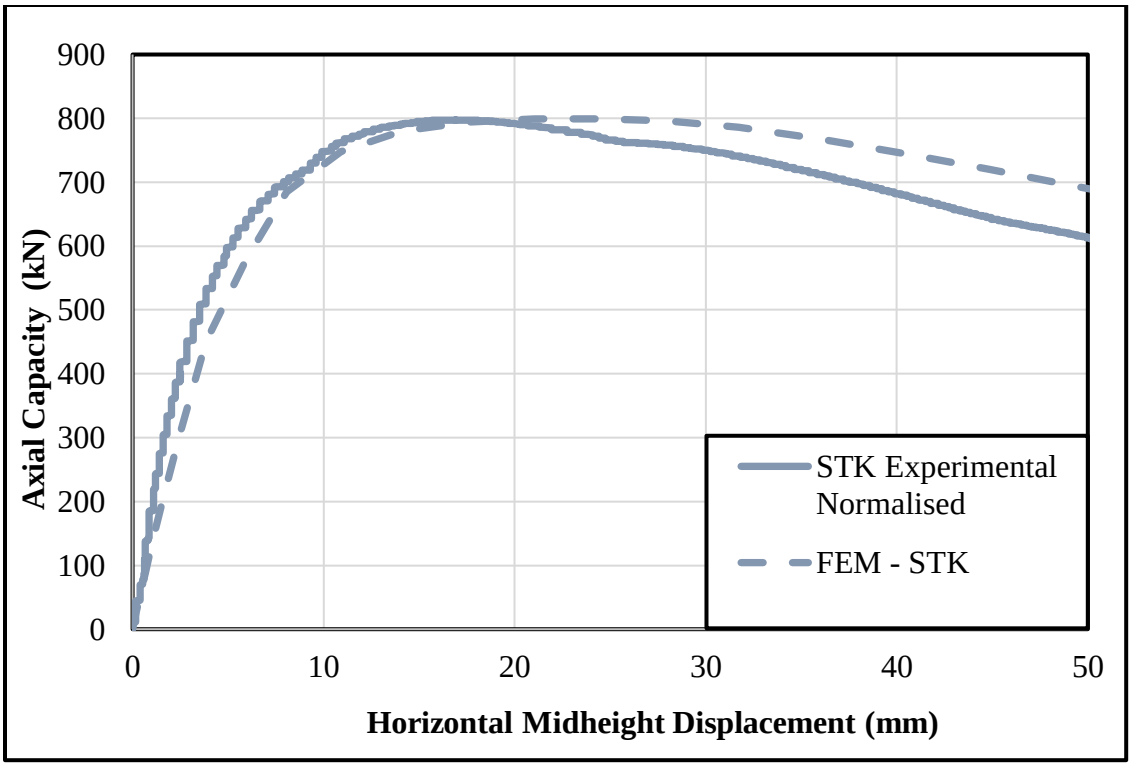

Figure 3.22: Comparison of the axial load vs midheight lateral deflection for the STK responses

The ultimate axial load for the STK FE and experimental responses displayed in Figure 3.22 are 799 kN and 798kN respectively, resulting in an error of 0.21%.

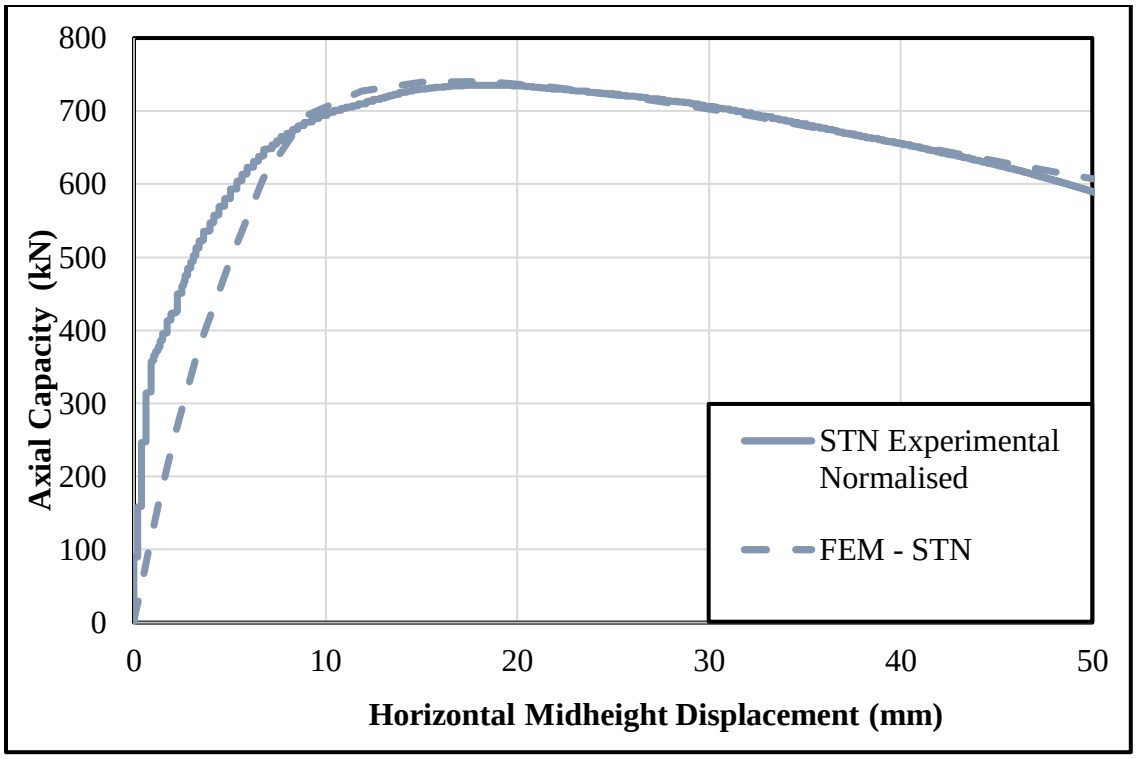

Figure 3.23: Comparison of the axial load vs midheight lateral deflection for the STN responses

The ultimate axial load for the STN FE and experimental responses displayed in Figure 3.23 are 740 kN and 736 kN respectively, resulting in an error of 0.64%.

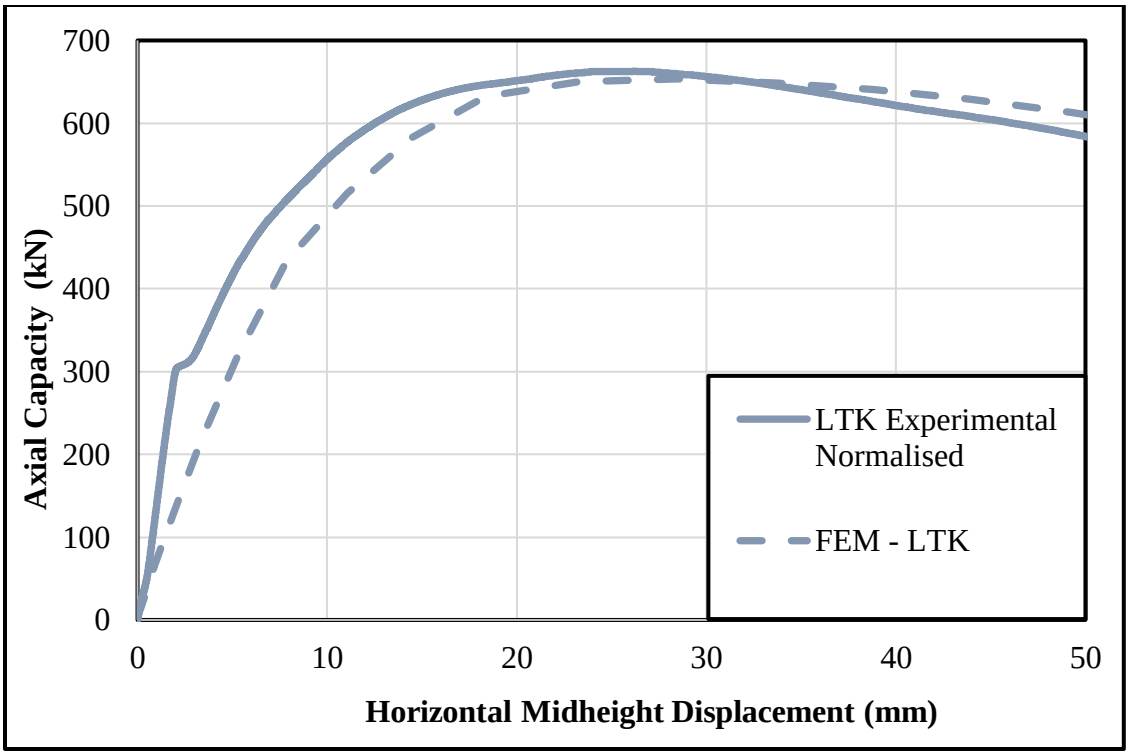

Figure 3.24: Comparison of the axial load vs midheight lateral deflection for the LTK responses

The ultimate axial load for the LTK FE and experimental responses displayed in Figure 3.24 are 652 kN and 663 kN respectively, resulting in an error of -1.67%.

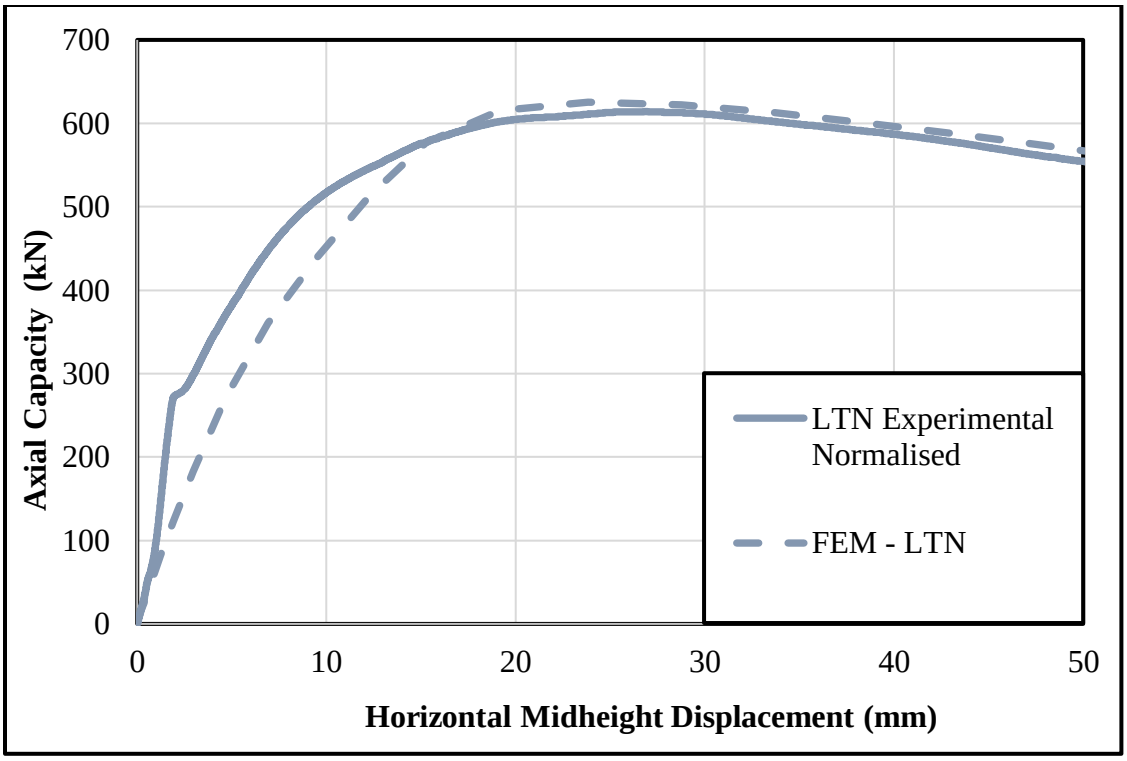

Figure 3.25: Comparison of the axial load vs midheight lateral deflection for the LTN responses

The ultimate axial load for the LTN FE and experimental responses displayed in Figure 3.25 are 633 kN and 614 kN respectively, resulting in an error of 2.98%.

3.6 RESULTS ANALYSIS AND SUMMARY

The results obtained from Figures 3.22 to 3.25 yields a maximum percentage difference of 3% between the FE and experimental test responses. This was obtained by calibrating the FE model to the experimental STK model, making minor adjustments to the FE STK model before validating this model against the experimental STK columns. The calibrated STK model was then used to validate the modelling approach against the STN, LTK and LTN columns. Based on the maximum percentage difference between the FE and experimental responses, it can be concluded that the general FE model is calibrated and properly validated. With this confidence in the general FE model, a sensitivity analysis was conducted on the parameters, which significantly influences the column's ultimate load as described in Chapter 4.

CHAPTER 4

SENSITIVITY ANALYSIS

A sensitivity analysis was conducted to investigate the effect that certain parameters have on the column's response when subjected to eccentric loading. The main parameters studied in this sensitivity analysis are; inner tube thickness, outer tube thickness, concrete strength, steel strength, column curvature, load eccentricity, support fixity and the concrete damage plasticity (CDP) parameter values (dilation angle, viscosity parameter, flow potential eccentricity, compressive meridian, ratio of compressive strength under biaxial loading to uniaxial compressive strength).

In conducting the sensitivity analysis, it is important to note that a single parameter is changed at a time while the remaining parameters are kept constant.

4.1 Effect of the Inner Tube Thickness on the Ultimate Load

A parameter study was conducted to obtain the column's behaviour when the inner tube thickness was varied. The base column model of the 4 specimens have inner tube thickness of 3mm. The sensitivity analysis was conducted for inner tube thicknesses of 4mm, 5mm and 6mm.

Figure 4.1 presents the axial load vs midspan displacement responses for the STK, STN, LTK and LTN columns when the inner tube thickness is varied.

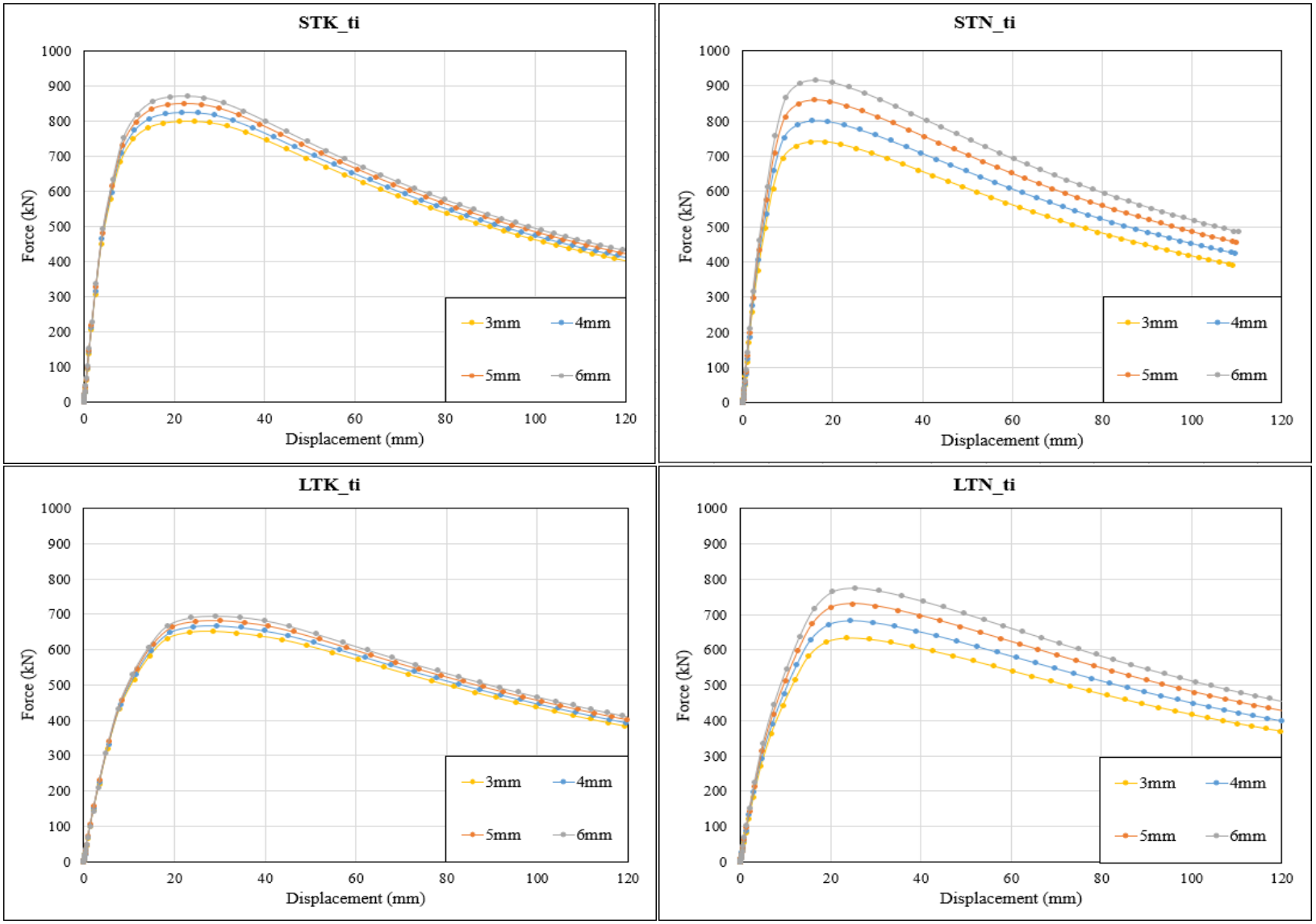

Figure 4.1: The effect of increasing the thickness of the inner tube on the column's peak load

From Figure 4.1, it can be observed that an increase in the thickness of the inner tube leads to a corresponding increase in the peak axial load. Furthermore, it is also observed that the change in the thickness of the inner tube has a greater effect on the TN columns than on the TK columns.

Table 4.1 presents the peak axial load of the columns for a change in the inner tube thickness, while Table 4.2 presents the same information in terms of percentage increase using the 3mm response as the base.

Table 4.1: Peak axial loads obtained by varying the inner tube thickness

Inner tube thickness (mm)	**STK (KN)**	**STN (KN)**	**LTK (KN)**	**LTN (KN)**
3	**799**	**740**	**654**	**633**
4	825	801	668	683
5	849	860	683	730
6	871	916	696	776

Table 4.2: Percentage increase in the axial load for an increase in the thickness of the inner tube

Inner tube thickness (mm)	**STK (%) (Base response = 799 kN)**	**STN (%) (Base response = 740 kN)**	**LTK (%) (Base response = 654 kN)**	**LTN (%) (Base response = 633 kN)**
3	**0**	**0**	**0**	**0**
4	3.3	8.2	2.1	7.9
5	6.3	16.2	4.4	15.3
6	9.0	23.8	6.4	22.6

From Table 4.2, it is observed that the percentage increase in peak axial load is greater for the TN columns compared to the TK columns. An increase of 1 mm in the thickness of the inner tube results in an average increase of approximately 3% in the TK column's peak axial load as opposed to an average increase of approximately 8% in the TN column's peak axial load. From Table 4.2, it can also be observed that varying the lengths of the column for the same cross-sectional area does not significantly affect the impact that the inner tube thickness has on the column's response.

Figure 4.2 presents a graphical representation of the column's peak axial load against an increase in the inner tube thickness.

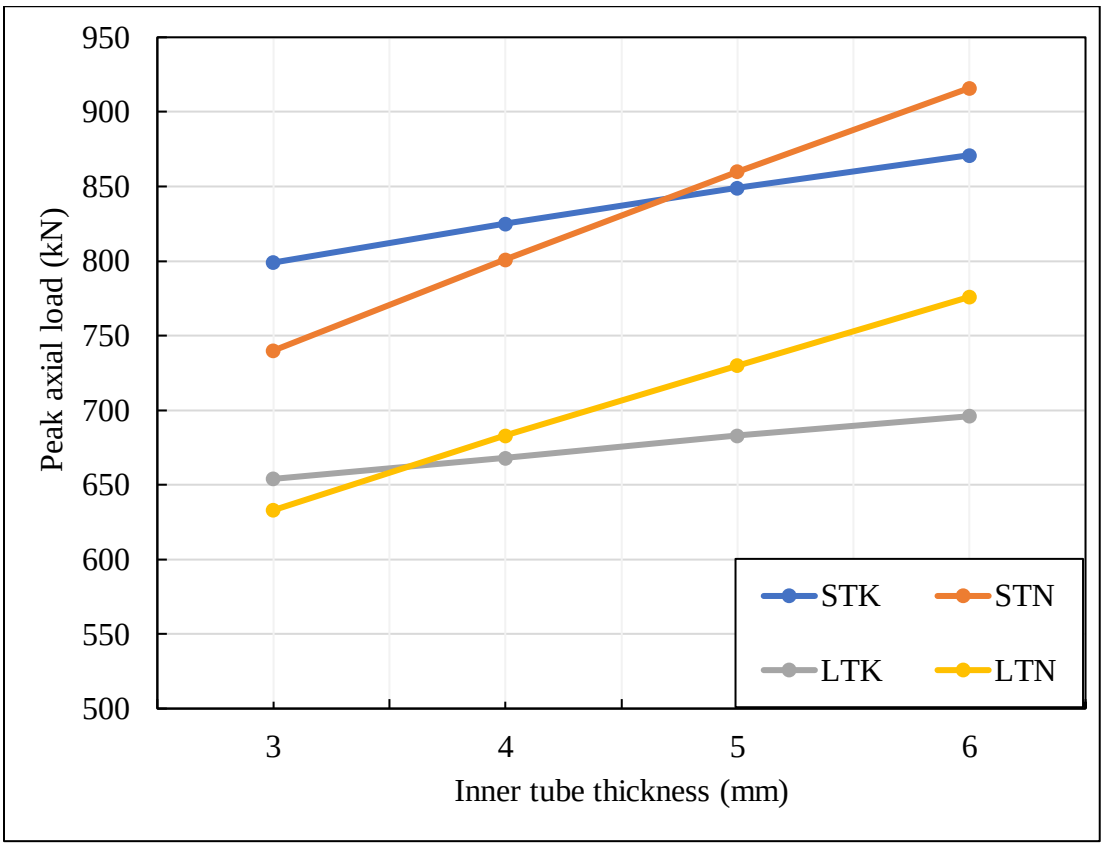

Figure 4.2 : Column's peak axial load response to change in inner tube thickness

Figure 4.2 portrays a novel observation not observed in previous research studies. For a column with different cross sections, TN and TK, but with the same length (S or L), the initial TK models have a greater peak load at 3 mm compared to the TN models, however the TN models peak load increases beyond the TK models as the inner tube thickness increases. This is counterintuitive that the TN model will produce greater peak loads compared to TK models as the inner tube thickness increases. This finding is significant as all other work, which considered variations of thickness only considered a single column configuration and would thus not have noticed this peculiar column behaviour. It is also interesting to note that a thicker inner tube is required for the short columns (± 4.6mm) as opposed to the long columns (± 3.6mm) to reach the transition where the

TN columns produce greater ultimate loads compared to the TK columns, for this particular configuration.

The above observation shows that by simply increasing the inner tube thickness, a column with a smaller concrete cross section can be developed to yield a greater axial load compared to a column with a larger concrete cross section if all other material properties and parameters are kept constant. This shows that a column with a thinner concrete thickness can be developed to produce a greater axial load than a column with a thicker concrete annulus, by simply varying its' inner tube thickness.

4.2 Effect of the Outer Tube Thickness on the Ultimate Load

Figure 4.3 presents the axial load versus vs midspan displacement response obtained by varying the outer tube thickness of the columns. The base model of each column has an outer tube thickness of 3mm, with outer tube thickness variations of 4mm, 5mm and 6mm.

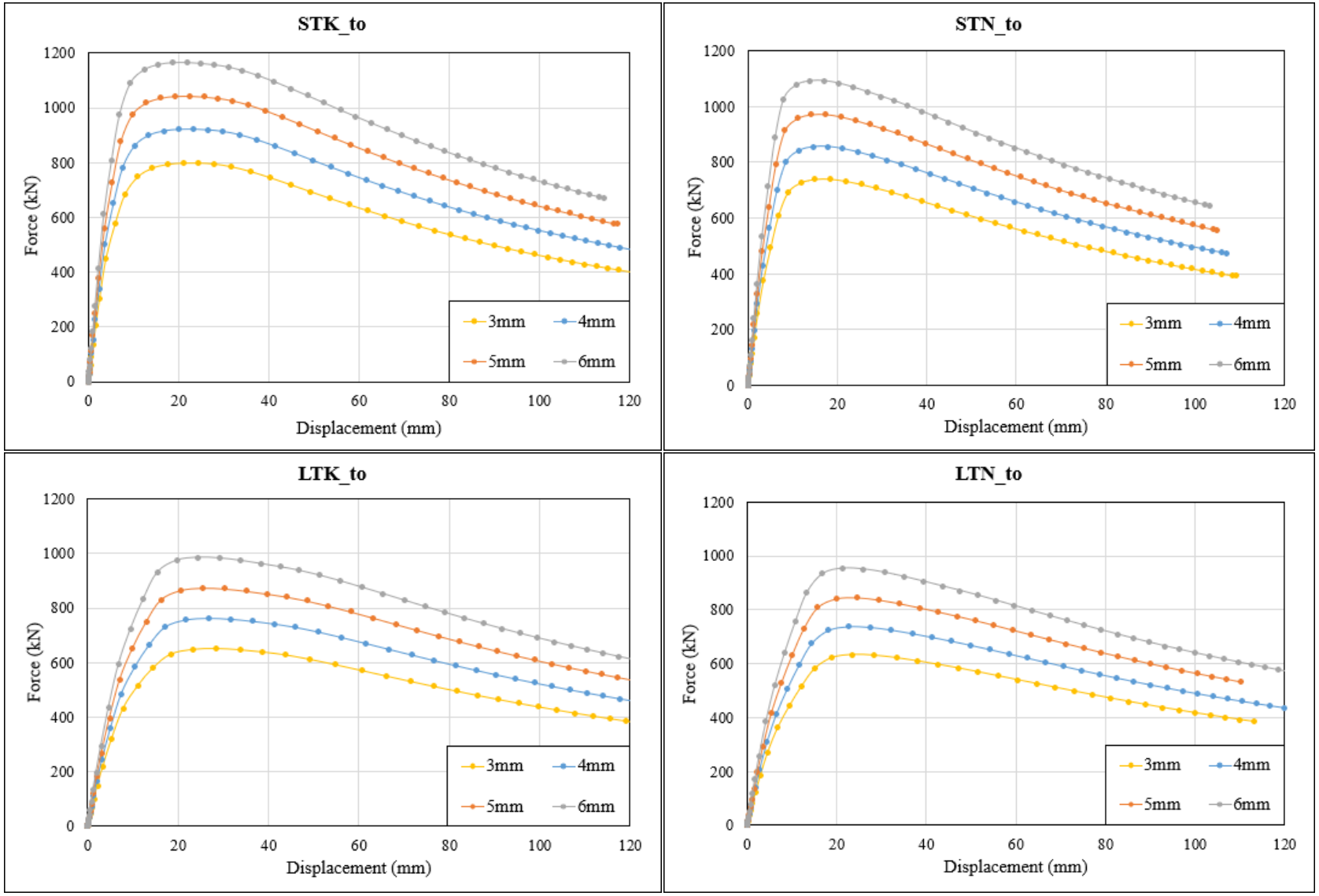

Figure 4.3: The effect of increasing the thickness of the outer tube on the column's peak load

From Figure 4.3, it can be observed that an increase in the thickness of the outer tube leads to a corresponding increase in the peak axial load. Furthermore, it is also observed that the change in the thickness of the outer tube has a similar effect on all the columns, irrespective of cross sections or lengths.

Table 4.3 presents the peak axial load of the columns for a change in the inner tube thickness in terms of percentage using the 3mm response as the base.

Table 4.3: Percentage increase in the axial load for an increase in the thickness of the outer tube

Outer tube thickness (mm)	**STK (%) (Base response = 799 kN)**	**STN (%) (Base response = 740 kN)**	**LTK (%) (Base response = 654 kN)**	**LTN (%) (Base response = 633 kN)**
3	**0**	**0**	**0**	**0**
4	15.3	15.6	17	16.6
5	30.5	31.5	34.0	33.5
6	45.8	47.5	51.0	50.6

From Table 4.3 we can conclude that increasing the outer tube thickness leads to a corresponding increase in the peak load of approximately 15% per millimeter for the short columns and approximately 17% per millimeter for the long columns.

Figure 4.4 shows the effect of increasing the outer tube thickness on the peak load of the columns.

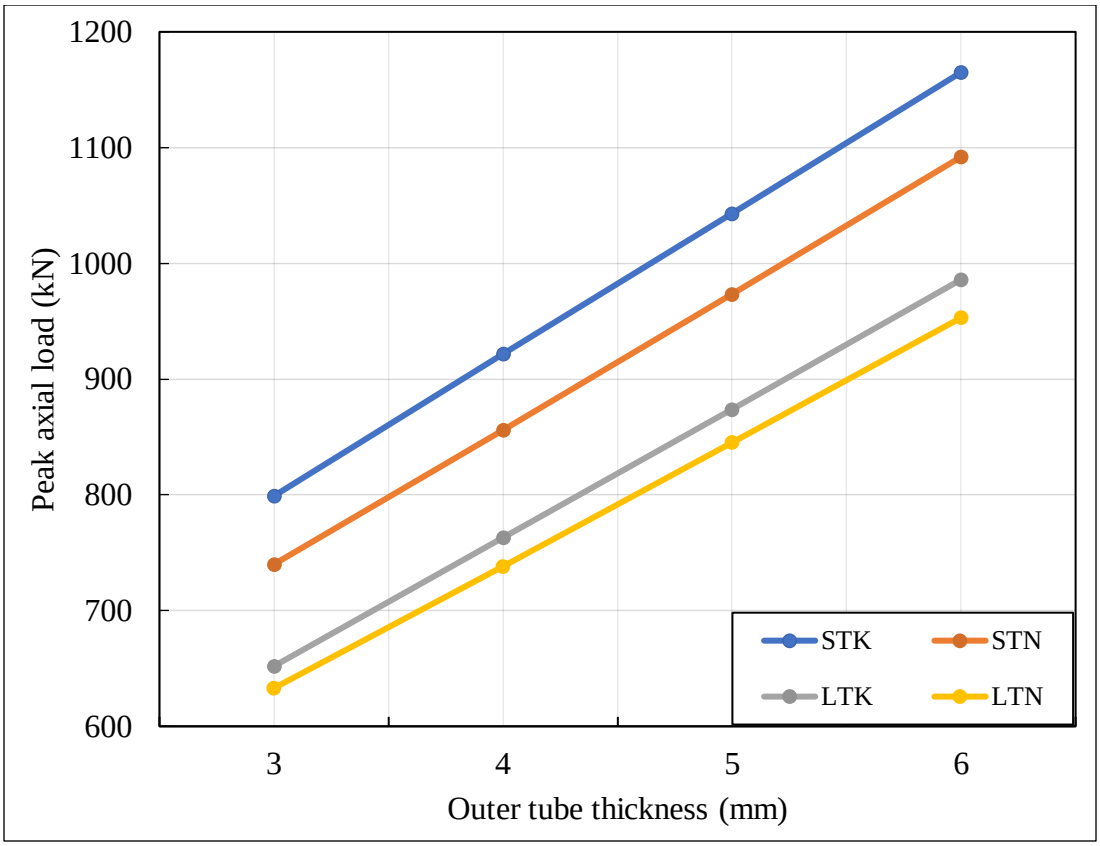

Figure 4.4: Column's peak axial load response to change in outer tube thickness

Figure 4.4 shows a linear increase in the column's peak load for a corresponding increase in the thickness of the outer tube. The difference between the TK and TN responses is similar for the same column length. There is also no cross over, where the TN columns become stronger than the TK columns as observed when the inner tube thickness is varied.

4.3 Effect of Concrete Strength on the Ultimate Load

The adjusted concrete strength of the base models in this experiment is 43MPa. The most commonly used concrete strength for construction projects varies between 35 and 55MPa. Also, the concrete strength can vary significantly whether the concrete is mixed on-site or whether ready mix concrete is procured. Therefore, it is important to determine the effect of the concrete strength on the peak load of the columns. Thus, a concrete strength sensitivity analysis was conducted using concrete strengths of 35MPa, 40MPa, 43MPa (base model), 45MPa, 50 MPa and 55MPa. The

concrete strength was incremented by 5MPa, to obtain a constant difference in results, which will help provide a better understanding of the column's behavioural response to changes of the concrete strength.

Figure 4.5 presents the effect of the concrete strength on the axial load of columns.

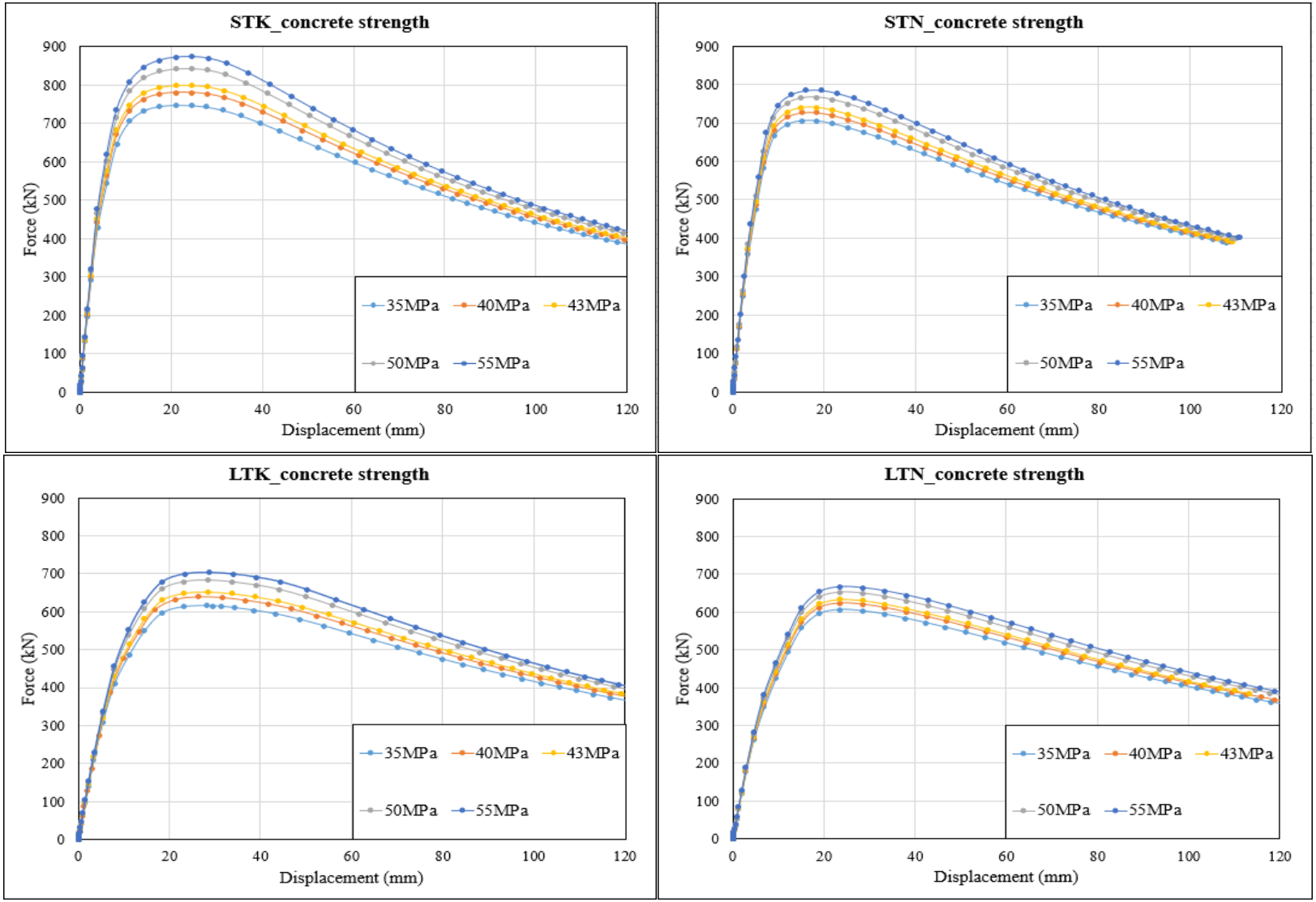

Figure 4.5: The effect of increasing the concrete strength on the column's peak load

From Figure 4.5 it is observed that an increase in concrete strength results in an increase in the column's axial load carrying capacity. Further observations are obtained from analyzing the results presented in Table 4.4.

Table 4.4: Percentage change of the column's axial load compared with the base model, obtained from varying the concrete strength

Concrete strength (MPa)	**STK (%) (Base response = 799 kN)**	**STN (%) (Base response = 740 kN)**	**LTK (%) (Base response = 654 kN)**	**LTN (%) (Base response = 633 kN)**
35	-6.4	-4.7	-5.6	-4.3
40	-2.4	-1.8	-2.2	-1.6
43	**0**	**0**	**0**	**0**
50	5.5	3.6	4.8	3.3
55	9.3	6.0	7.8	5.6

From Tables 4.4, it is observed that an increase in concrete strength results in an increase in column's axial load carrying capacity. The change in concrete strength has a greater effect on the TK models compared to the TN models.

Figure 4.6 presents a graphical representation of the column's peak axial load response to changes in concrete strength.

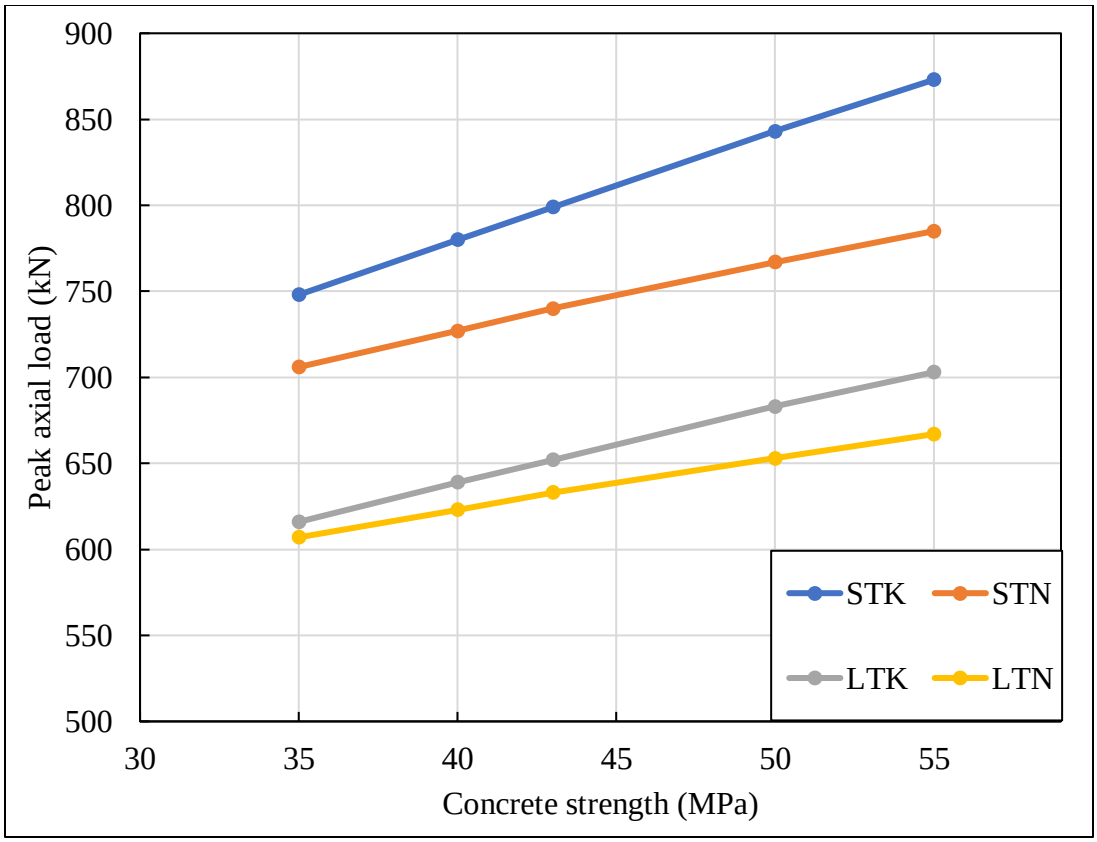

Figure 4.6: Column's peak axial load response to change in concrete strength

From Figure 4.6, we can deduce that the change in concrete strength does have a significant effect on the ultimate load carrying capacity of the column. It is also clear that as the concrete strength increases, the load carrying capacity between the TK and TN models become larger, i.e. the responses diverge. The divergence is more prominent in the short columns compared to the long columns. At the greatest concrete strength of 55 MPa, a difference in column's strength of 9.3% and 7.8% is observed between the short and long columns respectively, as opposed to an initial difference of 6.4% and 5.6% observed at 35 MPa.

Analyzing the results obtained from varying the concrete strengths and those obtained from varying the steel tube thicknesses shows that changing the tube thicknesses will be more efficient at increasing the column's axial load carrying capacity, compared to changing the concrete strength. Also, it is observed that changing the column's outer tube thickness is a more effective way of increasing the column's axial load carrying capacity, compared to changing the concrete

strength. This is because the results obtained from a 1mm increase in the steel outer tube thickness is the equivalent to a 10MPa increase in concrete strength.

4.4 Effect of a change in Steel Strength on the Ultimate Load

The column base models used in this study has a steel strength of 300MPa. The response of these columns to changes in steel strength was examined with steel strength values of 200MPa and 355MPa. Figure 4.7 presents the effect of the steel strength on the axial load of columns.

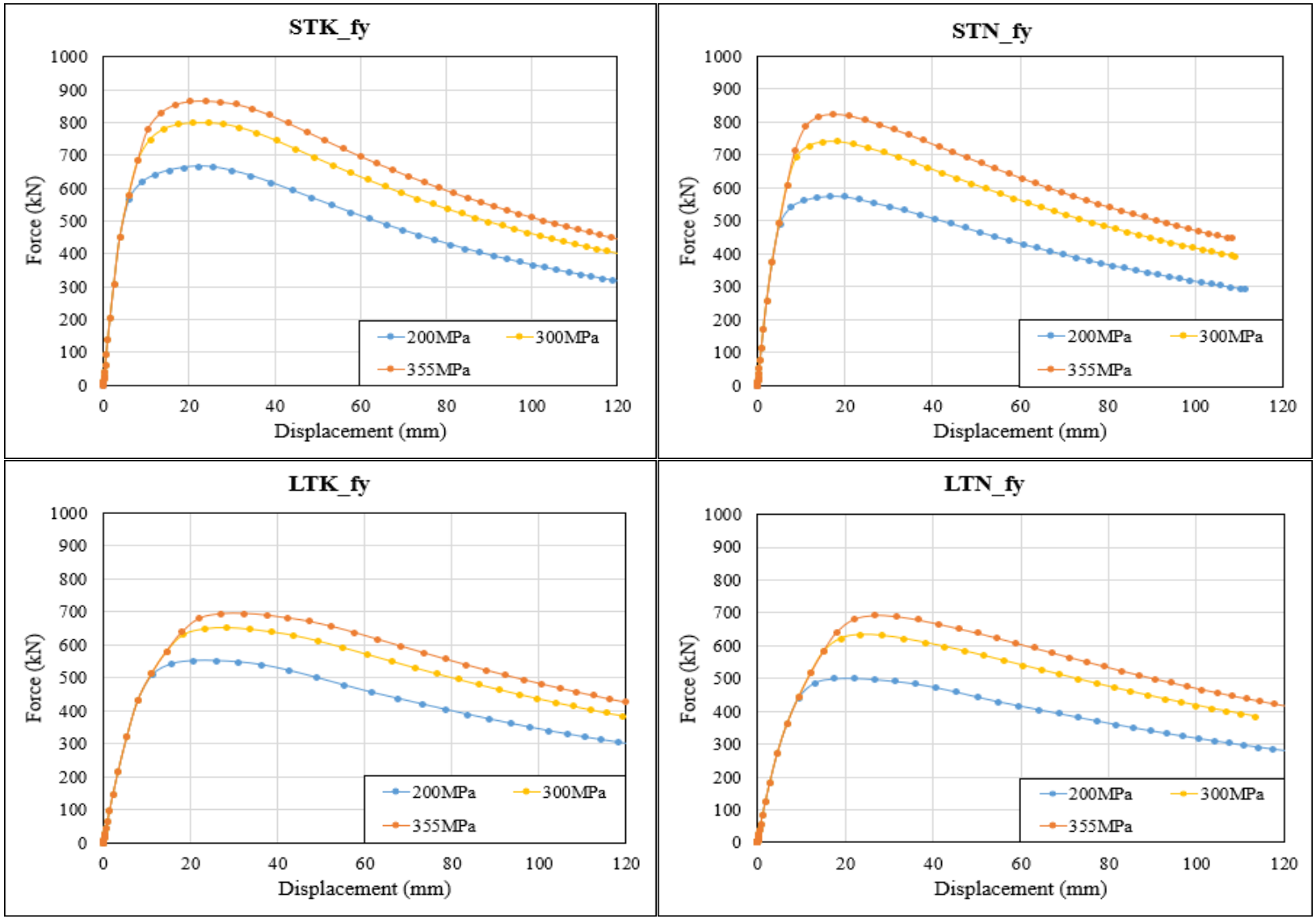

Figure 4.7: The effect of increasing the steel strength on the column's peak load

From Figure 4.7, it can be observed that an increase in the steel strength results in an increase in the column's axial load carrying capacity. Further observations are obtained from analysing the results presented in Table 4.5.

Table 4.5: Percentage change in column peak axial loads obtained for different steel strength magnitudes

Steel strength (MPa)	**STK (%) (Base response = 799 kN)**	**STN (%) (Base response = 740 kN)**	**LTK (%) (Base response = 654 kN)**	**LTN (%) (Base response = 633 kN)**
200	-16.6	-22.3	-15.3	-20.9
300	**-**	**-**	**-**	**-**
355	8.3	11.4	6.6	9.5

From Tables 4.5, it is observed that an increase in steel tube strength results in an increase in column's axial load carrying capacity. The change in steel strength has a greater effect on the TN models compared to the TK models.

Figure 4.8 is a graphical representation of the column's peak axial load response to changes in steel tube strength.

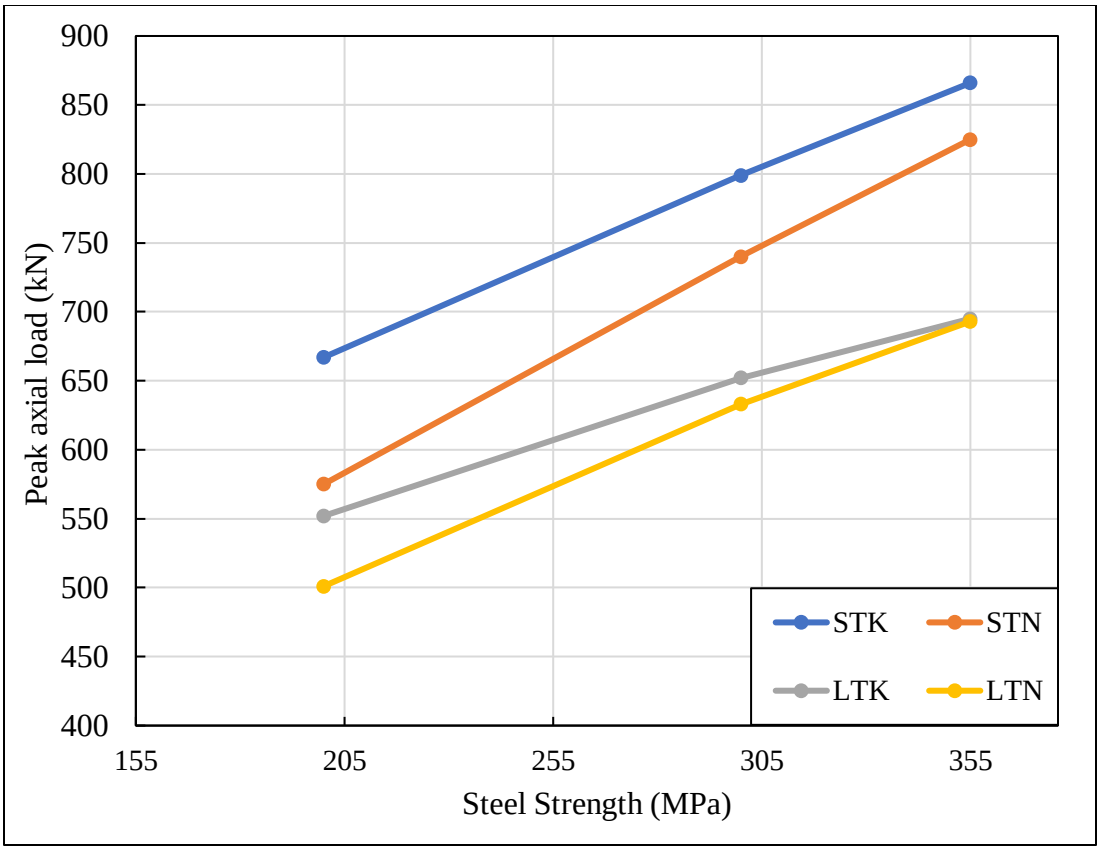

Figure 4.8: Column's peak axial load response to change in steel strength.

Figure 4.8 portrays another novel observation not observed in previous research studies. For a column with different cross sections, TN and TK, but with the same length (S or L), the initial TK models have a greater peak load when steel tubes are 200MPa compared to the TN models, however the TN model's peak load increases at a greater percentage than the TK columns as the steel tube strength increases. In Figure 4.8, the LTK and LTN columns with 355MPa steel strength have similar axial carrying load capacity, compared to a 10.4% difference at a steel strength of 200 MPa. It is counterintuitive that the TN column models with smaller concrete infill will produce similar peak loads compared to the TK models as observed in the LTK and LTN columns when the steel tube strength is increased from 200 to 355MPa. Therefore, an increase in steel tube strength has a greater effect on the peak axial load of columns with thinner concrete cross sections compared to those with thicker concrete cross sections. The short columns show a similar trend in that as the steel strength increases, the TK and TN peak loads converge.

Depending on the cost of the steel tubes and concrete, the results presented in Tables 4.1 to 4.8 is helpful in choosing the most efficient approach in increasing the column's axial load carrying capacity. Therefore, an analysis of all the parameters discussed in Sections 4.1 to 4.4 can assist in determining which method will be the most efficient in increasing the column's axial load carrying capacity. If unit prices of steel tube thicknesses, steel strength and concrete strength are taken into consideration, the results obtained in Section 4.1 to 4.4 will serve as a guide in choosing the most efficient and economical combination of parameters to obtain a desired column peak axial load.

4.5 Effect of Column Curvature on the Ultimate Load

Circular steel tubular columns measured in the laboratory showed that columns were not manufactured perfectly straight. These columns tend to have an initial curvature at mid length. The column curvature was observed to be insignificant of a few millimeters with the imperfection undetected to the human eye. A 2mm curvature imperfection was measured on the 2.5m long tubular column, which is undetectable to the human eye.

In the case of this experiment, the base model was considered having an initial curvature of 2mm.

A sensitivity analysis was therefore conducted to study the effect of the column's curvature on the axial load carrying capacity of the column. The column's curvature dimensions examined were 0mm, 0.5mm (for the short columns), 0.7mm (for the long columns), 1mm, 2mm (base model value), 3mm and 5mm. The reason why 0.5mm and 0.7mm was investigated for the short and long columns, respectively, is that An *et al* (2012) suggested an initial geometric imperfection value L/5000, where L represents the column length. Since the short column is 2.5m long and the long column is 3.5m in length, their geometric imperfection values were calculated as 0.5mm and 0.7mm, respectively.

The axial load versus midspan displacement graphs representing the different column responses to curvature change are shown in Figure 4.9.

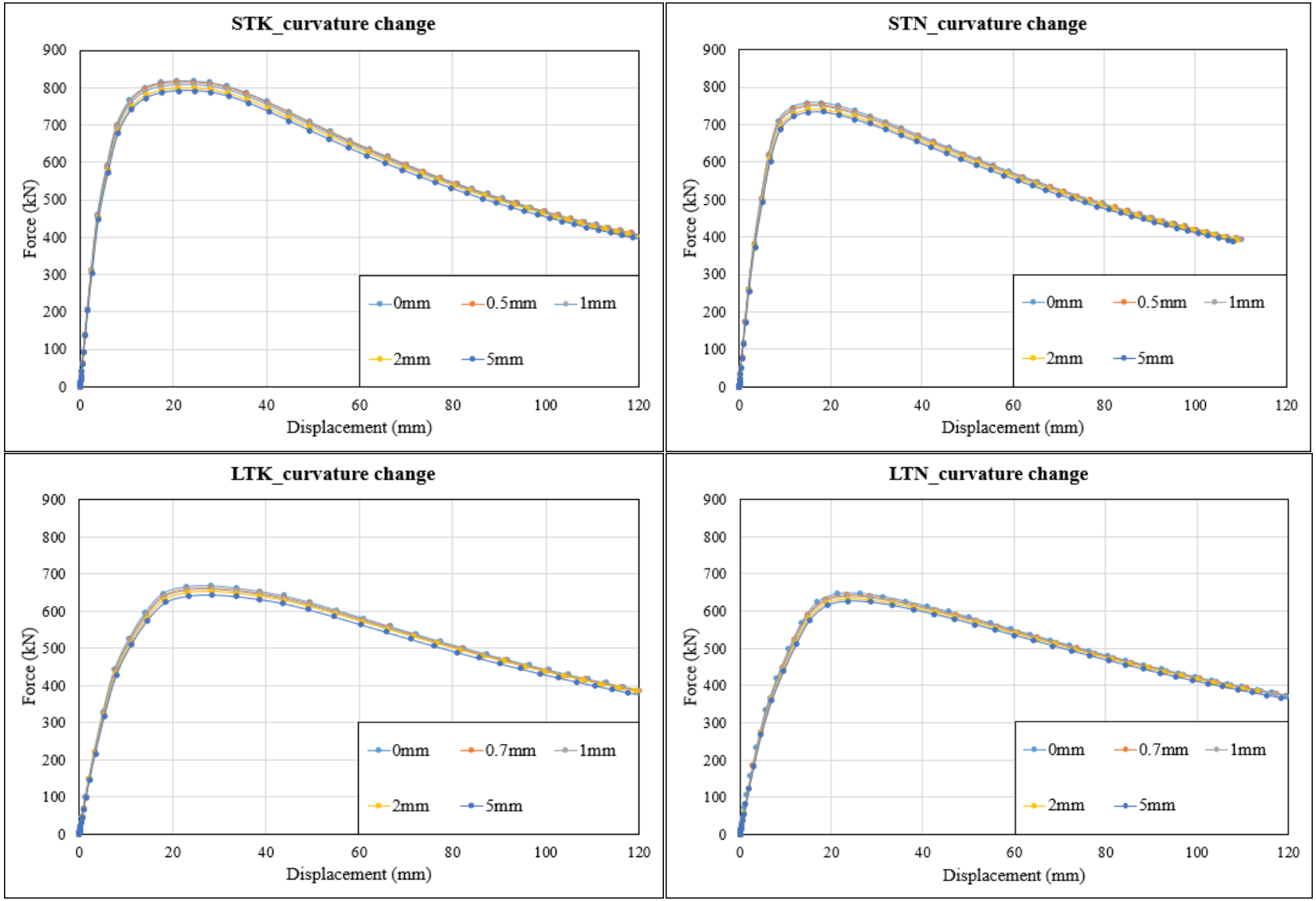

Figure 4.9: The effect of column curvature on the column's peak load

From Figure 4.9 it is observed that the impact of the change in curvature on the column's peak load is insignificant. An increase in column curvature results in a decrease in the column's axial load carrying capacity. Further observations are obtained from analysing the results presented in Table 4.6.

Table 4.6 presents the peak axial load of the columns for a change in the column curvature in terms of percentage using the 2mm response as the base.

Table 4.6: Percentage change in peak axial loads resulting from different column curvature magnitudes

Column curvature (mm)	**STK (%) (Base response = 799 kN)**	**STN (%) (Base response = 740 kN)**	**LTK (%) (Base response = 654 kN)**	**LTN (%) (Base response = 633 kN)**
0	2.5	2.3	2.6	2.4
0.5	1.8	1.7	-	-
0.7	-	-	1.6	1.6
1	1.2	1.2	1.3	1.2
2	**0**	**0**	**0**	**0**
5	-1.1	-0.9	-1.2	-1.0

From Tables 4.6, it is observed that an increase in column curvature results in a decrease in the column's axial load carrying capacity. The change in column curvature is observed to have a similar effect on all the column models. The column's peak load response to a change in column curvature is constant across the columns investigated.

Figure 4.10 shows the effect of increasing the column curvature on the peak load of the columns.

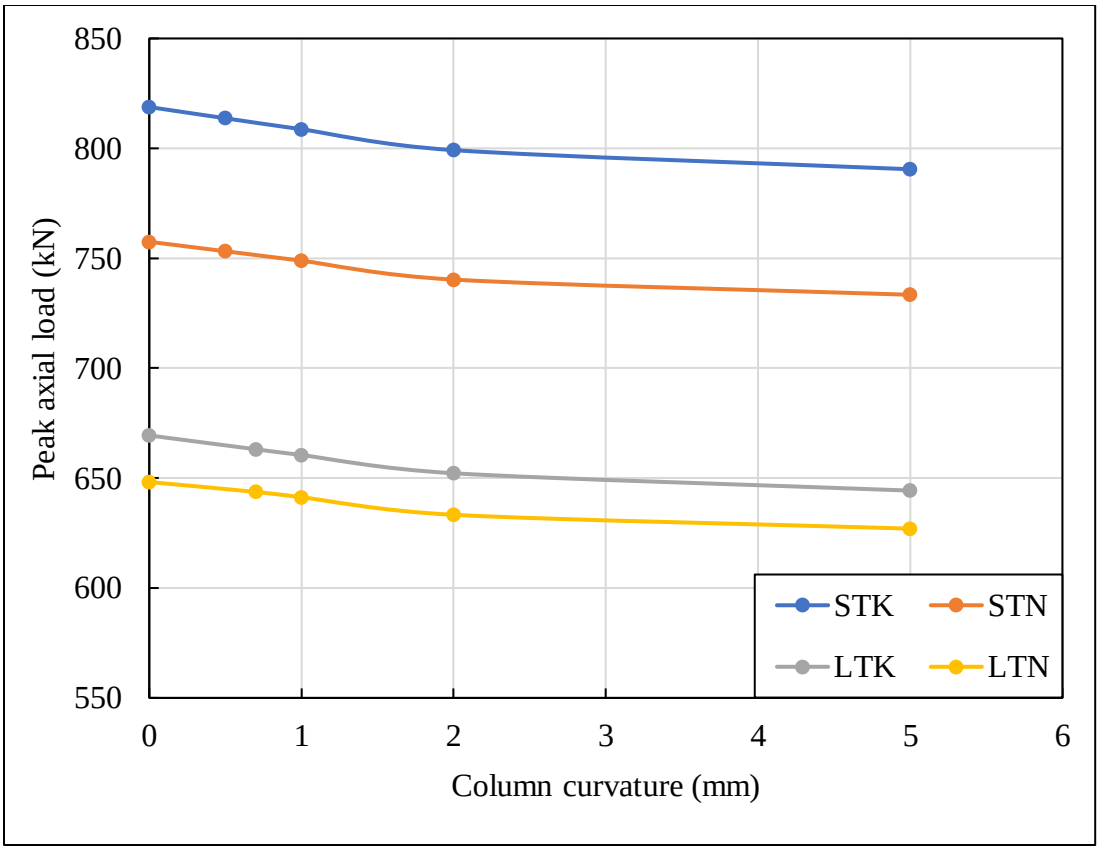

Figure 4.10: Column's peak axial load response to change in column curvature

Figure 4.10 shows an almost linear decrease in the column's peak load for a corresponding increase of the column's curvature. The difference in the peak loads is approximately the same across all the column models.

4.6 Effect of Load Eccentricity on the Ultimate Load

In practice, columns are loaded with some degree of eccentricity. The codes of practice also require the load to be applied eccentrically (SANS (10100-1) and EN 1992-1-1). A sensitivity analysis was therefore conducted to study the column's response to different load eccentricity magnitudes. Figure 4.11 presents the axial load versus midspan displacement response obtained by varying the load eccentricity on the cross section of the columns. The base model of each column was loaded with an eccentricity of 20mm, with eccentricity variations of 0mm, 1mm, 3mm, 6mm, 9mm, 12.5mm and 16mm.

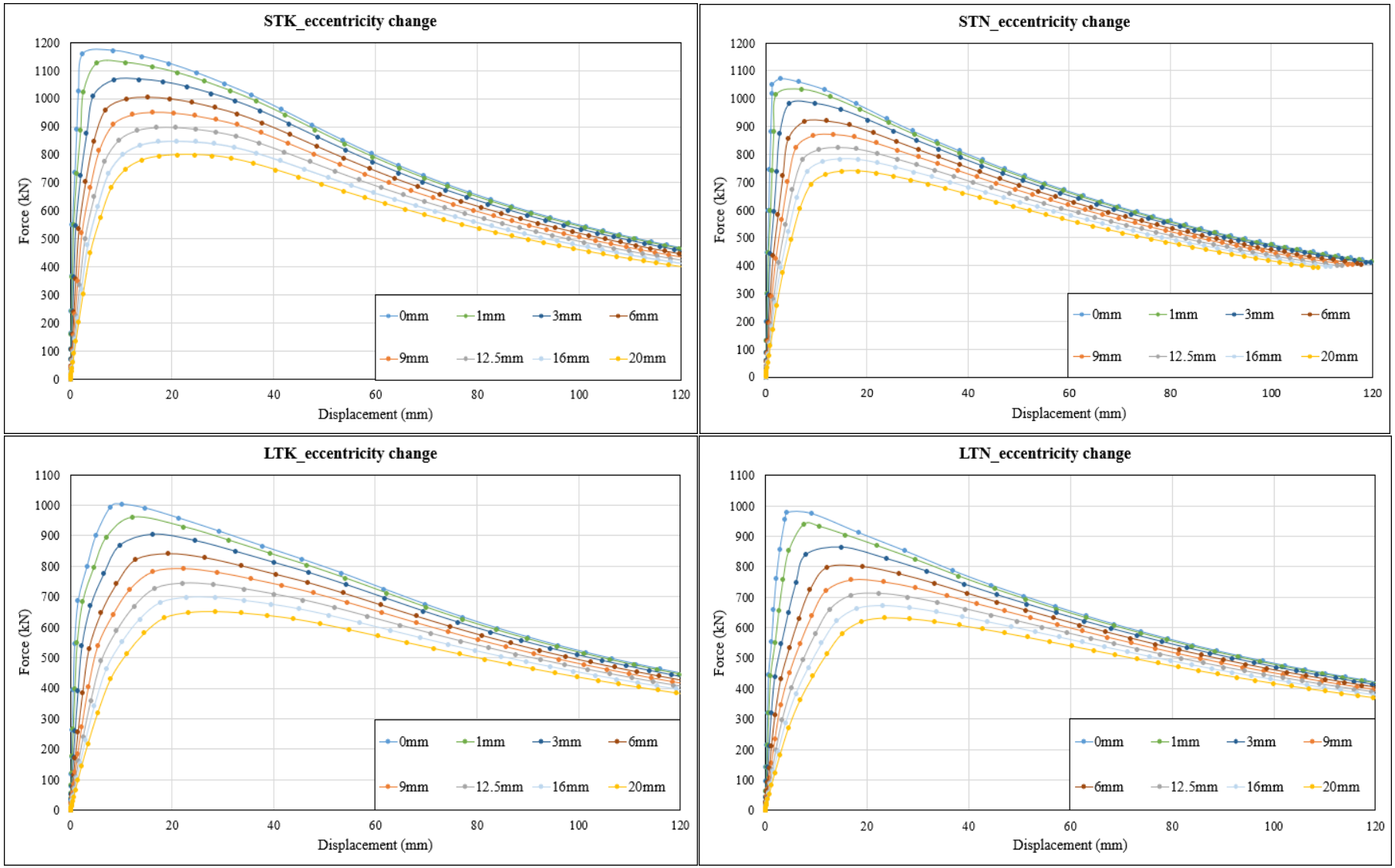

Figure 4.11: The effect of load eccentricity on the column's peak load

From Figure 4.11, it can be observed that an increase in the column's load eccentricity results in a decrease in the column's axial load carrying capacity. The increase in load eccentricity is observed to have a similar effect on all the column models investigated. Further observations are obtained from analysing the results presented in Table 4.7.

Table 4.7 presents the peak axial load of the columns for a change in the load eccentricity in terms of percentage using the 20 mm response as the base.

Table 4.7: Percentage change in the column's peak axial load obtained for different load eccentricity magnitudes

Eccentricity (mm)	**STK (%) (Base response = 799 kN)**	**STN (%) (Base response = 740 kN)**	**LTK (%) (Base response = 654 kN)**	**LTN (%) (Base response = 633 kN)**
0	46.7	45	54.9	54.7
1	41.2	39.9	47.4	48.5
3	33.7	32.7	38.8	36.7
6	25.8	24.5	29.3	26.4
9	19.1	17.8	21.8	19.6
12.5	12.3	11.5	14.0	12.5
16	6.3	5.8	6.9	6.3
20	**0**	**0**	**0**	**0**

A review of Table 4.7 leads to the observation that the column's peak axial load reduces by an average of 2.3% per 1 mm eccentricity for the short columns and 2.7% per mm for the long columns. Furthermore, it is also observed that the long columns are slightly more affected by the load eccentricity change than the short columns.

Figure 4.12 presents the effect of the load eccentricity on the peak load of the columns.

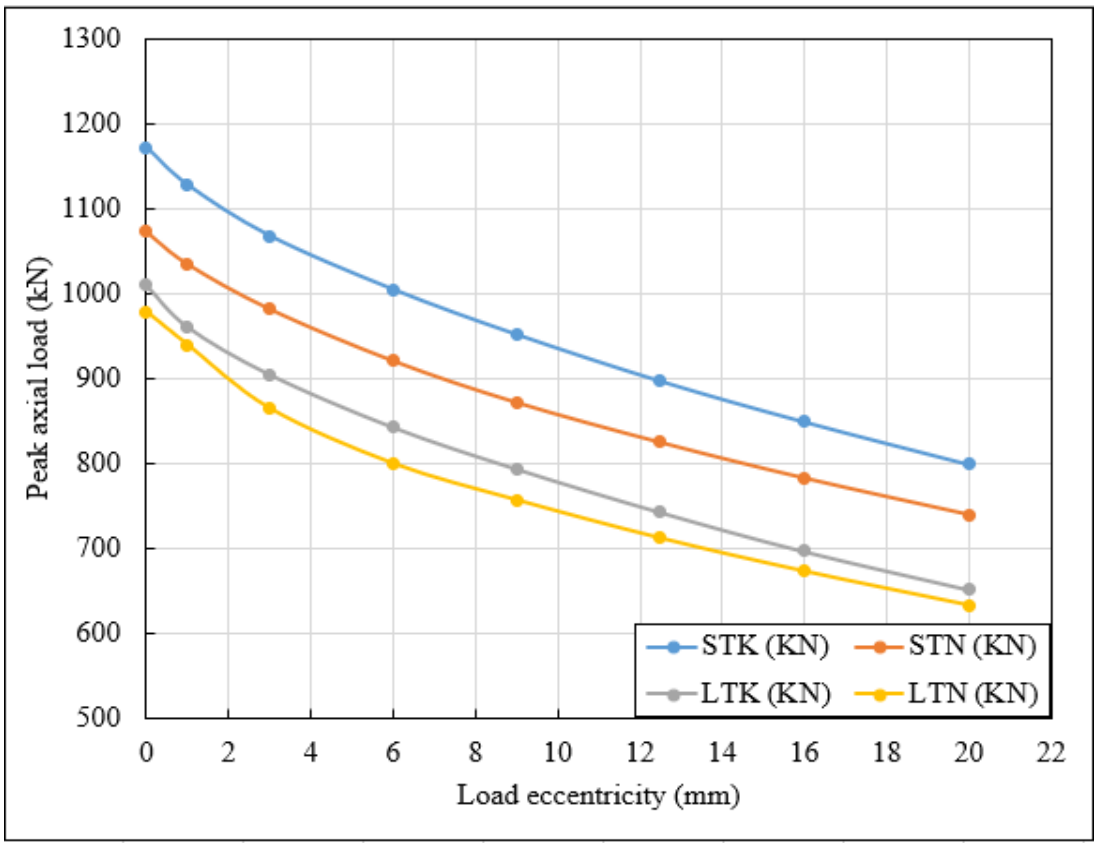

Figure 4.12: Column's peak axial load response to a change in the load eccentricity

From Figure 4.12 it is observed that the column's peak axial load and the load eccentricity have an inverse relationship. Therefore, an increase in the load eccentricity results in a decrease in the column's peak axial load. Also, from Figure 4.12 it can be observed that the column's response obtained by varying the load eccentricity is non-linear as that observed when the concrete strength and steel tube thicknesses are varied.

4.7 Effect of Fixity Conditions on the Ultimate Load

The column models in this research study were developed to replicate the pin support conditions Koen (2015) used in his experimental investigation. Thus, the FE models also used idealised pin support conditions. It should be noted that the FE model uses idealised support conditions which is not encountered in industry. The support conditions in industry varies between pin and fixed supports.

A sensitivity analysis was therefore conducted to examine the effect of using different types of column support. The column supports were changed from pin supports to fix supports. Figure 4.13 presents the axial load versus midspan displacement response obtained by varying the column fixity type.

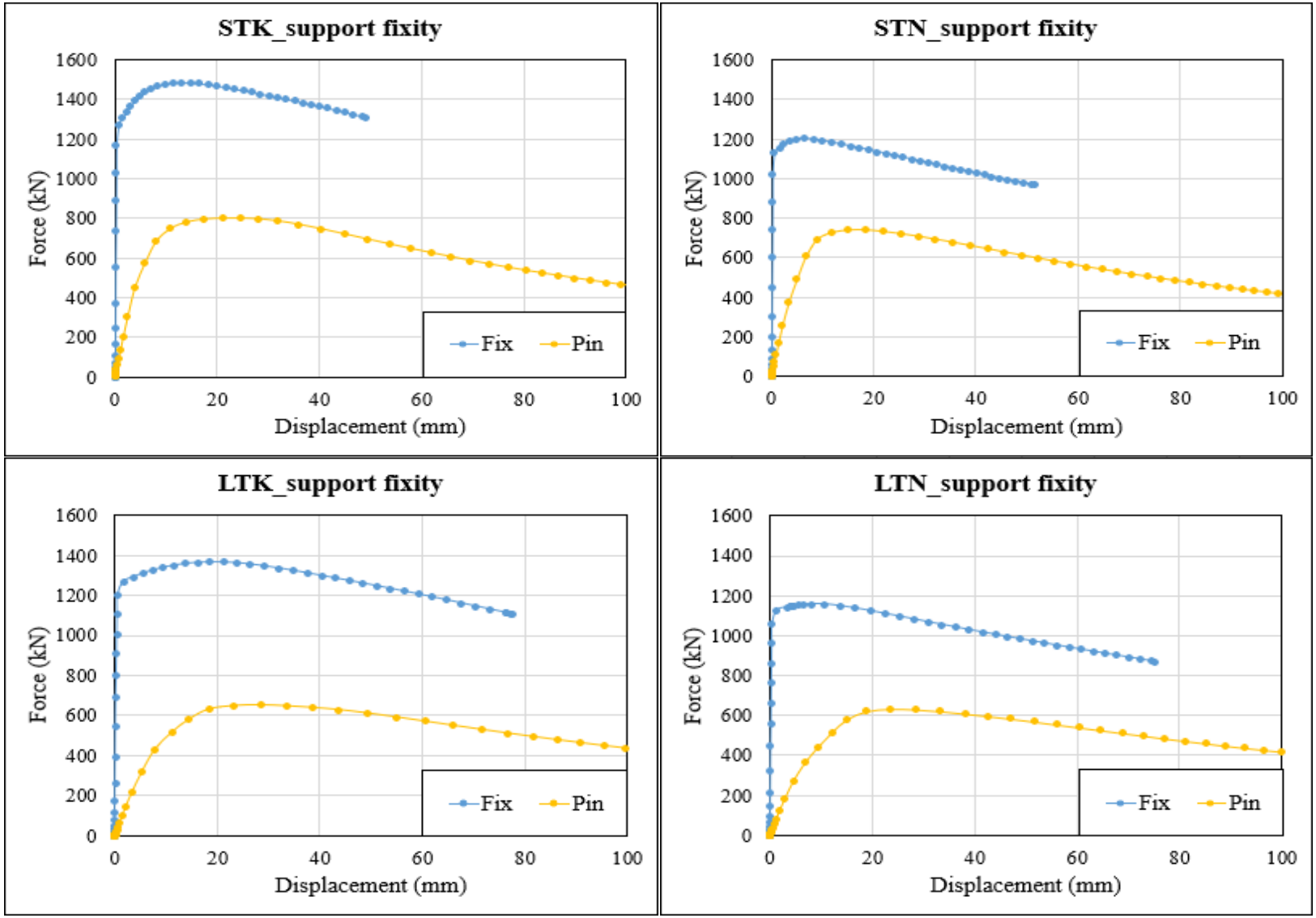

Figure 4.13: The effect of fixity on the column's peak load

An observation from Figure 4.13 shows that changing the supports from pin supports to fixed supports significantly increases the column's ultimate load, which is predominantly a result of a significant increase in the initial stiffness. The axial load carrying capacity of the fixed supported columns is approximately double of the pin supported columns.

Tables 4.8 presents the peak axial load of the columns for a change in support fixity in terms of percentage using the pin support response as the base.

Table 4.8: Percentage change in Column peak axial loads results obtained from changing the column support conditions

Support Fixity	**STK (%) (Base response = 799 kN)**	**STN (%) (Base response = 740 kN)**	**LTK (%) (Base response = 654 kN)**	**LTN (%) (Base response = 633 kN)**
Pin connection	**0**	**0**	**0**	**0**
Fix connection (top and bottom)	86.0	62.4	109.3	82.8

From Table 4.8 it is observed that a change in support condition from a pin support to a fixed support has a greater impact on the axial load carrying capacity of the long columns than the short columns. The increase is also more pronounced for the TK columns compared with the TN columns.

Figure 4.14 shows the effect of changing the support fixity on the peak load of the columns.

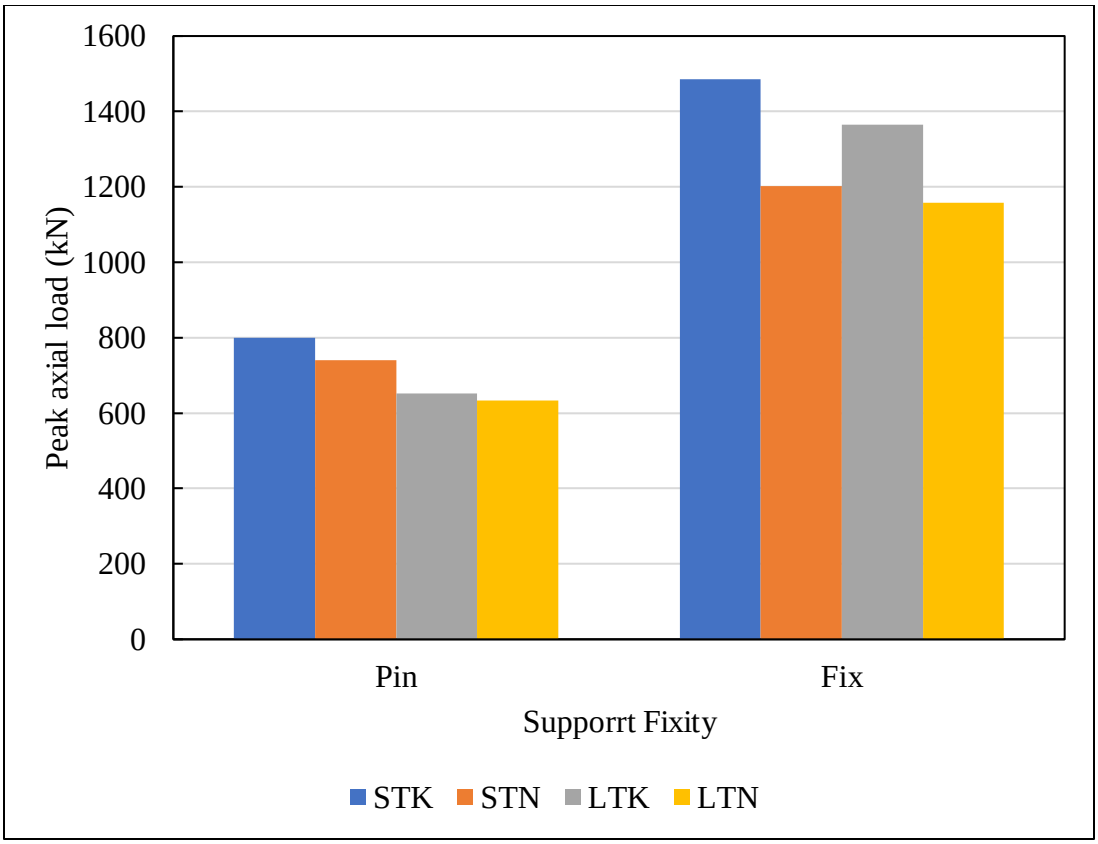

Figure 4.14: Column's peak axial load response to change in support fixity

From Figure 4.14 the fixed supported LTK column is observed to have a greater axial load carrying capacity than the fixed supported STN column. This, therefore, shows that a change in the column support conditions has a greater impact on columns with a thicker concrete cross section than on columns with a thinner concrete cross section. The response of the with fixed supports do not follow the normal behaviour of the pin supported columns.

4.8 Effect of the Concrete Damage Plasticity parameters on the Ultimate Load

The various parameters governing the concrete damage plasticity have already been discussed at length in this study under section 3.3.4.1.1.4. In this section a sensitivity analysis was conducted on these parameters to determine the impact they have on the column's response.

4.8.1 Effect of the Viscosity Parameter (μ) on the Ultimate Load

The Viscosity parameter, μ, is used for the viscoplastic regularization of the constitutive equations. It allows the model to slightly exceed the plastic potential surface in certain insufficiently small solution steps.

A sensitivity study was conducted on the Viscosity parameter. Tao *et al* (2013) in their research study, stated that a default value of 0 should be adopted as the magnitude of the Viscosity parameter in the CDP model for the modelling of confined concrete.

Figure 4.15 presents the axial load versus midspan displacement response obtained by varying the magnitude of the Viscosity parameter. The base model of each column has a Viscosity parameter of 0, with the Viscosity parameter varying between -1 and 1.

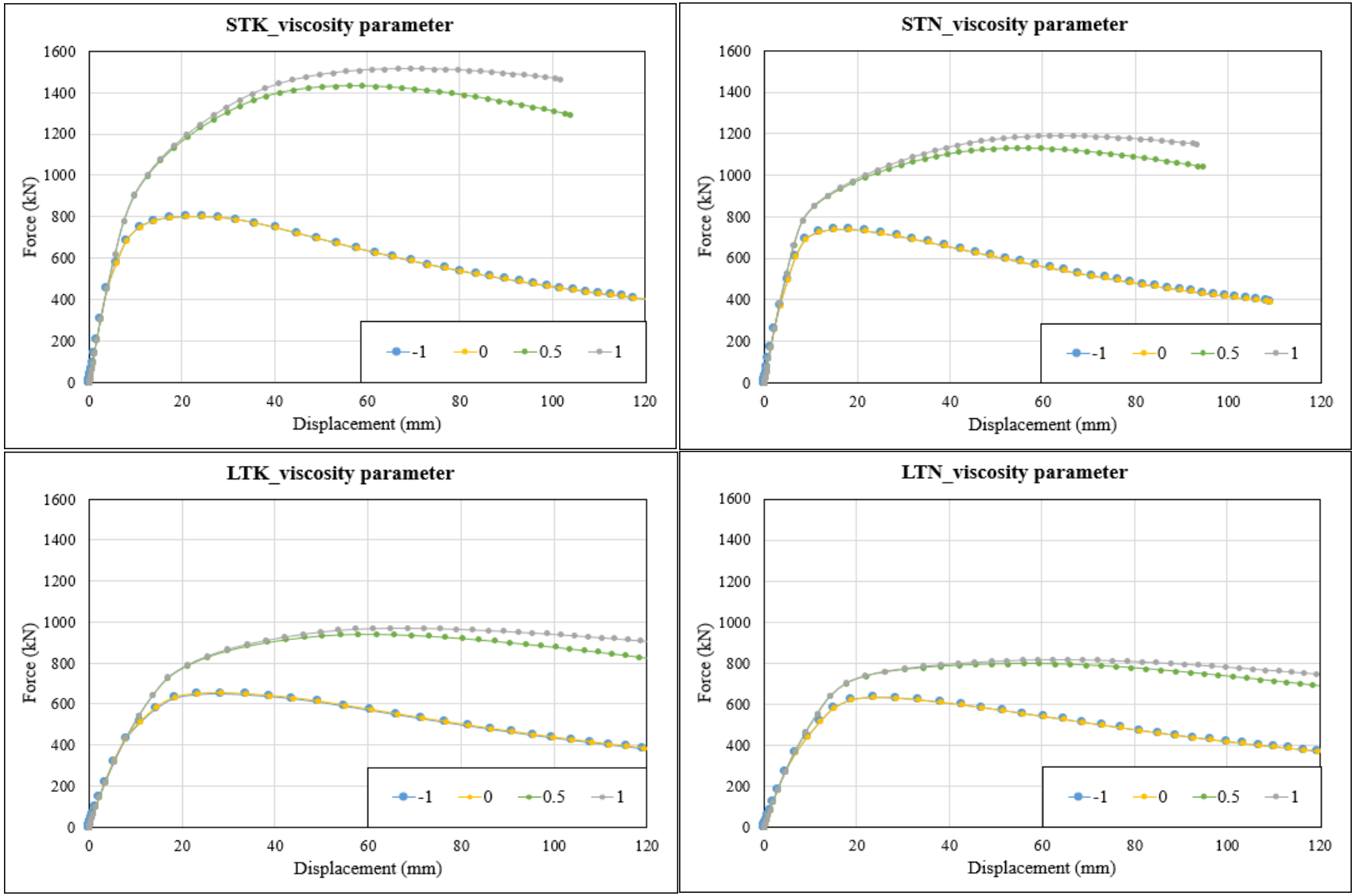

Figure 4.15: The effect of Viscosity parameter on the column's peak load

From Figure 4.15 it is observed that the responses for the Viscosity parameter of 0 and -1 lie on top of each other. This implies that the magnitude of the Viscosity parameter ≤ 0, has no effect on the load vs displacement response. However, magnitudes of the Viscosity parameter > 0 have a significant effect on the load vs displacement response. The effect of a small positive Viscosity parameter between 0 and 0.5 is significant on the load response, however the effect on the load response reduces for a Viscosity magnitude greater than 0.5.

Tables 4.9 presents the peak axial load of the columns for a change in the viscosity parameter in terms of percentage using the Viscosity parameter, μ = 0 response as the base.

Table 4.9: Percentage change in peak axial load, obtained from changing the Viscosity parameter

μ	STK (%) (Base response = 799 kN)	STN (%) (Base response = 740 kN)	LTK (%) (Base response = 654 kN)	LTN (%) (Base response = 633 kN)
-1	0	0	0	0
0	**0**	**0**	**0**	**0**
0.5	79.2	52.7	44.5	25.8
1	89.6	60.7	48.9	29.9

From Table 4.9 it is observed that accurate results are obtained when the magnitude of the Viscosity parameter ≤ 0, as observed by Tao *et al* (2013). Viscosity parameter magnitudes greater than 0, yields incorrect results. Therefore, based on the responses of the 4 columns it can be concluded that the magnitude of 0 as proposed by Tao *et al* (2013) is correct.

4.8.2 Effect of the Compressive Meridian (K_c) on the Ultimate Load

The Compressive Meridian parameter, K_c, is required for determining the yield surface of the concrete plasticity model. Equation 3.24 proposed by Yu *et al* (2010), is again presented for ease of flow and to view the composition of the Compressive Meridian parameter.

$$K_c = \frac{5.5}{5 + 2(f_c)^{0.075}}$$

The magnitude of the Compressive Meridian for the columns was obtained as 0.72. Han *et al* (2010), however, proposed a constant of 0.667 to represent the Compressive Meridian when modelling confined concrete using the CDP model. A sensitivity study was conducted on the Compressive Meridian to determine its effect on the axial load versus midspan displacement response which is presented in Figure 4.16. The base model of each column has a Compressive Meridian of 0.72.

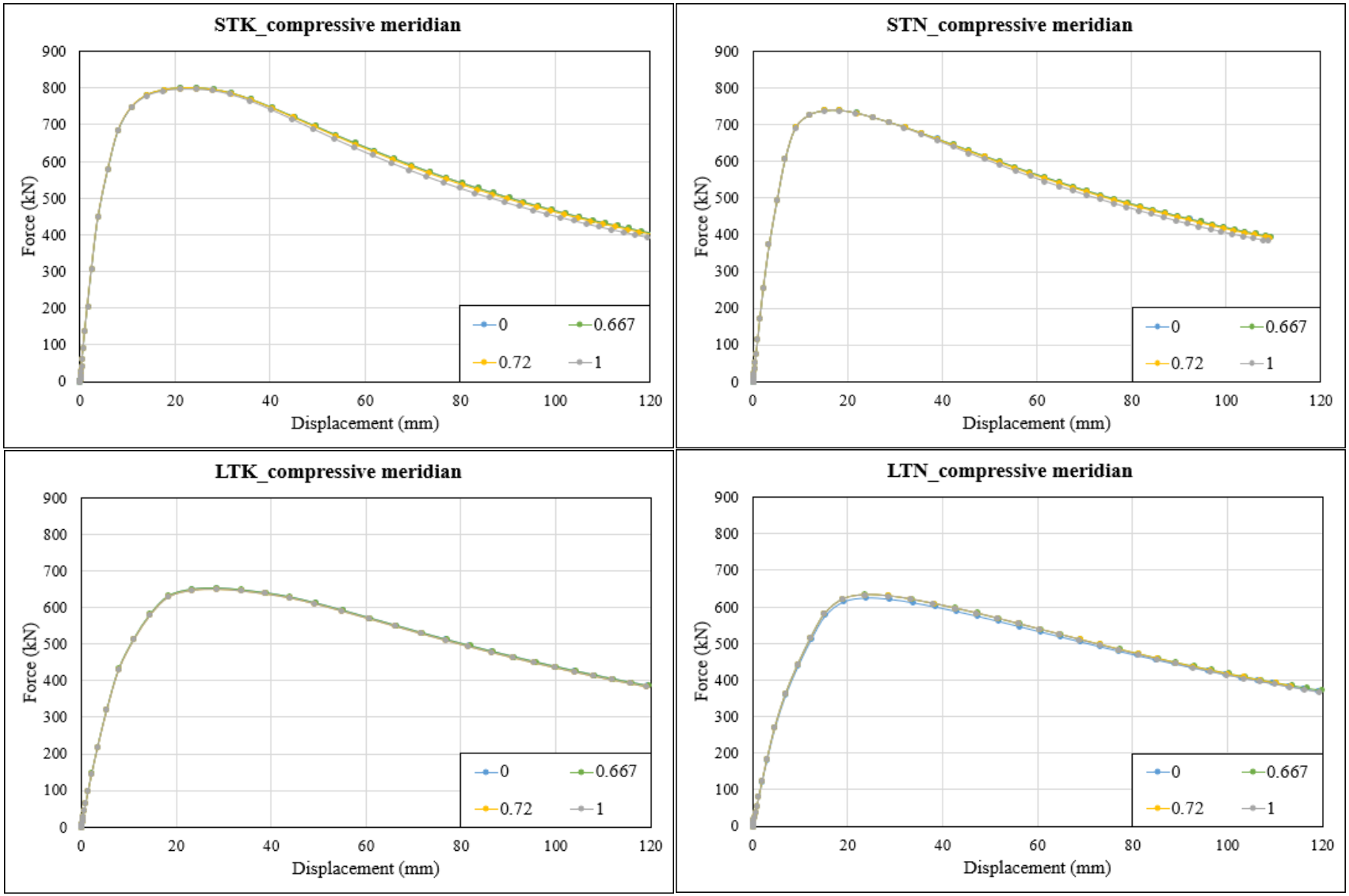

Figure 4.16: The effect of the Compressive Meridian on the column's peak load

Figure 4.16 shows that the change in the Compressive Meridian parameter has an insignificant effect on the axial force vs midspan displacement responses for all 4 columns, with a maximum percentage difference of less than 0.5%.

Table 4.10 presents the peak axial load of the columns for a change in the Compressive Meridian parameter in terms of percentage when a magnitude of 0.72 was used as the base response.

Table 4.10: Percentage change in peak axial loads in response to varying K_c

K_c	STK (%) (Base response = 799 kN)	STN (%) (Base response = 740 kN)	LTK (%) (Base response = 654 kN)	LTN (%) (Base response = 633 kN)
0	0.3	0.1	0.2	0.2
0.667	0.3	0.1	0.2	0.2
0.72	**0**	**0**	**0**	**0**
1	-0.4	-0.1	0	0

From Tables 4.10 it is observed that a percentage change of 0.3% is obtained when the column's Compressive Meridian parameter magnitude is changed from 0.667 to the calculated value of 0.72. Hence, using the default value proposed by Han *et al* (2010) is validated. Furthermore, a maximum percentage change of 0.4% is obtained when the column's Compressive Meridian parameter magnitude is changed from 0.72 to 1. Therefore, the column's response observed from using a Compressive Meridian parameter magnitude of unity (1) are similar to that obtained when a calculated value of 0.72 is used.

Hence, rather than using fractions to represent the magnitude of the Compressive Meridian parameter, it is proposed that a magnitude of 1 (unity) be implemented in the CDP model.

4.8.3 Effect of the Flow Potential Eccentricity (e) on the Ultimate Load

The Flow Potential Eccentricity, e, is defined as a small positive value which expresses the rate of approach of the plastic potential hyperbola to its asymptote. This parameter changes the shape of

the plastic potential meridian's surface in the stress space. From research work conducted by Tao *et al* (2013), a default value of 0.1 was proposed as the Flow Potential Eccentricity magnitude when modelling confined concrete.

A sensitivity study was conducted on the Flow Potential Eccentricity to determine its effect on the axial load versus midspan displacement response which is presented in Figure 4.17. The base model of each column has a Flow Eccentricity Potential magnitude of 0.1.

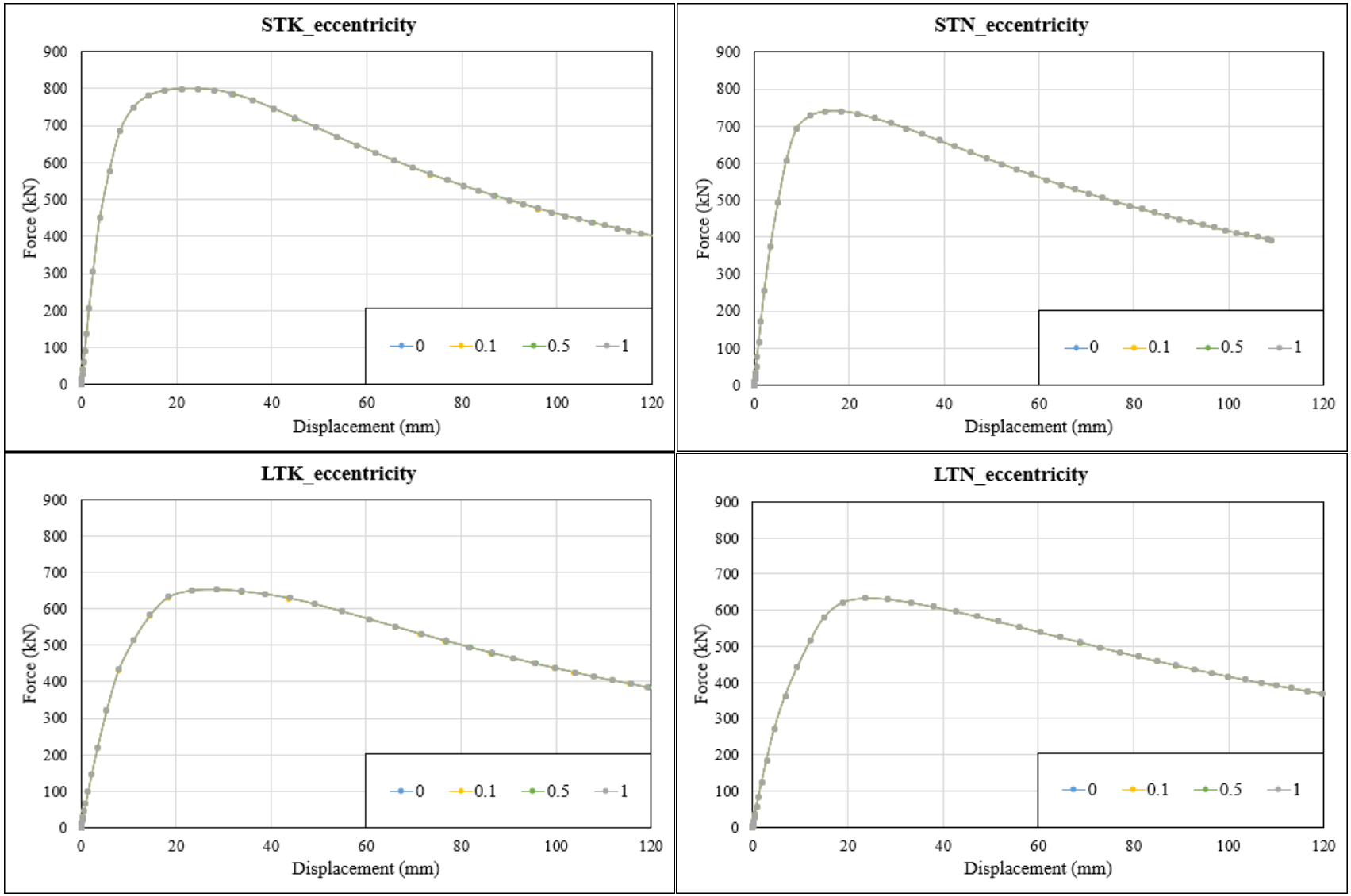

Figure 4.17: The effect of flow potential eccentricity on the column's peak load

Figure 4.17 shows that the change in the Flow Potential Eccentricity parameter has an insignificant effect on the axial force vs midspan displacement responses for all 4 columns.

Table 4.11 presents the peak axial load of the columns for a variation in Flow Potential Eccentricity values in terms of percentage using the Flow Potential Eccentricity magnitude of 0.1 as the base.

Table 4.11: Percentage change in peak axial loads obtained from varying e

e	**STK (%) (Base response = 799 kN)**	**STN (%) (Base response = 740 kN)**	**LTK (%) (Base response = 654 kN)**	**LTN (%) (Base response = 633 kN)**
0	0	0	0	0
0.1	**0**	**0**	**0**	**0**
0.5	0.003	0	0.003	0
1	0.013	0.003	0.012	0.002

From Tables 4.11 it is observed that varying the Flow Potential Eccentricity magnitude from 0 to 1 has an insignificant effect on the column's axial load carrying capacity. A percentage difference in column peak axial load of less than 0.02% is obtained when the column Flow Potential Eccentricity magnitude is changed from the default magnitude of 0.1 to 1 (unity).

Therefore, a value of unity (1) can conveniently be used as the default Flow Potential Eccentricity magnitude in the CDP model when modelling CFDST columns. In this research study a new default value of 1 (unity) is proposed for the Flow Potential Eccentricity magnitude when modelling confined concrete using the CDP model in ABAQUS.

4.8.4 Sensitivity to changes in Dilation angle (Ψ)

The Dilation angle, Ψ, is a material parameter determined from experimental data. This parameter is required by ABAQUS to determine the plastic flow potential. Equation 3.18, is presented for ease of flow and to view the contribution of the *Dilation angle parameter*.

$$\Psi = \begin{cases} 56.3(1-\xi_c) & for\ \xi_c \leq 0.5 \\ 6.672e^{\frac{7.4}{4.68+\xi_c}} & for\ \xi_c \geq 0.5 \end{cases}$$

Since the dilation angle is directly related to the confinement factor, the thick and thin columns are observed to have different dilation angles. From the calculation, the dilation angles for the TK columns was obtained as 24^0 while that of the TN columns was obtained as 19^0. Magnitudes of 20^0 and 30^0 are predominantly used by most researchers as the Dilation angle (Aziz *et al* (2017), Hassanein and Kharoob (2014), Hassanein *et al* (2017)).

A sensitivity study was conducted on the Dilation angle to determine its effect on the load response. Figure 4.18 presents the axial load versus midspan displacement response obtained by varying the magnitude of the Dilation angle. The base model of each column has a Dilation angle of 19^0 and 24^0 for the TN and TK columns, respectively.

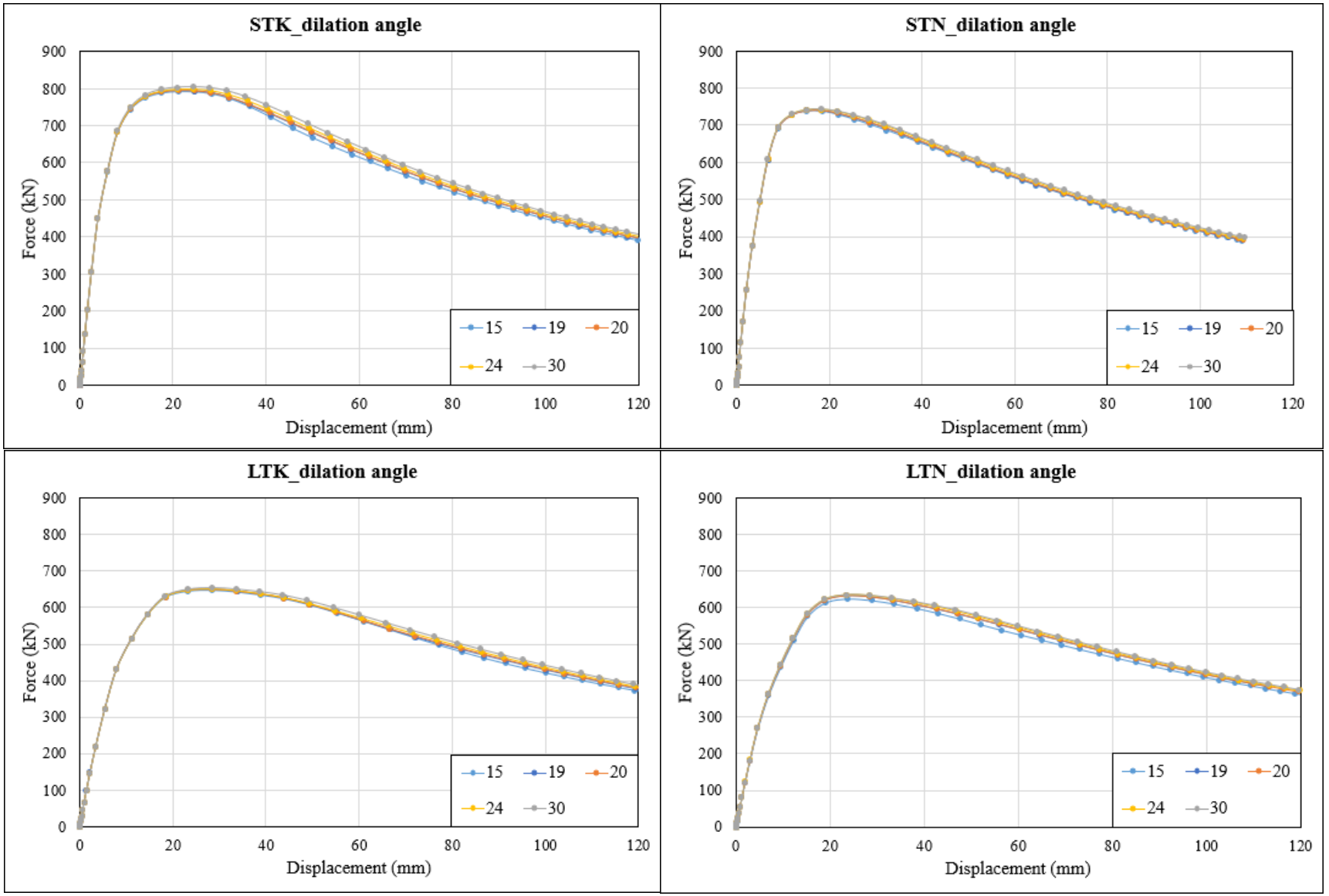

Figure 4.18: The effect of Dilation angle on the column's peak load

Figure 4.18 shows that the change in the Dilation angle parameter has an insignificant effect on the axial force vs midspan displacement responses for all 4 columns.

Table 4.12 presents the peak axial load of the columns in terms of percentage in response to variations in Dilation angle parameter with the Dilation angle magnitudes of 19^0 and 24^0 as the base for the TN and TK columns respectively.

Table 4.12: Percentage change in column peak axial load values obtained from changing Ψ magnitudes

Ψ (^{0})	**STK (%) (Base response = 799 kN)**	**STN (%) (Base response = 740 kN)**	**LTK (%) (Base response = 654 kN)**	**LTN (%) (Base response = 633 kN)**
15	-0.9	-0.3	-0.8	-0.2
19	/	**0**	/	**0**
20	-0.4	0.1	-0.5	0.2
24	**0**	/	**0**	/
30	0.8	0.5	0.3	0.3

From Tables 4.12 it is observed that a percentage change of -0.4% is obtained when the column's Dilation angle parameter magnitude is changed from the calculated value 19^0 and 24^0 (for the TN and TK columns respectively) to the assumed value of 20^0. Also, a percentage change of 0.8% is obtained when the column's Dilation angle parameter magnitude is changed from the calculated value 19^0 and 24^0 to the proposed value of 30^0.

From the observations made in Table 4.12, it is observed that a Dilation angle value of magnitude between 20^0 and 30^0 is adequate to be used as the default value to be implemented in the CDP model.

Hence, it is proposed that a default Dilation angle of 25^0 be implemented in the CDP model to represent the Dilation angle parameter.

4.8.5 Sensitivity to changes in the ratio of compressive strength under biaxial loading to uniaxial compressive strength (f_{bo}/f_c)

A magnitude of 1.16 has generally been used in research work to represent the magnitude of the Ratio of Compressive Strength under Biaxial Loading to Uniaxial Compressive Strength, f_{bo}/f_c. Equation 3.22 proposed by Papanikolaou and Kappos (2007) is presented for ease of flow and to view the composition of the Ratio of Compressive Strength under Biaxial Loading to Uniaxial Compressive Strength parameter.

$$\frac{f_{bo}}{f_c} = 1.5(f_c)^{-0.075}$$

Tao *et al* (2013) in their research study stated that a default value of 1.16 should be adopted as the Ratio of Compressive Strength under Biaxial Loading to Uniaxial Compressive Strength parameter magnitude in the CDP model for the modelling of confined concrete. A sensitivity study was conducted on the Ratio of Compressive Strength under Biaxial Loading to Uniaxial Compressive strength to determine its effect on the axial load versus midspan displacement response which is presented in Figure 4.19. The base model of each column has a Ratio of Compressive Strength under Biaxial Loading to Uniaxial Compressive strength magnitude of 1.15.

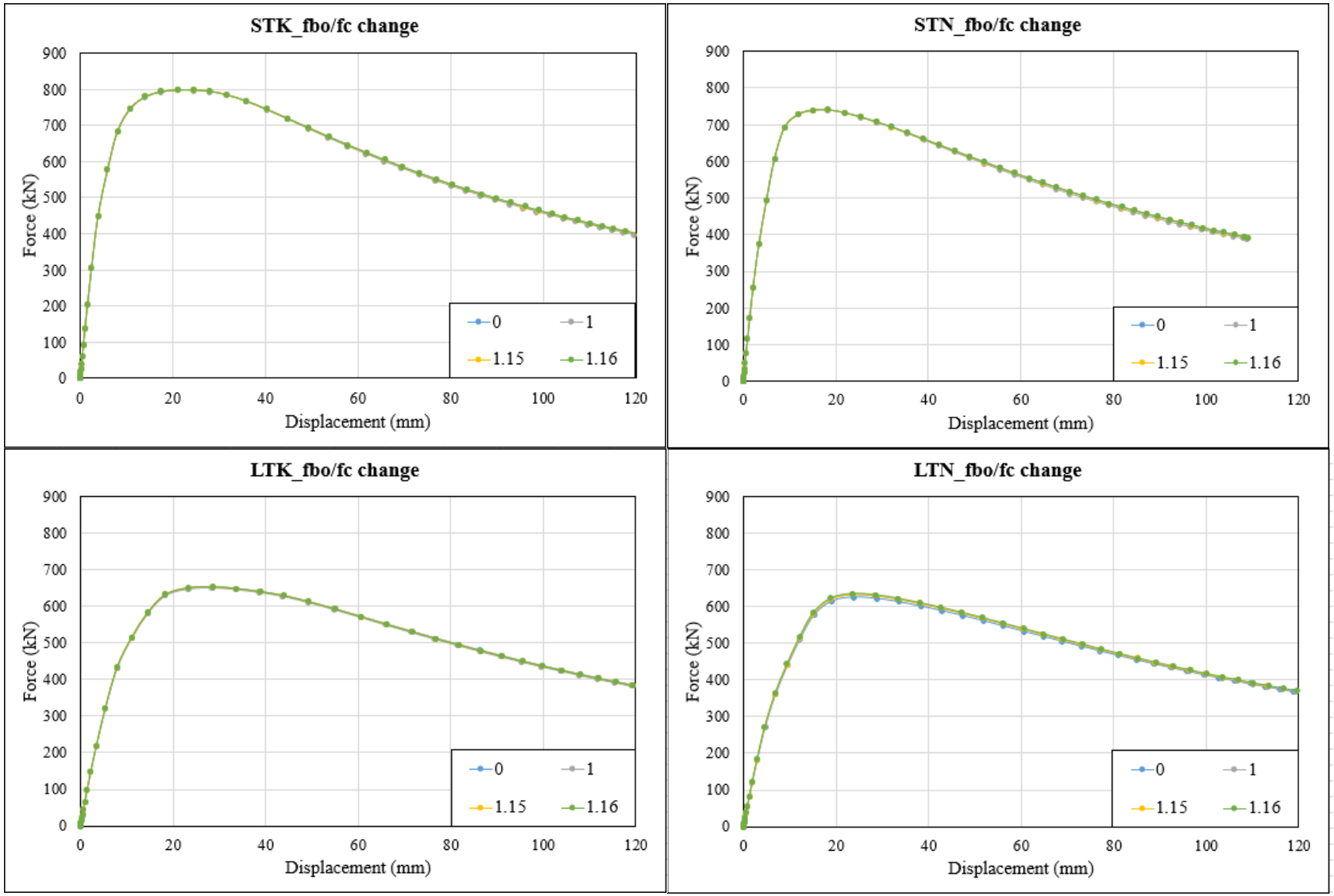

Figure 4.19: The effect of ratio of compressive strength under biaxial loading to uniaxial concrete strength (f_{bo}/f_c) on the column's peak load

Figure 4.19 shows that the change in the Ratio of Compressive Strength under Biaxial Loading to Uniaxial Concrete Strength parameter has an insignificant effect on the axial force vs midspan displacement responses for all 4 columns.

Tables 4.13 presents the peak axial load of the columns in response to varying the magnitude of the Ratio of Compressive Strength under Biaxial Loading to Uniaxial Concrete Strength parameter using the calculated value of 1.15 as the base.

Table 4.13: Percentage change of column peak axial load magnitude obtained from varying the f_{bo}/f_c magnitude

f_{bo}/f_c	**STK (%) (Base response = 799 kN)**	**STN (%) (Base response = 740 kN)**	**LTK (%) (Base response = 654 kN)**	**LTN (%) (Base response = 633 kN)**
0	0	0	0	0
1	-0.3	-0.1	0	0
1.15	**0**	**0**	**0**	**0**
1.16	0	0	0.3 %	0.3 %

From Table 4.13 it is observed that a percentage change of 0.3% is obtained when the column's Ratio of Compressive Strength under Biaxial Loading to Uniaxial Compressive Strength parameter magnitude is changed from the calculated value 1.15 to the proposed value of 1.16. Hence, using the default magnitude proposed by Tao *et al* (2013) is validated. Furthermore, a maximum percentage change of -0.3% is obtained when the column's Ratio of Compressive Strength under Biaxial Loading to Uniaxial Concrete Strength parameter magnitude is changed from 1.15 to 1. Therefore, the response of the columns observed from using a Ratio of Compressive Strength under Biaxial Loading to Uniaxial Concrete Strength magnitude of unity (1) are similar to those obtained when a calculated value of 1.15 is used.

Hence, rather than using fractions to represent the magnitude of the Ratio of Compressive Strength under Biaxial Loading to Uniaxial Concrete Strength parameter, it is proposed that a magnitude of

1 (unity) be implemented as the default magnitude of the Ratio of Compressive Strength under Biaxial Loading to Uniaxial Concrete Strength parameter.

CHAPTER 5

CONCLUSIONS AND RECOMMENDATIONS

5.1 OBJECTIVES

This research study focused on the FE modelling of eccentrically loaded CFDST slender columns. Koen's (2015) experimental work is used as a basis for calibrating and validating the eccentrically loaded FE CFDST column model developed. Also, a sensitivity analysis on certain parameters, most of which were not observed by previous researchers was conducted.

The objectives of this study were:

1. To calibrate a FE model which accurately predicts the behaviour of the STK column investigated by Koen (2015);
2. To use the FE STK column model as a generalised FE model, to accurately predict the behaviour of the 3 other columns; STN, LTK and LTN, tested by Koen (2015); and
3. To conduct parameter studies to critically analyse the sensitivity of the column responses to changes in load eccentricity, concrete and steel strength, curvature, fixity, inner and outer tube thicknesses and CDP parameter magnitudes.

All the objectives of this study were successfully achieved.

5.2 CONCLUSIONS

From literature reviewed and to the best knowledge of the author, no research study has been conducted on the development of a FE model which predicts the behaviour of eccentrically loaded CFDST slender columns. The FE model developed in this study accurately captures the behaviour of the axial load vs displacement response when the slender CFDST columns are subjected to eccentric loading, with a percentage difference of less than 3% between the FE model and experimental column responses.

During this study, the STK model was successfully calibrated. The modelling techniques used in calibrating the STK model was subsequently used to model the other columns, i.e. STN, LTK and LTN. After applying the changes to the length, outer tube and concrete diameters, and CDP parameters due to the cross section change, the STN, LTK and LTN models resulted in responses of 4.04%, -1.67% and 2.99% respectively. This was considered unacceptable since this error would be amplified during the sensitivity study and the degree of amplification is unknown. After careful review, it was observed that certain parameters required minor adjustment to ensure that the columns resulted in differences of less than 3% between the FE and experimental responses. Once the difference between the FE and experimental results were less than 3 %, the FE modelling approach was considered calibrated and properly validated. The FE models were thereafter used to conduct sensitivity analysis on changes in load eccentricity, concrete and steel strength, curvature, fixity, inner and outer tube thicknesses and CDP magnitudes.

Since a sensitivity analysis on 4 different columns was performed, the conclusions per parameter can be considered general, as opposed to previous researchers who generalised their work based on 1 column's sensitivity analysis.

A sensitivity analysis was performed to obtain the column's behaviour when the inner tube thickness was varied. It was observed that increasing the inner tube thickness of the columns result in an increase in the column's peak axial loads. The percentage increase in peak axial loads is greater for the columns with a thicker concrete cross section as compared to those with a thinner concrete cross section. For columns with the same length, the TK base models with inner tube thickness of 3mm have peak axial loads greater than that of the TN base column models. Yet, as the inner tube thickness increases, the TN models peak axial loads were observed to increase beyond that of the TK models.

Also, a sensitivity analysis was performed to obtain the column's behaviour when the outer tube thickness was varied. It was observed that an increase in the thickness of the outer tube resulted in a significant increase in the column's peak axial load. This change in thickness of the outer tube had a similar effect on all the columns, irrespective of their cross sections or length.

The effect of the concrete strength on the ultimate axial load of the columns was also investigated. It was observed that an increase in the column's concrete strength resulted in a significant increase in their peak axial load. This change in concrete strength was observed to have a slightly greater

effect on columns with a thicker concrete cross section compared to columns with a thinner concrete cross section.

A sensitivity analysis to study the effect of a change in steel strength on the ultimate load of the columns was conducted. It was observed that an increase in steel strength resulted in a significant increase in the column's peak axial load. This change in steel strength was observed having a greater effect on columns with thinner cross sections than on columns with thicker cross sections. This observation is opposite to what was observed when the concrete strength magnitude is varied, where the columns with thicker concrete cross sections showed greater increase in axial load as compared to those with thinner concrete cross sections.

A sensitivity analysis was performed to obtain the column's behaviour when the column curvature was varied. It was observed that an increase in the column curvature resulted in a decrease in the column's peak axial load. The impact of the change in curvature on the column's peak load was observed to be small. Also, the change in column curvature had a similar effect on all the column models, irrespective of their cross sections or length.

Also, a sensitivity analysis was performed to study the columns behavioural response to different load eccentricity magnitudes. It was observed that an increase in the column's load eccentricity resulted in a decrease in the column's axial load carrying capacity. The increase in load eccentricity is observed to have a similar effect on all the column models.

A sensitivity analysis was performed to obtain the column's behavioural response to different column fixity conditions. It was observed that changing the support fixity from pin to fix significantly increased the column's axial load carrying capacity due to a significant increase in the column's initial stiffness. The change in support fixity was observed to have a greater effect on the long column models compared to the short column models.

Another major observation was that some of the calculated and assumed concrete damaged plasticity (CDP) parameters had little or no change on the overall column model. After performing sensitivity analysis, new magnitudes proposed in this study to be used as default values for some of the CDP parameters are:

- Dilation angle (Ψ) = 25^0
- Compressive meridian (K_c) = 1

- Flow potential eccentricity (e) = 1
- Ratio of compressive strength under biaxial loading to uniaxial compressive strength (f_{bo}/f_c) = 1

The viscosity parameter, μ, remains zero (0) as suggested by Tao *et al* (2013).

5.3 RECOMMENDATIONS

- The FE model developed in this study accurately predicts the behaviour of eccentrically loaded circular CFDST columns. A similar study should be conducted in order to analyse and observe the behaviour of eccentrically loaded slender square and rectangular CFDST columns.
- Having obtained a working FE model able to predict the behaviour of circular CFDST slender columns, more research should be conducted to establish the best solutions on how these columns can be employed in civil engineering infrastructure.
- Finite element modelling, although being very accurate, is not very practical since most consulting engineers do not have the technical expertise and software to incorporate CFDST columns in their designs. In order to have CFDST columns used more in practice, mathematical models, which are an accurate and efficient computational and design technique need to be developed to allow implementation into design codes. Liang (2018) proposed a working mathematical model for determining the behaviour of circular CFDST slender columns. This model was developed with some assumptions such as:
    - The bond between concrete and steel tubes were assumed to be perfect,
    - The effect of concrete creep and shrinkage was ignored,
    - The local buckling of circular steel tubes was not considered,
    - Plane sections were assumed to remain plane after deformation, hence resulting in a linear distribution of strains through the depth of the cross-section,
    - Failure was assumed to occur when the concrete strain of the extreme compression fibre attained the maximum strain.

  Therefore, although Liang's (2018) mathematical model was observed to predict the behaviour of eccentrically loaded circular CFDST columns, the reliability of this model's accuracy remains questionable due to the many assumptions made in developing the model.

A more reliable model could be developed for predicting the behaviour of eccentrically loaded circular CFDST columns, taking in to account the effect of the parameters assumed by Liang (2018).

- Since most structural buildings make use of rectangular columns, it will be important to develop a mathematical model which accurately predicts the behaviour of eccentrically loaded square and rectangular CFDST columns.

CHAPTER 6

REFERENCES

ABAQUS. *Analysis User's Guide, Version 6.14*. Providence, RI: Dassault Systèmes Simulia Corp, 2014.

ABAQUS. *Standard User's Manual, Version 6.14*. Providence, RI: Dassault Systèmes Simulia Corp, 2014.

Alys, H. & Ben, S., 1999. *Structural Design for the Stage* (1st ed.). New Haven: Focal Press.

ACI. "Building code requirements for structural concrete and complementary", ACI-318-14. Detroit (USA): American Concrete Institute; 2014.

An, Y. F., Han, L. H. & Zhao, X. L., 2012. Behaviour and design calculations on very slender thin-walled CFST columns. *Thin-Walled Structures*, Volume 53, pp. 161–175.

Aziz, R. J., Al-Hadithy, L. K. & Resen, S. M., 2017. Finite element modelling of concrete filled double skin steel tubular columns under cyclic axial compression load. *Journal for Engineering Sciences*, Volume 20, Issue 2, pp. 326-340.

Bansal, R. K., 2010. A textbook of Strength of Materials, Laxmi Publications LTD, New Delhi.

Blake, A., 1986. *Handbook Of Mechanics, Materials, And Structures*. Wiley-Interscience, California.

Chen, W. F. & Chen, C. H., 1973. "Analysis of concrete filled steel tubular beam-columns." *International Association for Bridge and Structural Engineering Publications*, 33(11), pp. 37-52.

Dai, X. H. & Lam D., 2010. Numerical modelling of the axial compressive behaviour of short concrete-filled elliptical steel columns. *Journal of Construction Steel Research*, Volume 66, Issue 7, pp. 931–942.

Dai, X. H., Lam, D., Jamaluddin, N. & Ye, J., 2014. Numerical analysis of slender elliptical concrete filled columns under axial compression. *Thin-Walled Structures,* Volume 77, pp. 26–35.

DBJ/T13-51-2010. *Technical specification for concrete filled steel tubular structures*. Fuzhou, China: The Construction Department of Fujian Province; 2010[in Chinese].

Dong, C. X. & Ho, J., 2012. Uni-axial behaviour of normal-strength CFDST columns with external steel rings. *Steel and Composite Structures,* Volume 13, Issue 6, pp. 587-606.

Duggal, S. K., 2014. *Limit state design of steel structures* (2nd ed., pp. 327). McGraw Hill Education Private Limited, New Delhi.

Dundu, M., 2012. Compressive strength of circular concrete filled steel tube columns. *Thin-Walled Structures*, Volume 56, pp. 62-70.

Elchalakani, M., Zhao X. L. & Grzebieta, R. H., 2002. Tests on concrete filled double-skin (CHS outer and SHS inner) composite short columns under axial compression. *Thin-Walled Structures*, Volume 40, Issue 5, pp. 415–441.

Elchalakani, M., Karrech, A., Hassanein M.F. & Yang B., 2016. Plastic and yield slenderness limits for circular concrete filled tubes subjected to static pure bending. *Thin-Walled Structures*, Volume 109, pp: 50–64.

Ellobody, E., Young, B. & Lam, D., 2006. Behaviour of normal and high strength concrete filled compact steel tube circular stub columns. *Jounal of Constructional Steel Research,* Volume 62, Issue 7, pp. 706-715.

Espinós, A., Romero, M. L., Portolés, J. M. & Hospitaler A., 2014. Ambient and fire behaviour of eccentrically loaded elliptical slender concrete-filled tubular columns. *Journal of Constructional Steel Research,* Volume 100, pp. 97-107.

Essopjee, Y. & Dundu, M., 2015. Performance of concrete-filled double-skin circular tubes in compression. *Composite Structures,* Volume 133, pp. 1276-1283.

EN 1992-1-1. Eurocode 2: design of concrete structures. Part 1-1: general rules and rules for buildings. 2004.

Fanggi, B. A. L. & Ozbakkaloglu, T., 2013. Compressive behavior of aramid FRP-HSC-steel double-skin tubular columns. *Construction and Building Materials*, Volume 48, pp. 554-565.

Farahi, M., Heidarpour, A., Zhao, X. L. & Al-Mahaidi, R., 2016. Compressive Behaviour of Concrete-Filled Double-Skin Sections Consisting of Corrugated Plates. *Engineering Structures*, Volume 111, pp. 467-477.

Farojpourbonab, E., 2017. Effective parameters on the behaviour of CFDST columns. *Journal of Applied Engineering Science*, Volume 15, pp. 99-108.

Gardner, N. J. & Jacobson, E. R., 1967. Structural behaviour of concrete-filled steel tubes. *American Concrete Institute Journal*, 64(7), pp. 404-412.

GB50017-2003. Code for design of steel structures. Beijing: *China Planning Press*; 2003 [in Chinese].

Giakoumelis, G. & Lam, D., 2004. Axial capacity of circular concrete-filled tube columns. *Journal of Construction Steel Research*, Volume 60, Issue 7, pp. 1049–68.

Gopal, S. & Manoharan, P., 2006. Experimental behaviour of eccentrically loaded slender circular hollow steel columns in-filled with fibre reinforced concrete. *Journal of Constructional Steel Research*, Issue 62, pp. 513-520.

Haas, T. N. & Koen, A., 2014. Eccentric loading of CFDST columns. *World Academy of Science*, Engineering and technology.

Han, L. H. & Huo, J. S., 2003. Concrete-filled hollow structural steel columns after exposure to ISO-834 standard fire. *Journal of Structural Engineering*, Volume 129, Issue 1, pp. 68–78.

Han, L. & Yang, Y., 2001. Influence of concrete compaction on the behaviour of concrete filled steel tubes with rectangular sections. *Advances in Structural Engineering*, Volume 4, Issue 2, pp. 93-100.

Han, L.H., Li, W. & Bjorhovde, R., 2014. Developments and advanced applications of concrete filled steel tubular (CFST) structures: members. *Journal of Construction Steel Research*, Volume 100, pp. 211–228.

Han, L. H., Li, Y. J. & Liao, F. Y., 2011. Concrete-filled double skin steel tubular (CFDST) columns subjected to long-term sustained loading. *Thin-Walled Structures*, Volume 49, Issue 12, pp. 1534-1543.

Han, T. H., Stallings J. M., & Kang Y. J., 2010. Nonlinear concrete model for double-skinned composite tubular columns. *Construction and Building Materials*, Volume 24, Issue 12, pp. 2542–2553.

Hanswille, G., 2008. *Eurocode 4, Composite Columns* [Presentation]. Retrieved from https://eurocodes.jrc.ec.europa.eu/doc/WS2008/EN1994_4_Hanswille.pdf

Hassan, A., & Sivakamasundari, M. S., 2014. Study of Structural Strength and Behaviour of Concrete Filled Double Skin Columns. *International Journal of Engineering trends and technology*, Volume 18, Issue 6, pp. 272–275.

Hassanein, M. F. & Kharoub, O. F., 2014. Analysis of circular concrete-filled double skin tubular slender columns with external stainless steel tubes. *Thin-Walled Structures*, Volume 79, pp. 23-37.

Hassanein, M. F. & Patel, V. I., 2018. Round-ended rectangular concrete-filled steel tubular short columns: FE investigation under axial compression. *Journal of Constructional Steel Research*, Volume 140, pp. 222-236.

Hassanein, M. F., Elchalakani, M., Karrechi, A., Patel V.I. & Yang, B., 2018. Behaviour of concrete-filled double-skin short columns under compression through finite element modelling: SHS Outer and SHS inner tubes. *Structures*, Volume 14, pp. 358-375.

Hassanein, M. F., Elchalakani, M. & Patel, V. I., 2017. Overall buckling behaviour of circular concrete-filled dual steel tubular columns with stainless steel external tubes. *Thin-Walled Structures*, Volume 115, pp. 336-348.

Hassanein, M. F., Kharoob, O. F. & Liang, Q. Q., 2013. Circular concrete-filled double skin tubular short columns with external stainless steel tubes under axial compression. *Thin-Walled Structures*, Volume 73, pp. 252–263.

Ho, J. C. M. & Dong, C. X., 2014. Improving strength, stiffness and ductility of CFDST columns by external confinement. *Thin-Walled Structures*, Volume 75, pp. 18-29.

Hu H. T., & Su, F. C., (2011). Nonlinear analysis of short concrete-filled double skin tube columns subjected to axial compressive forces. *Marine Structures,* Volume 24, pp.319–337.

Hu, X. & Su, F., "Nonlinear analysis of concrete-filled double skin tube columns subjected to axial compressive forces", Abaqus Taiwan Users' Conference (2010).

Hu, H. T. & Schnobrich, W. C., 1989. Constitutive modelling of concrete by using none associated plasticity. *Journal of Materials in Civil Engineering*, Volume 1, Issue 4, pp. 199–216.

Huang, H., Han, L. H., Tao Z., & Zhao, X. L., 2010. Analytical behaviour of concrete-filled double skin steel tubular (CFDST) stub columns. *Journal of Constructional Steel Research*, Volume 66, Issue 4, pp. 542–55.

Ibañez, C., Romero, M., Espinos, A., Portolés, J. M. & Albero, V., 2017. Ultra-high strength concrete on eccentrically loaded slender circular concrete-filled dual steel columns. *Structures*, Volume 12, pp. 64-74.

İpek, S. & Güneyisi, E. M., 2019. Ultimate axial strength of concrete-filled double skin steel tubular column sections. *Advances in Civil Engineering*, Volume 2019, Article ID 6493037.

Johansson, M., 2002. *Composite Action and Confinement Effects in Tubular Steel-Concrete Columns*. Ph.D. thesis, Chalmers University of Technology, Goteborg, Sweden.

Karim, S. A. & Ipe, B., 2016. Comparative study on CFRP concrete filled double skin tube (CFDST) columns. *International Journal of Innovative Research in Technology*, Volume 3, Issue 4, pp. 148-155

Koen, J. A., 2015. *An investigation into the axial capacity of eccentrically loaded concrete filled double skin tube columns*. MSc Thesis, Stellenbosch University.

Krunal, R. (2020, January 31). CivilJungle. *Difference between short column and long column*. Retrieved from https://civiljungle.com/difference-between-short-column-and-long-column/

Kumari, B., 2018. Concrete filled steel tubular (CFST) columns in composite structures. *IOSR Journal of Electrical and Electronics Engineering*, Volume 13, Issue 1, pp.11-18.

Kurian, S. S., Paulose, D. & Mohan, S., 2016. Study on Concrete Filled Steel Tube, *IOSR Journal of Mechanical and Civil Engineering*: ISSN:2278-1684, pp 25-33.

Li, W., Ren, Q. X., & Han L. H., 2012. Behaviour of tapered concrete-filled double skin steel tubular stub columns. *Thin-walled structures*, Volume 57, pp. 37-48.

Liang, Q. Q., 2018. Numerical simulation of high strength circular double-skin concrete-filled steel tubular slender columns. *Engineering Structures*, Volume 128, pp. 205-217.

Liang, Q. Q. & Fragomeni, S., 2009. Nonlinear analysis of circular concrete-filled steel tubular short columns under axial loading. *Journal of Constructional Steel Research*, Volume 65, pp. 2186-2196.

Liew, J. Y. R. & Xiong, M., 2015. *Design Guide for Concrete Filled Tubular Members with High Strength Materials to Eurocode 4*. Research Publishing, Chennai.

Lin, C. Y., 1988. "Axial capacity of concrete infilled cold formed steel columns." Proc. of Ninth International Specialty Conference on Cold-Formed Steel Structures. St. Louis, Missouri, USA.

Lin, M. L. & Tsai, K. C., 2001. *Behavior of double-skinned composite steel tubular columns subjected to combined axial and flexural loads*. In: Proceedings of the first international conference on steel & composite structures, pp. 1145–52.

Lu, H., Zhao, X. L. and Han, L. H., 2010. Fire performance of self-consolidation concrete filled double skin tubular columns: experiments. *Fire Safety Journal*, Volume 45, Issue 2, pp. 106-115.

Lu, Z. H. & Zhao, Y. G., 2010. Suggested empirical models for the axial capacity of circular CFT stub column. *Journal of Constructional Steel Research*, 66, pp. 850-862.

Mander, J. B., Priestley, M. J. N., & Park, R., 1988. Theoretical Stress-Strain Model for Confined Concrete. *Journal of Structural Engineering*, ASCE, V.114, No. 8, p. 1827- 1849.

Montague, P., 1978. The experimental behaviour of double skinned, composite, circular cylindrical shells under external pressure. *Journal of Mechanical Engineering Science* 1978, Volume 20, Issue 1, pp. 21–34.

Mursi, M. & Uy, B., 2003. Strength of concrete filled steel box columns incorporating interaction buckling. *Journal of Structured Engineering* ASCE, Volume 129, Issue 5, pp. 626–639.

Naderi, M., Sheibani, R. & Shayanfar, M. A., 2009, Comparison of different curing effects on concrete strength. *3rd International conference on concrete &development***,** pp 507-516.

Pagoulatou, M., Sheehan, T., Dai, X. H. & Lam, D., 2014. Finite element analysis on the capacity of circular concrete-filled double-skin steel tubular (CFDST) stub columns. *Engineering Structures*, Volume 72, pp. 102–112.

Papanikolaou, V. K., & Kappos, A. J., 2007. Confinement-sensitive plasticity constitutive model for concrete in triaxial compression. *International Journal of Solids Structures*, Volume 44, Issue 21, pp. 7021–7048.

Portolés, J. M., Romero M. L., Bonet, J. L. & Filippou, F. C., 2011. Experimental study of high strength concrete-filled circular tubular columns under eccentric loading. *Journal of Constructional Steel Research*, Volume 67, Issue 4, pp. 623–633.

Ren, Q. X., Han, L. H., Lam, D., & Li, W., 2014. Tests on elliptical concrete filled steel tubular (CFST) beams and columns. *Journal of Constructional Steel Research*, Volume 99, pp. 149-160.

Richart, F. E., Brandzaeg A. & Brown, R. L. *A study of the failure of concrete under combined compressive stresses*. Bull. 185. Champaign (IL, USA): University of Illinois Engineering Experimental Station; 1928.

Romero, M. L., Ibañez, C., Espinos, A., Portolés, J. M. & Hospitaler, A., 2017. Influence of ultra-high strength concrete on circular concrete-filled dual steel columns. *Journal of Structures*, Volume 9, pp. 13-20.

Saenz, L. P., 1964. Discussion of Equation for the stress–strain curve of concrete by P. Desayi, and S. Krishnan. *Journal of American Concrete Institute*, Issue 61, pp. 1229-1235.

Schneider, S., Kramer, D. & Sarkkinen, D., 2004. The design and construction of concrete filled steel tube column frames. s.l., *13th World Conference on Earthquake Engineering*, Paper number 252.

Shanmugam, N.E. & Lakshmi, B., 2001. State of the art report on steel-concrete composite columns. *Journal of Constructional Steel Research*, Volume. 57, pp. 1041-1080.

Shen, Q., Wang, J., Wang, W. & Wang, Z., 2018. Performance and design of eccentrically-loaded concrete-filled round-ended elliptical hollow section stub columns. *Journal of Constructional Steel Research*, Volume 150, pp. 99-114.

SIMULIA, 2014. *ABAQUS 6-14 Documentation.* s.l.:s.n.

Soliman, K. Z., & Arafa, T. M., 2013. Review of design codes of concrete encased steel short columns under axial compression. *HBRC Journal*, Volume 9, Issue 2, pp. 134-143.

South African National Standard, 2000. SANS 10100-1: The Structural Use of Concrete. Part 1: Design.

Tao, Z., Han, L. H. & Zhao X. L., 2004. Behaviour of concrete-filled double skin (CHS inner and CHS outer) steel tubular stub columns and beam-columns. *Journal of Construction Steel Research*, Volume 60, Issue 11, pp.1129–1158.

Tao, Z. B., Uy, B., Liao, F. Y. & Han, L. H., 2011. Nonlinear analysis of concrete-filled square stainless steel stub columns under axial compression. *Journal of Construction Steel Research*, Volume 67, pp. 1719-1732.

Tao, Z., Wang, Z.-B. & Yu, Q., 2013. Finite element modelling of concrete-filled steel stub columns under axial compression. *Journal of Constructional Steel Research,* Volume 89, pp. 121–131.

Tsuda, K., Matsui, C. & Ishibashi, Y., 1995. "Stability design of slender concrete filled steel tubular columns." Proc. *Fifth Asia-Pacific Conference on Structural Engineering and Construction (EASEC-5)*.

Uenaka, K., Kitoh, H. & Sonoda, K., 2010. Concrete filled double skin circular stub columns under compression. *Thin-Walled Structures*, Volume 48, Issue 1, pp. 19–24.

Wan, C. Y. & Zha, X. X., 2016. Nonlinear analysis and design of concrete-filled dual steel tubular columns under axial loading. *Steel Composite Structures*, Volume 20, pp. 571–597.

Wei, S., Mau, S. T., Vipulanandan, C. & Mantrala, S. K., 1995. Performance of new sandwich tube under axial loading: experiment, *Journal of Structural Engineering ASCE*, Volume 121, Issue 12, pp. 1806–1814.

Xiong, M. X., Xiong, D. X. & Liew, J. Y. R., 2017. Axial performance of short concrete filled steel tubes with high-and ultra-high-strength materials. *Journal of Engineering Structures*, Volume 136, pp. 494-510.

Yu, T., Teng J. G., Wong Y. L., & Dong S. L., 2010. Finite element modelling of confined concrete-I Drucker–Prager type plasticity model. *Engineering Structures*, Volume 32, Issue 3, pp. 665–79.

Yu, M., Zha, X., Ye, J. & Li, Y., 2013. A unified formulation for circle and polygon concrete-filled steel tube columns under axial compression. *Engineering Structures,* Volume 49, pp. 1-10.

Zeghiche, J. & Chaoui, K., 2005. "An experimental behaviour of concrete-filled steel tubular columns." *Journal of Constructional Steel Research*, 61, pp. 53-66.

Zhao, X., Han, B. & Grzebieta, R., 2002. Plastic mechanism analysis of concrete-filled double skin (SHS inner and SHS outer) stub columns. *Thin-Walled Structures*, Volume 40, Issue 10, pp. 815–833.